1-1-2019

The Evolution Of Coral Snake Mimicry

Renan Janke Bosque

THE EVOLUTION OF CORAL SNAKE MIMICRY

A dissertation

Submitted to the graduate faculty

in partial fulfillment of the requirements

for the degree of Doctor of Philosophy

in the Biology Department

The University of Mississippi

by

Renan Janke Bosque, B.S; M.S.

December 2019

ABSTRACT

Scientists have regarded mimicry as one of the most amazing examples of the power of natural selection. Early observations by naturalists of the mimetic association between venomous New World coral snakes of the genus *Micrurus* and harmless mimics has stimulated an intense debate about the causes and consequences of mimicry that persists today. Despite its medical, evolutionary and historical importance our understanding of evolution within the genus *Micrurus* is negligible. My dissertation explores the evolution of mimicry within South American coral snakes and their mimics using a multi-scale framework involving macroevolutionary (Chapter I), geographic/morphological concordance (Chapters II and III), behavioral (Chapter IV), and phylogeographic (Chapter V) approaches. I show that warning coloration is widespread, liable and positively correlated with speciation rates. I found that *Micrurus* species behave as Müllerian mimics. *Oxyrhopus guibei* is a potential mimic of the genus *Micrurus* and mimetic precision is independent of model's species richness but dependent on which part of the snake's body is being studied. I also demonstrate that social interactions might be an underappreciated factor on the evolution of mimicry. Finally, I explore the phylogeographic history of *M. surinamensis* and *M. lemniscatus* and provide an interpretation of their distinct patterns of evolution with implications for *Micrurus'* taxonomy.

DEDICATION

My family, friends and all the people who are tormented with the apparent rising of obscurantism, superstition and polarization in our present time

ACKNOWLEDGEMENTS

First I would like to thank my wife Marcella Gonçalves Santos for embarking on this adventure with me, being patient, for always being there to support me in every situation and for helping me work through my mistakes (which occur quite frequently). Thank you for helping me with my analyses and thoughtful discussions of my work. Thank you for giving me a lovely family. You are an inseparable part of my life. Thanks too to Nico for always having a smile to cheer up our day after long hours of work.

Thanks to all my family in Brazil specially my mother Karin Janke and father, José Carlos Bosque for helping me to build my way towards the achievement of my goals. This work is also dedicated to my brother Rafael Janke Bosque of whom I am extremely proud, in part for his current academic achievements. My sister Karina Janke Bosque and Barbara Bosque for all the hours chatting on the phone that helped me to cope with living so far from home. I would like to express my gratitude to my grandfather André Bosque and grandmother Maria Inez de Oliveira Bosque for the unconditional love and care they have always shown.

I would like to give to give a special thanks to my mother-in-law Fernanda Gonçalves and to my father-in-law Marcello Santos for all the support, love and resilience in coping with the distance.

I am particularly thankful to all the support and friendship of my advisor Brice Noonan and his family. Brice never measures efforts to support us in our goals and always sees the good

side even in bad situations. Thanks to his wife, Danielle Noonan for being an outstanding friend and extending her kindness and love to our son.

I would like to thank all the students that helped with my dissertation, specially the undergraduates: Nicholas, Alexander, Matthew, Leon, Rachel, Jenna, Eduardo, Jacob, Maria Luiza, Camila, Matt, Adriana, Bailie, Dylan and Terrence. You helped me not just with my project, but also with my formation of mentoring and advising students. Many thanks to Chaz for helping me with analyses and translating old German manuscripts and Isis for helping me with molecular analyses. Thanks Almir de Paula for helping me during my visit to MZUSP.

I am extremely thankful to Laís Veludo for the help provided while visiting the herpetological collections in Brazil. Laís was fundamental to the success of this adventure, helping me not just with lab work but also with all the logistics of the entire trip. This trip was particularly stressful for me (pending fatherhood and a gastritis crisis just to name a few of the stressors) and without your help I would have been totally lost. For all your friendship and dedication I am thankful. Thanks Nelma and Emílio (Laís' aunt and uncle) for all the support while visiting the MPEG.

Thanks to Fabrícius Maia Chaves Bicalho Domingos for years of friendship and science discussion. Fabrícius has been a companion since my early days in the herpetology and an excellent person to have by my side during field trips or lab work. Fabrícius was almost like an advisor during my PhD, giving large contributions for the development of this work.

Many thanks to Nelson Jorge da Silva Júnior for helping me with many aspects of my dissertation. Nelson has a remarkable knowledge of coral snakes and was always very eager to

discuss the results of my research. Nelson also provided financial support for travel to the International Symposium on Coralsnakes, where I was able to contact several researchers with similar interests including Janis Roze.

Thanks to all of the curators, lab managers and students of Centro de Estudos e Pesquisas Biológicas da PUC Goiás, Coleção Herpetológica da Universidade Federal da Paraíba, Coleção Herpetológica da Universidade de Brasília, Instituto Nacional de Pesquisas da Amazônia, Laboratório de anfíbios e répteis da Universidade Federal do Rio Grande do Norte, Museu de História Natural Capão da Imbuia, Museu Nacional do Rio de Janeiro, Museu Paraense Emílio Goeldi, Museu de Zoologia da Universidade Federal da Bahia, Museu de Zoologia da Universidade de São Paulo, and Universidade Federal do Mato Grosso for providing all the support and access to specimens in their respective collections during my visit to Brazil. A special thanks to Guarino Colli for his friendship and ongoing academic guidance since 2005.

Thanks to all my lab mates Andrew Snyder, Isis Arantes, Timothy Colston, JP Lawerence, Stuart Nielsen and Megan Smith for making the work in the lab less tedious and for being really good friends. Quality of life in Oxford definitely decreased after y'all left.

Finally, many thanks to Conselho Nacional de Desenvolvimento Científico e Tecnológico (CNPq) and the Science Without Borders program for providing the fundamental financial support during my PhD. I want to express my gratitude to Marcela Colognesi de Sá who was my lifeline with CNPq and helped to solve innumerable bureaucracies. Thanks for the Graduate School of the University of Mississippi for the financial support of a dissertation fellowship in the Spring of 2019.

TABLE OF CONTENTS

LIST OF TABLES

LIST OF FIGURES

CHAPTER I:

THE EVOLUTION OF WARNING COLORATION IN SNAKES

Introduction

Coloration and its associated biological and ecological functions play a major role in the evolution of organisms (Ruxton et al. 2004). Color can be used by animals in intraspecific (social displays, mate choice) and interspecific (predator avoidance/deterrence) communication (Houde 1997; Ellers et al. 2003; Ruxton et al. 2004; Hoekstra 2006; Macedonia et al. 2013).

Although cases of color evolution via genetic drift have been reported (Protas and Patel 2008), selection is thought to be the major force driving changes in coloration. From a macroevolutionary perspective, the evolution of coloration has also been associated with shifts in diversification rates (Santos et al. 2014). Clades containing species that display warning coloration may have more than twice the number of species compared to cryptic sister groups (Przeczek et al. 2008). Studies suggest that diversification rates of lineages with warning coloration are higher due to the combined effects of high survival and the isolating effects of localized predator avoidance (Vamosi 2005). Once established, warning coloration may increase diversification if it allows conspicuous species to explore unavailable resources and niches otherwise inaccessible due to predation pressure (Santos et al. 2014). Under a different selective

regime, populations that display warning coloration may ultimately be reproductively isolated from populations with cryptic color.

Despite decades of study on the subject, only recently has the scale of evolutionary analyses allowed for the study of the macroevolutionary patterns associated with warning coloration within a comparative framework (Arbuckle and Speed 2015; Davis Rabosky et al. 2016b). In a pioneering study, Arbuckle *et al.* (2015) showed that while extinction rates were not different, the speciation rate of vividly colored anurans was three times higher than clades characterized by cryptic coloration, indicating that coloration is an important driver of diversification.

Red coloration is a visual signal widely used to convey information to other organisms (Pryke 2009; Pravossoudovitch et al. 2014). The purpose of red coloration can be dependent on the species bearing the color, the way in which it is presented, and the context through which individuals of the same or a different species perceive and react to that coloration (Cox and Davis Rabosky 2013). In some animals red coloration may function as a signal to attract mates (Gray 1996), while in others it may be used to warn predators of potential danger such as venom or poison (Rowe and Guilford 2000). The same visual signal can even be used in both ways, targeting both conspecifics and potential predators, and may depend on light conditions and background contrasts (Endler 1992).

Snakes employ a myriad of strategies to avoid predation but the use of visual warning signals is one of the most common. Several snake taxa use red color as a deterrent that has even been shown to elicit innate avoidance by predators (Smith 1975). The conspicuous warning coloration in some snake groups provides an opportunity to study the influence of color on species diversification rates. Field and laboratories studies (Smith 1975; Brodie 1993) have

shown that warning coloration in snakes may dramatically reduce predation rates relative to cryptic coloration, and this may lead to faster diversification. Numerous extant snake taxa exhibit what might be considered warning coloration, many of which are Batesian (harmless) mimics of dangerous, aposematic species (Kikuchi and Pfennig 2010; Akcali and Pfennig 2014). Notably, each instance of mimicry within snakes effectively doubles the number of clades capitalizing upon the diversification-promoting forces associated with warning coloration. Batesian mimicry can promote diversification by disfavoring immigrants that are locally unfit and by selecting against mimetic hybrids from different populations (Pfennig et al. 2015).

The pattern in which the red signal is displayed is another important factor. For example, *Bothrophthalmus lineatus* (Lamprophiidae) has a red and black striped pattern which is widely accepted to be a pattern facilitating escape behavior (Brodie 1992), while red rings (several Elapidae, Colubridae and Dipsadidae species) have been shown to be a warning pattern. Despite the possible different functions of the two patterns (escape vs. warning), stripes and rings might have similar outcomes when combined with red coloration. When not moving, a snake with red stripes may signal potential danger to predators, but when moving the stripes may make it hard for the predator to focus and aim a strike (Allen et al. 2013). In a similar fashion, red rings can also aid in escape if the predator cannot distinguish between red and black rings when the snake is moving. The blur caused by movement makes the snake appear steady for the receivers a phenomenon known as "flicker fusion effect" (Titcomb et al. 2014).

While many invertebrates, and some vertebrates, derive their red coloration through the ingestion and sequestration of carotenoids (Toews et al. 2017), snakes, produce red drosopterin pigments (Olsson et al. 2013; Kikuchi et al. 2014). This physiological pathway may have enabled the independent evolution of warning signals in different clades under similar selective

pressures. Analysis of the distribution of warning coloration across the snake tree of life could enhance our understanding of the macro evolutionary patterns in this group and the influence of warning color on biotic diversification.

The objective of this work is to answer the following questions: 1) How many times has warning coloration evolved within Serpentes? 2) How many reversals from warning coloration to non-warning coloration occurred during snake evolution? 3) Does warning coloration affect diversification or extinction rates in snakes?

Methods

Snake phylogeny and color

We produced a matrix with coloration data for all 1,262 snake species present in the species-level squamate phylogeny published by Pyron *et al.,* (2013), accounting for approximately 36 percent of all described snake species. The phylogeny presented by Pyron *et al.,* (2013) was used to calculate the phylogenetic signal and ancestral state estimation while the phylogeny produced by Pyron *et al.,* (2013) was used calculate transition and diversification rates. All the metrics and analysis performed in this chapter were based on the species-level squamate tree trimmed for the Serpentes clade. As a proxy for warning signal we counted only species with red coloration on the dorsum, which is the largest section of the body and the one most often exposed to visually oriented predators. Each species in our data matrix was coded as either 1 = possessing red coloration on the dorsum and 0 = lacking red coloration on the dorsum. Red coloration in snakes is known to follow a Mendelian pattern of inheritance, being unlinked to sex (Davis Rabosky et al. 2016a) which contributes to an easier understanding of the role that

this color can play in the evolution of the group. Snake colors were assessed based on photos (print and digital) and original descriptions. Images of snakes were obtained through searches of Google images and the website http://reptile-database.reptarium.cz (Uetz and Hošek 2019). When necessary, the identification of species was confirmed by comparison to original descriptions and/or available taxonomic keys.

Phylogenetic signal

To determine whether the evolution of warning coloration exhibits phylogenetic signal we calculated lambda (λ), a measure of the strength of phylogenetic signal (1=strong to 0=weak) associated with a character, which is robust to incomplete taxon sampling (Pagel 1999; Molina-Venegas and Rodríguez 2017). The calculated value of λ is then compared with simulated trees (999 simulations) where λ =1 and λ=0 considering a Brownian motion evolution of the trait. After that, the fit of the models was evaluated using a likelihood ratio test. We estimated λ using the R package *phytools* (Revell 2012). We also calculated the D statistic, using 1000 permutations, which tests if the presence of warning color is phylogenetically conserved (D=0) or randomly distributed (D=1) across the phylogeny (Fritz and Purvis 2010) using the R package *phylobase* (R Hackathon et al. 2019) with the function *phylo.d*. All analyses were performed using the free software R (R Core Team 2017).

Ancestral state estimation

To infer ancestral character states we performed a stochastic character mapping of discrete traits on the phylogeny of Pyron *et al*, 2013 using SIMMAP (Bollback 2006) in the R

package *phytools* (Revell 2012). Inferred ancestral states were plotted using the function density map (Revell 2013) with 1000 stochastic mapped trees. This visualization has the advantage of combining results of the stochastic mapping of binary traits and plotting the posterior density on the tree using a color gradient.

Transition rates of warning color

Since we are dealing with a large tree, such that different parts of the phylogeny may have different transitions rates between warning and non-warning signal, we estimated the transition rates using a "hidden rates model" (HRM) with two hidden (slow and fast) states (Beaulieu et al. 2013). This analysis was used to assess evidence for varying rates of evolution of warning coloration across the phylogeny.

Warning color as a diversification factor

To infer whether the warning coloration has an effect on diversification parameters (speciation rate, extinction rate and rate of transition between states) compared to lineages without warning coloration we used binary-state speciation and extinction model (BiSSE), as proposed by Maddison *et al.* (2007). We tested whether the differences in species number among lineages were caused by asymmetrical character change (red to non-red and non-red to red), or asymmetrical extinction or speciation using appropriate likelihood ratios. These analyses were performed using the package *diversitree* in R (FitzJohn 2012).

Results

Of the 1262 species analyzed, 121 possess red coloration. Within genera the frequency of red coloration varied widely from complete absence to all species displaying red color. As expected, venomous coral snakes of the Elapidae and the presumed mimics within the Dipsadidae and Colubridae were the groups with the highest number of species displaying red coloration. (Fig. 1, all the figures of the dissertation are presented in the appendix B).

Phylogenetic signal

Red coloration showed a strong phylogenetic signal (λ=0.90 ; $p<0.001$; D=0.15; probability of (D) resulting from no phylogenetic structure = 0, Probability of (D) resulting from phylogenetic structure: 0.262), indicating that the phylogeny alone can explain red coloration evolution in snakes.

Ancestral state estimation

Our inference of the evolutionary history of warning coloration demonstrates that red coloration is a labile trait. Using the SIMMAP function, we identified an average of 81.75 state changes, with 68.45 transitions from non-warning to warning coloration and only 13.30 reversions (Fig 1). Most of the reversions occurred in the families Colubridae and Dipsadidae.

Transition rates of warning color

The parameters calculated using HRM for coral and non-coral coloration showed differences within transition rates. At the slow rate class the transition to a non-coral coloration (coralènon-coral: 0.097) is several orders of magnitude higher than a transition to a coral coloration (non-coralècoral: 2.061e-09). On the other hand, the fast rate class has a much higher transition to a coral coloration (non-coralècoral: 7.843e-03) than the reverse (coralènon-coral: 2.061e-09). It is easier for a transition to occur towards a slow rate class in both color states – non-coral: (slow rate classèfast rate class: 4.228e-03); (fast rate classèslow rate class: 0.016); coral: (slow rate classèfast rate class : 2.061e-09); (fast rate classèslow rate class: 4.901e-02).

Warning color as a diversification factor

Using BISSE, we found that the variation in speciation rate is explained by the presence of red color (best log-likelihood value = -5198.4; Chi Squared$_4$ = 138.299; $p<0.0001$). Clades with red coloration were found to have, approximately 5.16 times the speciation rate of clades without it. There were no differences in extinction rates between clades with red coloration and clades with non-red coloration.

Discussion

Species traits are commonly shaped by balancing forces that allow individuals to secure resources, access mates, and avoid predation (Schall and Pianka 1980; Hawlena et al. 2006). One important trait that is usually subject to strong selection is color, and we found that warning coloration is not randomly distributed across the snake phylogeny (Fig 1 and phylogenetic signal estimates), reinforcing the suitability of red coloration for diversification studies in snakes. The

inferred frequent independent origin of warning coloration (average 81.75 transitions to red coloration) indicates an important role for this trait in the diversification of snakes that may have been facilitated by the use of the same genetic building blocks (Olsson et al. 2013; Kikuchi et al. 2014). The repeated evolution of warning coloration in distantly related snake clades (Fig. 1) suggests a selective advantage for species displaying red coloration on their dorsum, which is corroborated by field (Brodie 1993) and laboratory (Smith 1975) studies.

The ability of certain clades to occupy new niches or areas is highly correlated with an increase in diversification rate (Davis Rabosky et al. 2016b). We found that clades with red coloration have a five-fold increase in speciation rates, which can be illustrated by Colubridae, Dipsadidae and Elapidae. Signaling potential danger to predators may have enabled species that display red coloration to explore more niches since they have a natural buffer to predation. Additionally, the use of warning coloration by harmless species might have further increased the diversification in some clades since they do not carry the burden of producing toxins. The production of secondary compounds consumes resources (McCue 2006) that can, otherwise, be allocated to reproduction, adding another effect that can might explain the diversification of harmless and conspicuous snakes.

Reversals to a non-red coloration occurred in both venomous and non-venomous species, indicating that the selective advantage of having red coloration is not absolute and might shift depending on the context. The factors that are determinants to trigger reversals towards a non-red state still require further investigation, but some plausible explanations might include lack of predators (extinction of predator or colonization of areas without predators), extinction of model species (mimics returning to a non-red coloration), genetic drift, and environmental constraints. For example, *Micrurus albicinctus* has a bicolor pattern with black and white rings, despite most

Micrurus species displaying some sort of red coloration. The absence of red coloration in *M. albicintus* might have been selected for by low light conditions in forest habitats (França 2008).

Phylogenies with many terminals are expected to span heterogeneous evolutionary rates for many traits that may be a result of different selective regimes, extinctions, and reproductive modes (Beaulieu et al. 2013; Garamszegi 2014). However, we found that only the slow rate was present, showing that color evolves in a uniform manner. This uniform evolution of the red coloration may be a result of a shared pathways producing the red coloration among all snake clades. At the slow rate class, it is unlikely for a clade to switch to red coloration. The combination of non-red coloration and slow class may be viewed as an absorbing state probably because when a red morph first appears in a population it is expected to be exposed to greater predation pressure. This may hold because predators do not recognize a new red snake as a potential threat and being conspicuous, they are promptly attacked. This fitness valley between a species that does not display a warning signal and a species that does display a conspicuous warning signal is probably deep and hard to cross. At the same time, once the fitness valley is crossed, we expect faster diversification, which is in accordance with our results.

In conclusion, our results demonstrate that warning coloration is widespread within Serpentes and is correlated with higher speciation rates. Despite the apparent selective advantage, warning coloration is a liable trait and we found several reversals to non-warning coloration. Field and laboratory tests might be performed to investigate the possible causes of transition between states. Similarly, investigating the mechanisms responsible for promoting diversification in lineages that attain warning coloration will greatly benefit our understanding of coloration evolution.

CHAPTER II:

COLORATION PATTERNS OF SYMPATRIC NEOTROPICAL CORAL SNAKES SHOW EVIDENCE OF MÜLLERIAN MIMICRY

Introduction

New world snakes of the genus *Micrurus*, commonly known as coral snakes advertise potential danger via their aposematic (warning) coloration, frequently a combination of red, black, and light (white or yellow) colored bands (Roze 1996). This aposematic genus, protected by neurotoxic venom, serves as model for several mimic species, providing well described examples of Batesian mimicry (Greene and McDiarmid 1981), where a number of harmless New World species display similar color patterns to deceive predators (Ruxton et al. 2004).

Surprisingly, despite decades of study of the genus, no formal tests have been performed to evaluate the extent in which *Micrurus* species engage in Müllerian mimicry, the assumption instead relying upon anecdotal reports (Greene and McDiarmid 1981; Roze 1996; Marques 2002). Müllerian mimicry, the sharing across defended species (e.g. species of *Micrurus*) of both an aposematic signal and the cost of training predators to avoid said signal by dangerous or unpalatable species (Müller 1878; Ruxton et al. 2004; Sherratt 2008). This phenomenon has been documented in other snake groups (Sanders et al. 2006), but has yet to be tested in coral snakes.

The paucity of studies of Müllerian mimicry in coral snakes might be because the majority of studies have been performed in the United States, where only a few species of coral snakes exist in non-overlapping geographic areas. However, throughout its range the genus *Micrurus* has approximately 80 recognized species, with up to 11 species co-occurring in some

areas, such as the western Amazon (Bosque et al. 2016), making this an ideal area for the evolution of Müllerian interactions.

The high diversity of *Micrurus* in the neotropics creates an opportunity for similarly-defended aposematic species to share the cost of training predators to avoid these color patterns, and/or to share the benefit of evolved innate avoidance of coral snake coloration (Smith 1976). *Micrurus* species tend to be locally rare which imply less opportunity for predator learning and weaker selection for innate avoidance. Because of its rarity, Müllerian mimicry might play an underappreciated role in the evolution of coral snake coloration. If two or more such species engage in Müllerian mimicry, a convergence in morphology is expected in areas where they co-occur (Kapan 2001), with a relaxation of selection for signal similarity outside the range of distributional overlap. In this study, we integrated morphology, coloration and geographic distribution data for several *Micrurus* species to test for the existence of Müllerian mimicry.

Materials and methods

Species

To test whether coral snakes engage in Müllerian mimicry, we examined museum specimens of the subset of Amazonian species that possess a tricolored, triadal (red bands separated by a sequence black-white-black-white-black bands) aposematic signal (Savage and Slowinski 1992). We selected species with overlapping and non-overlapping geographic distributions across the range of each species, and which were well represented in museums. After an initial exploration of the available material, the species selected for this study were

Micrurus brasiliensis, M. frontalis, M. ibiboboca, M. lemniscatus and *M. surinamensis.* Geographic coordinates where the specimens were sampled were obtained from the museums.

Morphology and color quantification

We took high quality digital photographs from the dorsum of 1528 preserved snakes deposited in Brazilian herpetological collections (CEPB, CHUFPB, CHUNB, INPA, LARUFRN, MHNCI, MNRJ, MPEG, MZUFBA, MZUSP and UFMT; Fig. 2 and Appendix C). After excluding damaged snakes, we retained 1458 individuals for our analysis. From each image we recorded the following measurements: total length (from the tip of the snout to the end of the tail), number of black, red and white bands. We also selected one triad at mid-body to measure the length of the first, second, and third black bands; length of the first and second white bands and the length of the red band anteriorly to the selected triad. The length of the white bands as well as the first and third black bands were nearly identical, so we calculated averages of the two for further analyses. After checking which variables were highly correlated (≥ 0.9), using a spearman correlation test, we selected 5 variables to be used in further analyses: number of red bands, proportion of red bands (width of red band/total length), proportion of external black bands ((width of black band 1 + width of black band 3/total length)/2), proportion of white bands ((width of white band 1 + width of white band 2/total length)/2), and proportion of internal black bands (width of black band 2/total length). All images were analyzed using the software ImageJ version 2.0.0-rc-69/1.52i.

Statistical analysis

All statistical analyses were performed using the statistical software R (R Core Team 2018). To calculate morphological variation along the geographic distribution of each species, we used a multivariate spatial analysis (spatial principal component analysis: sPCA), with the function *multispati* from the package *adespatial* (Dray et al. 2018), which maximizes the product of variance and spatial autocorrelation. To test for spatial autocorrelation at broad geographic scales in the morphological data, we ran a Monte Carlo test of global spatial structure with 999 simulations using the function *global.rtest* from the package *ade4* (Dray and Dufour 2007). To calculate the number of nearest neighbors and the spatial weights (using row standardized style) we used functions *knearneigh* and *nb2listw,* respectively, using the package *spdep* (Bivand 2002). In order to produce maps of the morphological variation of each species, we interpolated the sPCA lagged scores using the function *interp* from the *Akima* package (Akima and Gebhardt 2016).

To test whether each species pair is more morphologically similar where their distributions overlap we created a grid with cells of one degree latitude x longitude (ca. 111 km^2) for each species. We extracted the lagged scores from each cell to generate a matrix where the geographic grid cells are the rows and the columns are the species. If multiple samples of the same species were found in the same cell, we averaged their lagged score to obtain a single value for that particular cell. After that procedure we compared each pair of species performing t-tests, to check if their lagged scores were similar where they co-occur and if they were different where they do not co-occur. We repeated this procedure for the first three sPCA axes.

Additionally, we tested if morphological dissimilarity between pairs of species increases with geographic distance by performing a Mantel test (999 permutations) using the package

ecodist (Goslee and Urban 2007) with a dissimilarity matrix of the Euclidean distances of each PCA score and geographic distance of each individual with the package *geosphere* (Hijmans 2017).

Results

After a first exploration of the data we concluded that coral snakes do not have an ontogenetic variation in the number of rings (correlation test between number of red bands and total length: rho= -0.003; p=0.905). That is, juveniles tend to maintain a constant number of rings along their life, only increasing the length of each ring. Accordingly, we performed analyses using all the available individuals (adults and juveniles). The first three spatial principal components explain 93% of the variance in the original morphological variables (Fig 3). From the Monte-Carlo simulation we rejected our null hypothesis of no spatial structure in our data (Monte-Carlo test: observed: 0.08, simulated p-value: 0.001). The first spatial principal component (sPCA1) alone accounted for 47% of the variance and number of bands and length of the internal black bands best were the most important variables (Table 1 and Fig. 4; all the tables of the dissertation are presented in the appendix A).

On the second principal component (sPCA2), which explains to 30% of the variance, length of white bands was the variable with the greatest contribution (Table 1 and Fig. 5). On the third principal component (sPCA3, 16% of the variance), the length of external black bands was the variable that contributed the most (Table 1 and Fig. 6).

In general, the maps produced by the interpolation clearly separate each species in specific color pattern groups (Fig. 3), with the exception of *M. lemniscatus*. Despite indicating that species can be grouped based on color pattern, the maps produced by interpolation reveal

that there are similar trends between species for length and number of bands (i.e., species tend to be more similar where they overlap, Fig. 4 and Table 1). On the sPCA1, *M. lemniscatus* is clearly the species with the largest variation of morphological measurements, which is unsurprising given that *M. lemniscatus* has the largest, most discontinuous geographic distribution of all analyzed species (Fig 3). *M. surinamensis* shows long internal black bands and a reduced number of bands, while *M. frontalis* shows an increased number of bands with short internal black bands (Table 2).

The t-tests showed that where a pair of species does not overlap in their geographic distribution they are not similar in appearance (7 out of 10 comparisons; Fig. 7). When a pair of species does overlap in their geographic distribution, they tend to look similar (10 out of 10 comparisons; Fig. 7 and Table 3).

The Mantel test results indicate that, in general, dissimilarity between species pairs increases with distance (Table 4 and Fig. 8). The only exception to this pattern occurred when comparing *M. surinamensis* against *M. frontalis*/*ibiboboca*/*lemniscatus*.

Discussion

Micrurus species have long been considered models for several harmless mimics. Numerous studies have shown that these species engage in Batesian mimicry (Brodie 1993; Davis Rabosky et al. 2016b; Akcali and Pfennig 2017), yet there has been no formal demonstration that *Micrurus* species increase their protection against predation by converging on similar coloration in sympatry. Our study is the first to demonstrate that *Micrurus* species also behave as Müllerian mimics by displaying similar color patterns where they co-occur.

Given that density of individuals is generally lower towards the edge of a species' distribution, we expect even more similarity between two species in such areas (Harper and Pfennig 2007). This phenomenon is believed to occur because predators have fewer encounters with coral snakes at the edge of their geographic distribution, leaving little room for deviations of the local pattern. Selection favoring better mimicry at the edge of distribution was tested in a previous study of coral snake replicas, indicating that Batesian mimics are more similar to their model at the edge of the distribution of the model (Harper and Pfennig 2007). The low density of individuals at the edge of the distribution is probably a factor that is accelerating the convergence towards coloration similarity between multiple *Micrurus* species. This edge-density effect might be another factor contributing to the strong patterns that we found in the present study.

The length of the red bands was not an important variable in any of the three sPCA. This might indicate that the length of red bands is under strong selection even at larger geographic scales and may be functioning as a generalized signal for predator deterrence (Pryke 2009). However it should be noted that there are some *Micrurus* species, like *M. albicinctus*, that do not have red coloration, which indicates that the banding pattern itself is another way to transmit a deterrence signal (Brodie 1993). The red coloration is usually attributed to a broadly avoided coloration pattern (Pryke 2009; Pravossoudovitch et al. 2014) and banding patterns are used as a signal in other taxa such as hymenopterans (Williams 2007) and lepidopterans (Ingalls 1993). Further investigation is warranted to understand the interaction between coloration and banding patterns in *Micrurus* snakes, and its role in signaling unprofitability.

Although our results indicate a pattern of Müllerian mimicry, Batesian and Müllerian mimicry likely work together in complex mimicry systems and sometimes distinction between these two types of mimicry can be blurred (Speed and Turner 1999; Balogh et al. 2008). The

difficulty of distinguishing between these two types of mimetic interactions can be exacerbated by the fact that distinct *Micrurus* species vary in their venom composition (Lomonte et al. 2016), which might pose different levels of threat to each predator species. Neotropical coral snakes and their harmless mimics also show overlapping coloration patterns (Bosque et al. 2016), but it remains to be tested whether there is coloration similarity in areas of geographic overlap of *Micrurus* and harmless snakes. Field tests of predation avoidance and quantification of population densities of coral snakes would also provide an important source of evidence for the evolution of such signals in local communities.

Future directions

To further investigate the evolution of mimicry in such a diverse clade, a comprehensive *Micrurus* phylogenetic hypothesis that includes both intra- and interspecific structure is essential, particularly one that includes representative sampling of species with large geographic distributions. Estimates of population demography, particularly with respect to distributional core and periphery, would provide additional context for further tests of coral snake mimicry.

CHAPTER III:

CORAL SNAKE BATESIAN MIMICRY AND THE EFFECTS OF MODEL DIVERSITY AND SYMPATRY ON MIMIC FIDELITY

Introduction

A mimic's similarity to its model varies widely among known systems and includes extreme cases of dramatic intraspecific polytypism, frequently associated with geographic structure (Mallet and Joron 1999; Symula et al. 2001). There are also examples of a gradation of levels of mimicry, from nearly perfect to those that bear little resemblance to their models within and between mimic species (Savage and Slowinski 1992; Akcali and Pfennig 2017). Such variation in mimetic fidelity has been attributed to many factors, including the relative abundance of models and mimics, their degree of sympatry, the presence of multiple models, the level of protection of the model, or the evolutionary stage of the mimic relationship (Edmunds 2000; Sherratt 2002; Kikuchi and Pfennig 2013). The factors involved in mimetic fidelity can act jointly to create a mosaic of different degrees of similarity along the mimic's geographic distribution.

In areas where the model is rare, selection may drive mimics to be more similar to models due to predation pressure (Harper and Pfennig 2007; Pfennig et al. 2007). In contrast, poor mimics may persist through gene flow from central to peripheral areas of their putative

model distribution (Harper and Pfennig 2008). Furthermore, in areas where aposematic species of many different color patterns overlap in their distributions, mimics may attain an intermediate mimetic phenotype, not resembling any specific model (Edmunds 2000).

Mimetic precision might also be affected by how predators interact with their prey. It is know that some avian predators have a tendency to aim a strike toward the head of prey as a mechanism to avoid a counterstrike which is particularly important when preying on dangerous animals like venomous snakes (Smith 1976; Brodie 1993). Predators relying only on cues of certain parts of the body to decide whether or not to attack will select mimics that have a more precise resemblance in that particular part of the body. In contrast, the parts of the body not targeted by predators might be under relaxed selection pressure for mimetic fidelity. Overall, a mimic might look imprecise (at least in our perception (Cuthill and Bennett 1993)), but precise resemblance at only certain parts of the body might be enough to dissuade predators and avoid an attack.

One of the most debated example of mimicry in vertebrates occurs in several harmless snake species that deceive predators by mimicking the color of the deadly coral snakes of the *Micrurus* (Savage and Slowinski 1992; Roze 1996; Campbell and Lamar 2004). Coral snakes warn predators by using a combination of red, black, and yellow-or-white bands arranged several patterns (Savage and Slowinski 1992; Roze 1996; Silva Jr. et al. 2016). The same coloration is found in a diverse group of harmless snakes even in distantly related taxa (Davis Rabosky et al. 2016b).

One widely-presumed Batesian mimic of the genus *Micrurus* is *Oxyrhopus* (Zaher and Caramaschi 1992; Brodie and Janzen 1995; Buasso et al. 2006; França 2008), which has an overlapping geographic distribution and similar coloration pattern to Neotropical *Micrurus*

(Bosque et al. 2016). *Oxyrhopus* species have intraspecific morphological variation that includes the number and width of bands, color of the head and total length (Zaher and Caramaschi 1992; Lynch 2009; Bernardo et al. 2012). *Oxyrhopus* has a geographic distribution that overlaps with many model species of the genus *Micrurus* that might be contributing for the great morphological variation found in *Oxyrhopus*.

Oxyrhopus guibei individuals exhibit a tricolor pattern with red, black, and white rings (Fig. 9) with a geographic distribution concentrated in Southern Brazil, a region with several potential *Micrurus* models that have a similar coloration pattern. The overlapping distribution with multiple models and various degrees of sympatry makes *O. guibei* an ideal candidate to test hypothesis related to mimic-model fidelity. This work aims to identify which species *O. guibei* is mimicking, test whether the number of model species present in a particular area affects the mimic's fidelity and test if *O. guibei* tend be more morphologically similar to models near the head.

Materials and Methods

Color and morphological quantification

We took high quality digital photographs from the dorsum of 557 preserved snakes deposited in many of the largest Brazilian herpetological collections (CEPB, CHUFPB, CHUNB, INPA, LARUFRN, MHNCI, MNRJ, MPEG, MZUFBA, MZUSP and UFMT; see Appendix C and D for complete specimen information and museum acronyms). After excluding damaged snakes, we retained 479 individuals. Since *Oxyrhopus* species are known to have incomplete bands (i.e., in a sagittal plane, left side of the band does not encounter the correspondent color on the right

side (Fig 10), we randomly chose one side (in a sagittal plane) to take the measurements as described below. From each image we recorded the following measurements: total length (from the tip of the snout until the end of the tail), distance from the tip of the snout to the intersection of the parietal scale, number of black, red and white bands. We also selected one triad in the mid portion of the total length of the snake and another at the first complete triad closest to the head (referred as neck from now on) to measure: the length of the first, second and third black bands; length of the first and second white bands, the length of the red band and the mismatch between left and right side of the triads (the length a color band did not match the same color on the other side). Additionally, we counted the number of incomplete triads on the first and second half of each snake. As the length of the first and the second white bands and the external black bands (first and third) were, respectively, almost identical, we averaged them for subsequent analyses. For the analysis we used the following variables: number of triads, proportion of external black bands (black band 1 + black band 3/total length), proportion of white bands (white band 1 + white band 2/total length) and proportion of internal black bands (black band 2 /total length), half triads (1^{st} and 2^{nd} half) and mismatch between triads (Fig. 10). We also used the morphological measurements of presumed model species from chapter 2 (*M. brasiliensis*, *M. frontalis, M. ibiboboca, M. lemniscatus* and *M. surinamensis*). Since *Micrurus* species do not have great variation on ring size along the body (Silva Jr. and Sites 1999; Feitosa et al. 2007), we used the measurement made on the mid portion of the snake as a proxy for the measurements of the neck. All images were analyzed using the software ImageJ version 2.0.0-rc-69/1.52i.

Color variation of Oxyrhopus guibei and Micrurus

We performed two paired t-tests; one to evaluate if the number of half triads in the first and the second portion of the body of specimens of *Oxyrhopus guibei* are different, and another to evaluate if the mid-portion of the body of *O. guibei* is more prone to have mismatch between left and right triads than the triads near the head. Initially we performed a principal components analysis (PCA) with the raw data (not averaged per grid-cell) to explore how *O. guibei* morphological variation (excluding half triads and mismatch) overlaps with *Micrurus* species. We performed two separate PCAs, one for the variables of the neck, and another for the variables of the mid-body. To test which species *O. guibei* is mimicking we performed a linear discriminant analysis (LDA) with all *Micrurus* species patterns within the latitudinal and longitudinal limits of *O. guibei* and checked the amount of correct classifications. We performed this procedure for all the variables that measure the length of the bands (neck and mid-portion).

Geographic structure of coloration

In order to produce maps of color variation on each species we created a raster containing a grid with 1 degree cells in a range that encompass the maximum latitudes and longitudes for *O. guibei* (-82, -34, -30, 11: W,E,S,N – respectively). For each species we averaged the value measured for each morphological variable per cell totalizing 400 cells. Subsequently we extracted the mean value of each morphological variable per cell that overlapped with *O. guibei* distribution to create a data matrix for further analysis. The average of each cell can potentially estimate the mean morphology of a local population, which is ultimately how predators would perceive their prey. All raster generation and data handling were performed using the package

raster (Hijmans 2019) and maps were generated with aid of the packages *maptools* (Bivand and Lewin-Koh 2017), *prettymapr* (Dunnington 2017) and GISTools (Brunsdon and Chen 2014) in R (R Core Team 2018). We also performed an sPCA separately for the neck and mid-body regions and produced a matrix as described above. With the averaged lagged scores we used a paired t-test to check if *O. guibei* is, overall, morphologically more similar to *Micrurus* species in the neck or at the mid-portion of the body.

Effect of Micrurus species richness on Oxyrhopus guibei

To test the effect of *Micrurus* species richness on *Oxyrhopus guibei*, we constructed a matrix of *Micrurus* richness per 1º cell based on Bosque et. al,(Bosque et al.). The original matrix of Bosque et. al (2016) is based on geographic distribution maps of Roze, (Roze) and Campbell and Lamar,(Campbell and Lamar). We extracted the information of *Micrurus* species richness from the cells that overlapped with *O. guibei*. We used this information, to test if *Micrurus* species richness in each cell can explain mimetic precision on *O. guibei* we performed a generalized linear model with a Poisson regression. In our model the independent variable was *Micrurus* species richness and the dependent variable the number of half triads and mismatch between bands.

Results

Similar to their putative model species (see chapter 2), *O. guibei* does not exhibit ontogenetic variation in the number of rings (correlation test between number of red bands and total length: rho= 0.045; p=0.285).

We did not find differences between the number of half triads in the first and the second portion of the body of specimens of *Oxyrhopus guibei* (paired t test: t_{426} =0.814, p=0.416, and Fig. 11). The mid-portion of the body of *O. guibei* are more prone to have a mismatch between left and right triads than the triad adjacent to the neck (paired t test: t_{426}=-24.777, p<<0.001 and Fig 11). We found differences between the sPCA lagged scores of the mid-portion of the body between *Micrurus* and *O. guibei* (t_{34}=2.59, p= 0.012) but not in the neck (t_{34}=0.09, p= 0.9252). The number of bands seemed to vary more in *O. guibei* than all the *Micrurus* species (Fig. 12).

The most important variable for the first principal component was number of triads, followed by the internal black band length for mid-body (Table 5 and Fig. 13) and neck (Table 6 Fig 14). The majority of the overlap of the *O. guibei* internal black band length occurred with *Micrurus frontalis* and *M. brasiliensis* (Fig. 11, Fig 13 and Fig 14). For the second principal component the red band length was the most important variable for mid-body (Table 5 and Fig. 15), while white band length was the variable most important for the neck (Table 6 and Fig. 16). Conversely, the third principal component, the white band length, was the most important variable for mid-body (Table 5 and Fig. 15) while red band length was the variable most important for the neck (Table 6 and Fig. 16). The LDA analysis correctly classified *O. guibei* in 97% of the cases for mid-body and 96% of the cases for the neck. The misclassifications of the mid-body occurred at *M. frontalis* (n=2), *M. lemniscatus* (n=4); neck *M. brasiliensis* (n=5), *M. frontalis* (n=7), *M. ibiboboca* (n=1), *M. lemniscatus* (n=2).

The maps of morphological variation on *O. guibei* show an apparent geographic structure in some morphological variables. Individuals of *O. guibei* tend to have more triads towards the northern part of their distribution (Fig. 17), whereas the external black bands in the mid portion of the body and the neck are larger towards the southern portion of their distribution (Fig. 18, panel EB). A similar pattern is also found in the internal black bands at mid-body (Fig. 19), with the mismatch between bands greater towards the north, getting progressively smaller towards the south (Fig. 19). The other variables do not seem to show a strong geographic structure.

The maximum number of sympatric models was four *Micrurus* species per cell, which occurs in southeast and central Brazil (Fig. 20). We did not find a relationship between *Micrurus* species richness and our variables of mimetic imprecision (glm: mismatch neck, mismatch mid-body half triads neck, half triads mid-body F= 17.39, 1.71, -0.05, -0.04, p= 0.77, 0.86, 0.45, 0.62).

Discussion

By evolving coloration similar to species of the genus *Micrurus*, *Oxyrhopus guibei* individuals presumably reduce the chances of being attacked by visually oriented predators with a consequential benefit for survivorship and higher reproductive success. The advantage of resembling *Micrurus* has been demonstrated by several lab (Smith 1975) and field (Brodie and Janzen 1995; Buasso et al. 2006) studies, indicating a direct effect on mimics' evolutionary history (Davis Rabosky et al. 2016b). Here we showed that *O. guibei* resemble their models in several components of coloration, indicating a mimetic relationship between the two genera. Our results indicate that *O. guibei* morphologically overlaps with all the *Micrurus* species analyzed (Fig. 12), but has a small tendency to overlap more with *M. brasiliensis* and *M. frontalis* (Fig.

11). However, our LDA results, which encompass a larger geographic area where, did not misclassify *O. guibei* as *Micrurus*, which indicates that selection might be acting differently at large and small geographic scales.

We found no difference in the number of half triads between the first and the second half of the body, which might be related on how we measure this variable (the number of half-triads might be concentrated in both directions, towards the head and towards the tail). However, our results show that the portion near the head of *O. guibei* is more prone to precise mimicry (lower mismatch between left and right) indicating that predators might be targeting the head during an attack and consequentially selecting for precise mimicry in this area. This result is also in accordance with our sPCA results which show that at the local scale (1 degree cells) *Oxyrhopus* tend to look more similar to the local average *Micrurus* coloration towards the neck, but not the mid-body. These findings are in accordance with snake replica studies that show that predators tend to preferentially attack the head of a snake, especially when dealing with venomous species (Brodie 1993) indicating a stronger selection for precise mimicry in this area. Many predators have the tendency to attack vulnerable parts of the body specially the eyes, and many prey species uses several strategies to distract predators from aiming a strike towards the head, (Bustard 1969) before and during an attack. We believe that coral snakes and their mimics, use the portion of the head as a flag to signal potential danger to a predator. After the predator has committed to an attack, the flag is no longer useful and *Micrurus* adopt a strategy of concealing their heads and lifting their tails, a behavior also adopted by *Oxyrhopus* (Sazima and Abe 1991). The increased mismatch (or asymmetry) between left and right sides might further increase survival after the predator committed to attack (Cuthill et al. 2006). Asymmetric bands may reduce the capacity of the predator to target one part of the body while the snake is trying to

escape. Since warning signals that are symmetric are more easily recognized and remembered by predators then asymmetrical ones (Forsman and Merilaita 1999), we speculate that the asymmetric bands might also act as a way to predators to forget that a specific pattern of coloration is associated with a harmless and edible species. In summary, *Oxyrhopus guibei* might be using its bands of the neck to avoid an attack and using the bands of the mid-body as an aid to escape during an attack. The mid-body bands might also facilitate the disassociation warning signal to edibility by predators.

While geographic structure in color might be a product of neutral processes or association with model species present in an area (Brodie 1993), we can speculate about some other aspects that might be involved in the evolution of color in this group. It is well known that organisms' uses color to balance the amount energy received by the environment (Margalida et al. 2008), either for thermoregulation or protection against ultra-violet radiation (Cuthill et al. 2017). *Oxyrhopus* guibei populations that live in forested habitats in the Atlantic forest might have being selected to increase the length of the external black bands to maximize thermoregulatory efficiency.

We did not find an association between richness of models and mimetic imprecision in *Oxyrhopus guibei*. Mimetic precision between mimics and models is expected to decrease when the number of models increases due to relaxed selection in mimics (Kikuchi and Pfennig 2013). *Micrurus* species are well known by the toxicity of their venom, which can kill even large mammals (Bucaretchi et al. 2016). The extreme cost of mistakenly attacking a coral snake might grant protection to imprecise mimics of any kind reducing the effect of models richness in mimetic precision. Due to the difficulty of assessing population density, we did not consider the relative abundance of models and mimics in our study.

In conclusion we found that *Oxyhopus guibei* have similar colors of its co-occurring models but can still be recognized by its own unique characteristics of coloration. We showed that *O. guibei* is more similar to *Micrurus* near the head, which might be an indicative of a differential selection on this portion of the body. Tests of the dual purpose of coloration in *Oxyrhopus guibei* will benefit for future studies with predator avoidance on the field and laboratory. The clinal variation for certain aspects of color in *O. guibei* will be useful for future studies about the balance of mimetic interaction and the evolution to cope with thermoregulatory constrains.

CHAPTER IV:

DIVERSITY OF WARNING SIGNAL AND SOCIAL INTERACTION INFLUENCES THE EVOLUTION OF IMPERFECT MIMICRY

*Bosque, R.J., Lawrence, J.P., Buchholz, R., Colli, G.R., Heppard, J. & Noonan, B. (2018) Diversity of warning signal and social interaction influences the evolution of imperfect mimicry. Ecology and Evolution, **8**, 7490-7499.*

Introduction

Mimicry is an evolutionary strategy often employed by organisms to escape predation. Mimetic phenotypes can generally be classified as either camouflage/masquerade, e.g., insects mimicking leaves (Skelhorn and Ruxton 2010) or warning, i.e., co-opting the signal of a defended species (Ruxton et al. 2004). Color combinations including red, yellow, white, and black are broadly used as warning signals in many defended taxa, such as Hymenoptera (Hines and Williams 2012), Coleoptera (Bocak and Yagi 2010), Lepidoptera (Jiggins et al. 2006), Lissamphibia (Symula et al. 2001; Kraemer and Adams 2014) and Squamata (Campbell and Lamar 2004). These warning colors can elicit aversion in a wide variety of visually-oriented predators (Ruxton et al. 2004). The aversion of conspicuous prey can even be socially transmitted (Thorogood et al. 2017), reducing the predation pressure on newly evolved signals. Aversion can also be affected by individual variation in personality (Exnerová et al. 2010), which can be genetically inherited (Drent et al. 2003) and be accompanied by differences in morphological and physiological traits (Goerlich et al. 2012). Whether this aversion is innate,

self-learned or socially transmitted, warning signals are known to have a strong influence on how a predatory animal will explore and interact with prey (Lindstrom et al. 1999; Rowe and Guilford 2000; Ham et al. 2006)

At the community level, Batesian mimicry, where an undefended mimic benefits from a resemblance to a harmful model, is perhaps the most evolutionarily complex mimicry system (Bates 1862; Ruxton et al. 2004). Multiple predator species may co-occur with both multiple defended and multiple undefended prey species that employ a variety of warning colors and patterning, and the dimensionality of these components of the mimicry system can vary geographically. For example, New World coral snakes (*Micrurus*) and their mimics of the genus *Oxyrhopus* exhibit many combinations of model species number, mimic species number, pattern and coloration diversity (Fig. 21), Furthermore, the extent of geographic overlap between mimics and models may vary dramatically and extent of overlap between mimics and models (Roze 1996; Campbell and Lamar 2004; Bosque et al. 2016). Species of *Micrurus* transmit a clear warning signal to potential predators through varying combinations of contrasting red, black, yellow, and white rings (Smith 1976; Brodie 1993; Brodie and Janzen 1995). These same colors are also used by harmless snakes mimics, with varying fidelity in color and pattern to local *Micrurus* models, making this one of most remarkable examples of mimetic interaction (Savage and Slowinski 1992).

One interesting aspect of Batesian mimicry is that some mimic species range of broad geographic areas, sometimes exceeding the range of their presumed model, and often demonstrate regionalized phenotypic variation in their mimetic signal. Regional variation in the warning coloration of mimics could occur simply because different predators may interpret mimic-model resemblance using different sensory cues or cue components (Pekar et al. 2011;

Aubier and Sherratt 2015). Further, different populations of a mimic species may occur in areas with different predators, with local color variants emerging by predation pressure. Nonetheless, even within a single predator species, individual experience with model pattern richness (i.e., the number of different prey patterns) by direct contact or via social observation may also directly affect the evolution of mimetic lineages.

A particularly vexing problem in the macroevolutionary study of mimicry complexes that might benefit from a deeper understanding of predator learning is that, despite a presumed selective pressure to attain perfect resemblance with their models, imperfect mimics are not uncommon in nature. The factors that enable the persistence of imperfect mimics are still unclear but several authors have suggested plausible explanations (Kikuchi and Pfennig 2013; Kazemi et al. 2014). One explanation focuses on the selective pressures acting on the mimic when many models exist in the same area. When multiple models are present within a mimic's geographic distribution, mimics may be selected by predators to either resemble only one model or, if the models are not sympatric with each other, the mimics can adopt an intermediate phenotype (Edmunds 2000; Sherratt 2002). If just one model is present, selection is expected to drive mimics toward signal identity with the defended model (Ruxton et al. 2004). However, if several sympatric, defended models vary in phenotype, predators in this area may be conservative in the avoidance of harmless species with similar warning signals, even if mimetic fidelity to the defended models is inexact (Edmunds 2000). Experimental evidence demonstrates that predators indeed generalize a bad experience with one prey species to others (Hotová Svádová et al. 2013).

Model diversity may also drive generalization to novel patterns that are not even found in models (Ham et al. 2006; Kikuchi and Pfennig 2013). Historically, avoidance of novel prey has been attributed to innate neophobia; the avoidance of a previously unencountered signal simply

because it is new/unusual (Greenberg and Mettke-hofmann 2001). Because neophobia may disappear with exposure experience, the generalization and neophobia hypotheses for explaining novel mimic-like patterns make opposite predictions about the outcome of predator learning as the number of models increases. More models provide predators more cues from which to generalize, making them cautious about new prey patterns, but also increase the familiarity with novelty, thus fostering less neophobia towards it.

Previous researchers have demonstrated generalization of coral snake warning patterns by free-ranging avian predators. In these studies, the birds avoided a mimetic morph with a pattern that differed from the local model but with the same colors (Brodie and Janzen 1995; Kikuchi and Pfennig 2010). To investigate the evolution of more complex systems with multiple models and imperfect mimics, we tested whether the number of models that an avian predator experiences affects the breadth of its avoidance generalization to a novel pattern. In this study, a "novel pattern" is also an imperfect mimic, a pattern not seen previously by the subject, and yet incorporating features (colors and shapes) shared with the aposematic models. We also exposed chickens to different contexts using social and individual exposure as these may affect learned responses to distasteful prey (Thorogood et al. 2017). In order to understand how differences in individual development of chicks could impact their willingness to sample imperfect mimics, we investigated morphological traits that may reveal ontogenetic growth trade-offs between general investment in somatic growth (mass, tarsus and body condition) and organ specific development associated with immune preparedness (spleen mass) and sexual maturation (directional testis asymmetry). The spleen is an important immune organ in birds, the size of which reflects immune activity and possibly immunocompetence (John 1994). As in most bird taxa, the left testis is usually larger in mature phasianid birds such as the chicken (Calhim and Montgomerie

2015) and thus birds with greater asymmetry in this direction can be assumed to be on a more rapid trajectory towards the adult form. Directional asymmetry in adult testis size has been associated with male sexual ornamentation and mate quality in some birds (Møller 1994). We predicted that birds that invest more in organ maturation would be more motivated to feed and thus less likely to avoid a novel food item, despite having learned previously that similar cues were aposematic.

Methods

Study subjects and housing

As model predators we used approximately 10-day old, male domestic chickens (*Gallus gallus domesticus*). The capacity of chickens to discriminate between two objects based on their wavelength is comparable to several bird species (Hart 2001), which reinforces the adequacy of the species selected as a model predator. Birds are commonly used as model predators in warning coloration experiments because their color vision is well documented, and they are known to be the main predators of snakes, including coral snakes (Hinman et al. 1997; Buasso et al. 2006; Leynaud et al. 2008; Kikuchi and Pfennig 2010). Commercial feed (corn-meal) was provided *ad libitum* except for the 60 min immediately prior to exposure and testing sessions, so that the chicks were motivated to "attack." Housing and testing conditions were approved by the University of Mississippi Institutional Animal Care and Use Committee (#15-009). To replicate the snake patterns found in nature, we painted Wild Harvest™ tube feeders with brown spray paint to represent brown snakes and wrapped experimental feeders with colored electrical tape to represent the coral snake color pattern(s) present in three regions of South America (Fig. 21 and

Fig 22) (Bosque et al. 2016). We filled the aposematic (henceforth, we use aposematic and warning signal interchangeably) feeders with feed that was previously sprayed with 10% chloroquine solution, making the feed distasteful but not harmful (Lindstrom et al. 1997; Ruxton et al. 2004); brown feeders had normal feed. These feeders were not meant to be exact replicas of coral snakes, but simply represent a variety of patterns from which the chicks had to learn. To simulate natural encounters with aposematic prey, we used two different approaches: group exposure and individual exposure. Using these two approaches, we could not only identify how pattern richness affected generalization to a new pattern but also the effect of social exposure versus individual exposure.

Group exposure

Chicks were housed in three groups of 43 in poultry brooder cages during exposure to aposematic feeders. Each exposure group experienced only one of the pattern richness treatment levels (Fig 22): highest color pattern richness – H (8 patterns), intermediate color pattern richness – M (4 patterns), or low color pattern richness – L (1 pattern).

In addition to regular (trough-style) feeders, chicks were exposed to brown feeders for 8 h per day during the first four days. On the 5^{th} day, 16 feeders (8 brown and 8 aposematic) were positioned randomly along the perimeter of each enclosure for a 10 min exposure session. The feed in each feeder was weighed before and after each exposure session. This procedure was repeated an additional five times over two days. A final (6^{th}) exposure session before testing lasted 1 h, to ensure that chicks were completely avoiding the aposematic feeders. Notably, our group exposure training procedure allows for social learning (Slagsvold and Wiebe 2011) as the chicks in the same cage may learn from each other's negative reaction to the feed in aposematic

feeders. The learned aversion from conspecifics is still a theme that deserves investigation since contrasting results have been reported (Sherwin et al. 2002; Thorogood et al. 2017).

Group testing

After the conclusion of group exposure, we individually tested these chicks for their reaction to a feeder featuring either the imperfect mimetic pattern of the false coral snake (*Oxyrhopus rhombifer*) or a brown feeder. The testing arena consisted of a 60 cm x 60 cm wood box containing a small wire cage with two chick companions to prevent isolation stress of the test chick. Each chick was tested only once. Despite a broad geographic distribution, overlapping with many species of *Micrurus*, *Oxyrhopus rhombifer* has a tricolor pattern with black saddles bordered by white on a red dorsum (Fig. 21), a pattern not found in any *Micrurus* species. A previous study using plasticine replicas has demonstrated that the *Oxyrhopus rhombifer* phenotype does provide protection against free-range predators (Buasso et al. 2006), but the mechanisms of avoidance are still poorly understood.

We recorded the reaction to test feeder exposure as the hesitation time (time until the first peck). Each trial lasted up to five minutes or until the first attack (peck). If we did not observe any attack after five min, we stopped the trial. Before each trial, we offered small pieces of dry mealworm (*Tenebrio molitor*) to ensure that chicks were hungry and willing to attack. All trials were recorded using a digital camera (videos available upon request).

Individual exposure

In order to explore the impact of individual exposure to different model community diversity we deprived 27 chicks of food for one hour. We then individually exposed 14 chicks to high color pattern richness (Fig. 21) – H (8 patterns) and 13 chicks to low color pattern richness – L (1 pattern). Eight additional individuals were used as buddy chicks. The exposure (training) and testing arena consisted of a cardboard box 38 cm x 30 cm with two buddy chicks inside a small wire cage. In each treatment, we started by presenting one brown feeder for up to 2 min. Starting after the first peck, we allowed them to eat for a cumulative time of 10 seconds to prevent satiation. After that, we removed the brown feeder and presented a random aposematic feeder for up to 2 min. If the chick pecked the food, we allowed it to eat for up to a cumulative total of 10 seconds and then we removed the aposematic feeder. We repeated this procedure until all the 16 feeders were presented according to each subject's treatment group (H: 16 feeders with 8 different aposematic patterns; L: 16 feeders with 1 aposematic pattern – Fig. 22) and recorded the hesitation time i.e. time until the first peck. We did not record the quantity of feed eaten by chicks during individual training.

Individual testing

After the exposure described above, we presented a feeder with an imperfect mimic (i.e. *Oxyrhopus rhombifer*) pattern alongside a brown feeder in the testing arena. The arrangement (left or right) of the feeders was randomized to avoid lateralization bias. We recorded the hesitation time and first feeder choice. In order to evaluate whether morphological characteristics could explain individual variation in hesitation time, we took the following post-mortem

measures of each chick at the end of the experiment: tarsus length, body mass, directional testes length asymmetry, spleen mass and body condition. The entire length of each testis was measured, unless the organ was not fully differentiated, in which case only the length of the portion consisting of white (as opposed to purple-red) tissue was measured. Directional testis asymmetry was calculated as (left length – right length). Body condition was calculated as mass/tarsus length (Brown 1996).

Statistical analysis

We fitted Cox proportional hazards models to assess the dependency of hesitation time on predictor variables, using the *survival* package (Therneau 2015) in R (R Core Team 2017). Survival analysis models the time (i.e., survival time) it takes for a given event to occur and the factors that affect it (Moore 2016). For the group testing, we modeled hesitation time as a function of pattern richness exposure (H, M, or L), feeder type (aposematic or brown), and their interaction. For the individual testing, we modeled hesitation time as a function of pattern richness exposure (high or low), feeder type (aposematic or brown), their interaction, and the post-mortem morphological variables (tarsus length, body mass, testis length asymmetry, spleen mass and body condition). We used stepwise model selection based on the Akaike Information Criterion (AIC) to assess predictor importance. For each model we checked (1) the proportional hazards assumption by examination of scaled Schoenfeld residuals using the *cox.zph* function of package *survival*; (2) the nonlinearity assumption using Martingale residuals; and (3) the presence of influential observations using case deletion residuals (dfbetas) (Moore 2016). In all cases, we found no violation of assumptions nor any influential observation. When needed, we performed pairwise comparisons of treatments using the log-rank test as implemented by the

function *pairwise_survdiff* in package *survminer* (Kassambara et al. 2018), adjusting *P*-values with the Benjamini-Hochberg's method (Benjamini and Yosef 1995).

Results

Group exposure

Across the first five exposure sessions, mean consumption of feed from the aposematic feeders was lower (H: 1.40 ± 1.44 g; M: 1.99 ± 2.68 g; L: 1.85 ± 3.13 g) than from the brown feeders (H: 15.27 ± 8.42 g; M: 18.60 ± 8.36 g; L: 14.20 ± 7.43 g). This pattern was found for all three cages in all exposure sessions (Fig. 23). The last session (#6) demonstrated that the chicks were avoiding the aposematic patterns: brown feeders were nearly empty, whereas aposematic feeders were largely avoided (average of food left inside the feeders during the #6 session H: aposematic: 77.4%, brown: 17.10%; M: aposematic: 85.67%, brown: 8.06%; L: aposematic: 84.11%, brown: 27.22%).

During the testing, we recorded a wide range of attack latencies from 1 s to 228 s. In 16 trials chicks never attacked the feeder, and thus their trials were terminated at 5 min, and these data were right censored in our survival analysis. The final model derived from analysis of group exposure contained only one predictor: pattern richness exposure ($r^2 = 0.074$, Wald test = 8.48, df = 2, $P = 0.014$). Chicks exposed to low pattern richness had 0.47 times less risk of pecking the novel aposematic feeder than chicks in the high pattern richness treatment (log hazard ratio for low pattern richness exposure = -0.755, $Z = -2.848$, $P = 0.004$, Fig. 24 and Fig 25). The birds in the medium richness treatment showed only a marginal difference from the high pattern richness group in the risk of pecking the feeder (log hazard ratio for medium pattern richness exposure = -

0.47, Z = -1.898, P = 0.058, Fig. 24 and Fig 25). Hesitation time differed only between low and high pattern richness, based on pairwise comparisons (Benjamin-Hochberg adjustment; high–low: P = 0.001; high-medium: P = 0.081; low-medium: P = 0.293)

Individual exposure

When presented individually, feeder pattern (brown or aposematic-imperfect) was not a part of our final model, showing that chicks had no preference for feeder type. The final model contained only three predictors: pattern richness exposure (high vs low), spleen mass and directional testes asymmetry (r^2 = 0.445, Wald test = 13.3, df = 3, P = 0.004). Chicks exposed to low pattern richness were 3.63 times more likely to peck a feeder, regardless of color/pattern, than those exposed to high pattern richness (log hazard ratio for low pattern richness exposure = 1.291, Z = 2.552, P = 0.011, Fig. 26 and Fig 27). Chicks with higher spleen mass and higher testes asymmetry also had a much higher probability of pecking a feeder than less developed chicks (log hazard ratio for spleen mass = 7.771, Z = 2.304, P = 0.021; log hazard ratio for testes asymmetry = 3.916, Z = 2.437, P = 0.015, Fig. 26 and Fig 28). Body condition, body mass and tarsus length did not contribute to our final model of factors influencing predation.

Discussion

The evolution of novel aposematic patterns in nature is a theme of intense debate among evolutionary biologists (Mappes and Alatalo 1997; Lindström et al. 1999; Lawrence et al. 2019). If a novel aposematic pattern is not protected by previous predator education from similar warning patterns already extant in the region, the attention drawn to a bold, new pattern will subject it to a high degree of predator attack. Consequently, the intense predation on new patterns can slow or even inhibit their evolution (Turner 1988), leaving scientists puzzled as to the selective mechanisms by which new patterns can evolve. Our initial expectation was that greater pattern diversity exposure would lead to greater hesitation time to attack imperfect phenotypes, as birds are expected to transfer knowledge of diverse visual cues to new prey (Svádová et al. 2009). Instead we found that the effect of multiple aposematic models is dependent on the opportunity for social learning. Chicks exposed as a group to several patterns were less cautious than chickens exposed to one aposematic pattern. In contrast, when exposed individually, chickens are more cautious with a novel pattern when their previous aversive exposure involved multiple patterns.

Group exposure

Despite the low attack rate (food consumption) on aposematic feeders during the exposure phase, we found no evidence of discrimination between novel aposematic and brown prey during testing; whether previously exposed to low, medium or high color pattern training. This outcome suggests that novel imperfect mimics will not benefit from previous predator education on how to discriminate between harmless and defended prey. Instead all prey under

low pattern richness benefit because socially-trained predators are hesitant when facing any type of prey. In contrast, chicks exposed as a group to more than one aposematic pattern were less cautious and, thus, all prey patterns would be equally subjected to attack. This latter outcome has several possible causes. Young chickens may not be up to the cognitive task of integrating the many aposematic pattern features found in pattern-rich environments. Similarly, because chicks needed to navigate both social interactions and multiple patterns during training sessions, they were distracted such that they were not conditioned to aposematic cues. Alternatively, chicks may have indeed learned to avoid specific aposematic phenotypes, but also eventually learned from sampling so many feeders that there was little consequence of testing new prey.

Our results suggest that social predators can encourage the evolution of imperfect mimicry in areas of low model pattern diversity since imperfect mimics receive a crucial time to escape a predation attempt. However, once multiple color patterns are established in a particular area, the information overload received by social predators can hinder the evolution of imperfect mimics since predators promptly attack their prey.

Individual exposure

As with the socially exposed subjects, individually exposed subjects did not discriminate against the novel aposematic feeder. However, individuals exposed to multiple patterns had a higher hesitation to feed from either feeder during their test trials. In pattern-diverse areas, the uncertainty about the dangerousness of prey can make solitary predators more reluctant to try new food items presented to them. If so, in areas with many models and different aposematic patterns imperfect mimics are better protected because non-social predators will not immediately attack their prey, creating opportunity for escape.

Our individual subjects varied greatly in their latency to attack suggesting that motivational factors other than those caused by the treatments were at play. Difference in hunger is the most obvious explanation for this variation, but this seems unlikely given that chicks were fed *ad libitum* in their rearing brooder and each had equivalent opportunities to feed during the exposure events. Importantly, chick body condition did not explain latency to attack. Our results did, however, confirm our suspicion that the nutritional demands of alternative individual growth trajectories would contribute to explaining the variation in feeding hesitation by chicks. Although immune and reproductive development differs the most between strains of chickens, intra-strain differences among individuals in organ size or activity occur and can be found as early as day one (de Reviers and Williams 1984; Apanius 1998). Rapid growth of the spleen and development of adult-like asymmetry in the testes were associated with greater urgency to begin feeding in our study, independent of body condition. This result suggests that individual organ growth trajectories may create feeding motivations that are not reflected by external morphological measurements, but affect the opportunity for the evolution of novel aposematic prey types. Individual variation in the willingness to attack, also documented in other species like the quail *Coturnix japonica* (Marples and Brakefield 1995), can affect the evolution of new aposematic prey (Speed 2000). When individuals with rapid development are more prone to attack aposematic prey, this can enhance the risk of extinction of new conspicuous prey. On the other hand, slow growing individuals could initially ease the selection on new aposematic prey.

Although we conclude that the individual variation in attack latency results from the motivation to feed imposed by the energetic demands of different growth trajectories, growth and learning are not independent; feeding successfully results both in an increase in body size and reinforces learning about how to feed effectively (English et al. 2016). Individuals with bold

personalities often have a higher food intake rate (Biro and Stamps 2008; Kurvers et al. 2010). Thus early differences in individual personality traits, such as boldness and the propensity to quickly explore space, may allow some chicks to begin feeding sooner and develop faster relative to individuals that are shy and slow to explore. Consequently the weaker aversion to the novel imperfect mimic by our more developed subjects may be the direct and independent result of the bold personality itself, rather than simply a product of the growth trajectory initiated by their precocity at feeding. We did not measure personality traits in our subjects, but in another bird, the great tit (*Parus major*), fast explorers showed shorter attack latency for an aposematic insect than slow individuals (Exnerová et al. 2010), a result similar to our chicks with advanced organ development. Nevertheless the physiological demands of a bold personality may still be the driving force for the eagerness of such chicks to peck at aposematic prey. Bold individuals often have a higher metabolic rate than shy ones (Biro and Stamps 2008), are at greater risk of starvation (Lichtenstein et al. 2017), and thus may need to be less catholic in their feeding, showing greater resistance to learning to avoid noxious prey (Exnerová et al. 2010). Clearly the experimental disentanglement of predator personality, early development and motivation to feed discriminately is both relevant to our understanding of the evolution of mimicry and a complex challenge worthy of further research effort.

We demonstrated that color pattern diversity and social transmission of information might have an influence on the evolution of imperfect mimicry and mimicry in general, which corroborates mathematical models (Thorogood et al. 2017). However, we are aware that the evolution of imperfect mimicry may be facilitated by other extrinsic factors like niche preferences, predators with different visual systems (i.e., mammals vs. birds), and biogeographic history in areas with elevated model color diversity, as is the case for *Micrurus* in western

Amazonia (Bosque et al. 2016). There are few cases where predation of coral snakes has been observed in nature (DuVal et al. 2006) but it has been reported that in one specific site at least 90 species are potential predators of coral snakes (França 2008). Predators of coral snakes have sufficient opportunity for social learning, given the number of species in a particular area (interspecific leaning) and the various degree of sociality of each species, ranging from less social species (red legged seriema *Cariama cristata*), to highly social species (greater ani, *Crotophaga major*).

Interestingly, this empirical demonstration of the effects of model diversity and social interaction lends some insight into how mimicry systems arise at all. In low model-diversity systems, social predators facilitate the initial evolution of mimics while non-social predators are an opposing force. After a single color pattern model is established in a particular area, mediated by selection of social predators, the number of models/color patterns can further increase by selection of non-social predators (Fig 29). In this sense, in areas with high model color diversity, non-social predators will favor recently evolved mimics. Personal experience is probably more common than eavesdropped information, which might be another factor to explain why we find more mimics of coral snakes in areas of high color diversity of models (Davis Rabosky et al. 2016b).

Conclusion

Newly evolved patterns can be favored by social learning in areas of low pattern diversity and disfavored by individual learning. These findings can shed light on the evolution of imperfect mimicry (Kikuchi and Pfennig 2013), which were not previously explored. Our findings indicate that this phenomenon can be favored in areas of low and high model diversity by two distinct mechanisms. We suggest that imperfect mimicry can be favored in areas of high model diversity by reduced predation pressure as a result of attack hesitation by non-social predators. In areas of low pattern diversity, imperfect mimics can be better protected because social-predators are not so cognitively overloaded that they become less prone to attack prey. Furthermore, individual growth trajectory of predators may influence how they interact with their prey, making fast-growing individuals less hesitant to attack. Our understanding of how information overload, growth trajectory and the interrelationship between social and non-social predators on the evolution of imperfect mimicry will surely benefit from further consideration.

CHAPTER V:

COMPARATIVE PHYLOGEOGRAPHY OF *MICRURUS LEMNISCATUS* AND *M. SURINAMENSIS* USING GENOMIC DATA

Introduction

The Neotropical region is widely known to be the most biodiverse in the world (Zizka 2019). Yet despite centuries of biological investigation in the region our understanding the mechanisms that generate this biodiversity is still the subject of intense debate (Wiens et al. 2011; Rangel et al. 2018). While both climatic and tectonic events have been proposed to act as diversification mechanisms (Rull 2008; Wesselingh et al. 2011), the relative contribution of such events may vary greatly among regions and taxa (Hoorn and Wesselingh 2010; Hoorn et al. 2010). This variation in the response to biogeographic episodes can occur even among closely related species (Michaux et al. 2005), and may be related to specific life-history traits of these organisms.

Coral snakes of the genus *Micrurus* are distributed from southern North America to southern South America, with approximately 81 recognized species, and more than 100 described taxa (Uetz and Hošek 2019). Despite medical importance (venom research and snakebites) and intense evolutionary research interest (i.e., the evolution of mimicry), our understanding of the evolutionary history of the *Micrurus* genus is scant. There has yet to be a comprehensive phylogenetic study of the genus (Silva Jr. and Sites 2001; Davis Rabosky et al. 2016b; Lomonte et al. 2016). The pioneering phylogenetic study of coral snakes was performed

by Roze (1987) based on immunological, paleontological and meristic data. The first phylogenetic analysis of the genus *Micrurus*, that used molecular data dealt with only 11 species of South American coral snakes. That study employed allozyme and mitochondrial DNA (Slowinski 1995) to show that *Micrurus surinamensis* is sister to all other *Micrurus* species, and suggested that the widespread *M. lemniscatus* is polyphyletic. More recently, large phylogenies trying to solve broad scale relationships among snakes were published confirming the monophyly of the New World coral snakes (Zaher et al. 2009; Zaher et al. 2016), and presented some hypotheses about the relationships within *Micrurus* (Pyron et al. 2011) but with weak support. Pertaining 761 colubroid species among 4161 Squamata taxa Pyron et al., (2013) started to clarify the history of the genus *Micrurus* showing the separation of a North American clade + Monadal species as a sister group of the other South American species. Using Elapidae snakes Lee et. al, (2016), confirmed that *Micrurus* is sister to the genus *Micruroides* while also elucidating some relationships among sampled species of *Micrurus* . Zaher et. al, 2016 reaffirmed the Asiatic origin of coral snakes, with a divergence time of 27 million years (late Oligocene) between Asian and American coral snakes, with the origin and diversification of *Micrurus* occurring around 18 million years (early Miocene).

Past phylogenetic studies have been based on immunological, paleontological, meristic, allozyme, and mtDNA sampling of a small fraction of *Micrurus* species diversity. However, such studies focus on the interrelationships among taxa, not the phylogeographic history within them. Despite the impressive increase in the number of phylogeographic studies of Neotropical species, and the growing number of large scale phylogenetic studies of snakes globally, only one phylogeographic study of a species of the genus *Micrurus* has been published (Jowers et al.

2019). This work showed the patterns of colonization of Trinidad, establishing a Late Pleistocene vicariance of *M. diutius* from the mainland.

Within this genus, *Micrurus surinamensis* and *M. lemniscatus* are excellent subjects for a comparative phylogeographic study due to their intraspecific morphological variation and extensive geographic distribution across South America. The morphological variation found in these two species has fueled, in the last 20 years, an intense taxonomic debate that resulted in the formal recognition of several subspecies, some of them later elevated to species level (Silva Jr. and Sites 1999; Strarace 2013; Pires et al. 2014b; Feitosa et al. 2015; Silva Jr. et al. 2016; Jowers et al. 2019).

Micrurus lemniscatus is considered to be a species complex (Silva Jr. and Sites 1999), containing three morphologically distinguishable populations (Fig 30) that are recognized at as subspecies (*M. l. lemniscatus*, *M. l. carvalhoi*, and *M. l diutius*). *M. potyguara*, previously described as *M. lemniscatius,*, was recently described and elevated to species level (Pires et al. 2014a). Some authors considered consider *M. l. diutius* to be a species (Strarace 2013; Jowers et al. 2019) but due to volatility of the taxonomic rearrangements the debate is still open. The *M. lemniscatus* complex is widely distributed across South America, occurring in open and forested habitats (Terribile et al. 2018) and are a mainly terrestrial but can make some incursions in the aquatic environment (de Almeida et al. 2016). Some previously recognized subspecies (e.g., *M. l. frontifasciatus*) is currently considered as invalid. The ongoing taxonomic changes, indicates that further studies are necessary to evaluate the evolutionary status of the *M. lemniscatus* complex.

Micrurus surinamensis is one of the largest species of coral snakes (Fig. 30), and occurs throughout northern South America, with morphologically distinct populations (Schmidt 1952). Notably, this semi-aquatic species feeds primarily on fishes, having several anatomical

specializations related to the freshwater environment (Passos and Fernandes 2005; Olamendi-Portugal et al. 2008; Morais et al. 2016). In a revision of this species, morphological characters were used to split this species (with two subspecies) into two taxa: *M. surinamensis* (occurring in the Amazonas drainage) and *M. nattereri* (occurring in the Orinoco river system: (Schmidt 1952; Passos and Fernandes 2005).

The large distribution overlap between *M. surinamensis* and the *M. lemniscatus* complex, the morphological variation found among populations, and the recent taxonomic changes, provides a particular opportunity to investigate the biogeographic mechanisms that generate such high levels of variation in two closely related Neotropical species. Moreover, their ecological differences make them an ideal pair within which to explore factors influencing diversification. *Micrurus lemniscatus* is a typical coral snake with semi-fossorial habits, whereas *M. surinamensis* is primarily found in freshwater habitats. For these reasons, we hypothesize that the evolutionary history, and thus genetic structure, of *M. lemniscatus* were mainly influenced by South American neotectonic events (Hoorn et al. 2010) whereas the rivers and drainage evolution in the Amazon region will more strongly influence genetic structure within *M. surinamensis* (Hoorn et al. 2017). We anticipate that the genetic structure found in both species will correspond with documented patterns of morphological variation, which may reflect deeper evolutionary differentiation than previously recognized.

Herein, we present the first comprehensive comparative phylogeographic study of two coral snake species complexes (*Micrurus surinamensis* and *M. lemniscatus*) using genomic-level DNA sequence and morphological data. We explore the validity of current described taxonomic units, and test the role of South American biogeographic events and river drainages in structuring

populations of these species and evaluate whether morphological structure is coincident with genetic structure.

Materials and Methods

Sampling and DNA extraction

Tissue samples (liver, muscle, scale or blood) were obtained from multiple herpetological collections (see acknowledgments) covering most of the geographic range of both *Micrurus lemniscatus* and *M. surinamensis*. Tissue samples were preserved in 95% ethanol and kept at -80° C prior to extraction. In total we obtained 54 tissue samples of *M. lemniscatus*, and 41 samples of *M. surinamensis* spanning most of the known distribution of each species. We used two samples of *M. hemprichii* as outgroups for the *M. lemniscatus* complex and one sample *M. hemprichii* and another sample of *M. l lemniscatus* as outgroups of *M. surinamensis.*

DNA was extracted using the salt-extraction protocol, which has advantages to other methods of genomic DNA extraction in terms of efficiency (Aljanabi and Martinez 1997).

Library preparation

We used a Next Generation Sequencing method based on double-digest RADseq that has several advantages over previous methodologies, in particular lower quantities of DNA starting material, multiple enzyme compatibility of the adapters, lower cost and the capacity of obtaining thousands of loci (Peterson et al. 2012). In order to minimize the presence of adapter-dimmers we used a triple-enzyme RADseq library (Bayona-Vásquez et al. 2019). Initially, we digested 100ng of genomic DNA using the restriction enzymes XbaI, EcoRI and NheI. The enzymes were

selected based on *in silico* digestion of the python genome that resulted in a manageable number of target loci. After digestion, we ligated double-stranded adapters to each end of target fragments by running two cycles of 22°C for 20 minutes and 37 °C for 10 minutes followed by one cycle of 80°C for 20 min to cease enzymatic activity. Ligated fragments were cleaned using Sera-Mag speedbeads and a 96-well magnetic plate, washed twice with ethanol and resuspended in IDTE buffer. DNA fragments were amplified by polymerase chain reaction (PCR), using a unique combination of barcoded iTru5 and iTru7 primers per sample. PCR products were then pooled, followed by a cleaning and concentration step with MinElute™ PCR purification kit (QIAGEN). We size selected the amplified DNA fragments ranging from 390 to 460 base pairs, using Pippin Prep™ (SAGE science) with 1.5% agarose gel cassettes. Quantification of reduced representation DNA libraries was done with quantitative PCR (qPCR) using KAPA SYBR Fast qPCR kit (KAPABIOSYSTEMS). Sequencing was done at the National Center for Natural Products Research at the University of Mississippi on a NextSeq® 500/550 High Output Kit v2 flow cell with 75 cycles (Illumina).

Bioinformatics

1- Sequence processing

All sequence reads were processed using the Mississippi Center of Supercomputing research. Initially we downloaded raw data from the Illumina platform using the BaseSpaceDownloader_nothumb.py tool. Demultiplexing and conversion to fastq format was performed using the Illumina software bcl2fastq version 2.20. These Illumina tools and software can be found at https://www.illumina.com/index-d.html. Reads were trimmed to remove

barcodes and adapters and to limit our fragments to 62 base pairs using the fastx_trimmer toolkit (http://hannonlab.cshl.edu/fastx_toolkit/commandline.html).

2- Data set assembly

We assemble and analyzed our dataset using ipyrad v 0.7.3 (https://github.com/dereneaton/ipyrad). We used denovo assembly, with a cluster threshold of 0.85 and maximum barcode mismatch of 2. A locus was retained only when it was recovered from at least 50% of individuals. All the other parameters were kept at default values. For each species we ran ipyrad twice, with and without outgroups to perform phylogenetic and population analysis, respectively.

Data analyses

1- Genetic structure and admixture

To evaluate the extent of admixture between populations we performed a variational Bayesian inference using the software fastStrucrure (Raj et al. 2014) using the unlinked SNPs output from ipyrad. For the *M. lemniscatus* complex, we ran fastStrucrure using the simple prior with k ranging from 1 to 10 and selected the best range of ks using the utility tool chooseK.py (https://github.com/rajanil/fastStructure). Since our phylogenies of *M. surinamensis* pointed to weak genetic structure in our data (see Results), we also ran fastStructure using the logistic prior for each k selected with the simple prior runs. The logistic prior is more powerful for detecting weak population structure or when population structure is difficult to determine. The best k was

the one with the highest maximum-likelihood value among all the logistic prior runs. Admixture graphs were created using the R package *pophelper* (Francis 2017).

To investigate the phylogenetic relationships among individuals of each species we used the software RAxML version 8 (Stamatakis 2014) with a conditional likelihood method that minimizes overestimation of the branch length parameters by the exclusive use of variable sites (Lewis 2001). All the RAxML input files were preprocessed using the R package *phrynomics* to remove invariant and non-binary sites (Leaché et al. 2015). RAxML runs were performed using the k80 model of substitution with optimization of substitution and site-specific evolutionary rates (parameter -m ASC_GTRCAT). Additionally, we performed maximum likelihood analysis using the software IQ-TREE (Nguyen et al. 2014), with all loci (variant and invariant sites) concatenated into a supermatrix.

In order to verify that we had correct taxonomic identification of our samples we ran a RAxML analysis using RADseq data utilizing 40% of all *Micrurus* species with a total of 213 samples. This phylogeny comprise a separate study focusing on interspecific relationships within the genus (results not presented here). Curiously, *Micrurus filiformis* samples nested within *M. lemniscatus*, and for that reason we included *M. filiformis* samples in all of our *M. lemniscatus* analyses.

2- Divergence time

To estimate divergence times between *Micrurus surinamensis, M. hemprichii and M. lemniscatus* complex we used the software SNAPP(Bryant et al. 2012) which uses a Markov Chain Monte Carlo sampler with single nucleotide polymorphism data. We initially ran iPyrad

using similar procedures described above, except that we selected a subset of samples from each major clade within each species present in our RAxML analysis, including the outgroup *Micruroides euryxanthus*. The reduced dataset was necessary in order to obtain a tractable computation time. The constrains used in our divergence analysis were based on the results produced by Zheng et. al (Zheng and Wiens 2016). For dating the most recent common ancestor of the genus *Micruroides* and genus *Micrurus* we use a lognormal prior with 33.74 Mya of mean and sigma (standard deviation) of 0.15 Mya to allow a higher sampling probability around this value (quantiles: 5% =26.1 Ma and 95%=42.7 Ma) while avoiding hard boundaries. For the crown group of the *M. surinamensis, M.hemprichii* and *M. lemniscatus* complex we used a lognormal prior with 11.75 Mya of mean and sigma of 0.2 Ma to allow a higher sampling probability around this value (quantiles: 5% =8.29 Ma and 95%=16 Ma) while avoiding hard boundaries. And finally, for dating the most recent common ancestor of *M. hemprichii* and the *M. lemniscatus* complex we used a lognormal prior with 10.29 Mya of mean and sigma of 0.2 Ma to allow a higher sampling probability around this value (quantiles: 5% =7.26 Ma and 95%=14 Ma) while avoiding hard boundaries.

3- Niche modeling

We generated maps of potential habitat suitability using bioclimatic variables and altitude of both *Micrurus lemniscatus* and *M. surinamensis* with the software Maxent version 3.4.1 (Phillips et al. 2006). Initially we downloaded present bioclimatic variables Bio1-Bio19 from the website: https://www.worldclim.org using a resolution of 2.5 arc-minutes. After this procedure, we clipped our bioclimatic rasters to a rectangle corresponding to each species' latitudinal and

longitudinal limits (*M. lemniscatus* -82 W, -34 E, -30 S, 11 N and *M. surinamensis* -82 W, -34 E, -20 S, 10 N). We excluded highly correlated (correlation ≥ 0.7) bioclimatic variables using variance inflation factor, a stepwise technique used to deal with multicollinearity (Naimi et al. 2014). After selecting the subset of variables with reduced correlation we ran Maxent using distribution data obtained by confirmed identifications collected while visiting major herpetological museums in Brazil, complemented with data obtained from http://vertnet.org. In total we obtained 678 samples points for the *M. lemniscatus* complex and 246 sample points for *M. surinamensis*. We randomly choose 25% of the sample points to test the model accuracy and verified the performance of the predictions by checking the area under the curve (AUC). We performed a jackknife test while running Maxent to check which environmental variable was the most important to the predictive model of each species. We projected our set of trained bioclimatic variables on last glacial maximum (~21,000 years) bioclimatic data in order to infer the impact of past climatic fluctuation on the distribution of both species.

4 -Morphology and color quantification

We took high quality digital photographs from the dorsum of *Micrurus lemniscatus* and *M. surinamensis* specimens deposited in some of the largest Brazilian herpetological collections (CEPB, CHUFPB, CHUNB, INPA, LARUFRN, MHNCI, MNRJ, MPEG, MZUFBA, MZUSP and UFMT; Fig. 2). After excluding damaged snakes, we retained 424 individuals of *M. lemniscatus* and 185 individuals of *M. surinamensis* in our analyses. From each image we recorded the total length (from the tip of the snout to the end of the tail) and number of black, red and white bands. We also selected one triad at midbody to measure the length of the first,

second, and third black bands; length of the first and second white bands and the length of the red band anterior to the selected triad. The length of the white bands as well as the first and third black bands were nearly identical, so we calculated averages of the two for further analyses. From these measurements, we selected 5 variables to be used in further analyses: number of red bands, proportion of red bands (width of red band/total length), proportion of external black bands ((width of black band 1 + width of black band 3/total length)/2), proportion of white bands ((width of white band 1 + width of white band 2/total length)/2), and proportion of internal black bands (width of black band 2/total length). All images were analyzed using the software ImageJ version 2.0.0-rc-69/1.52i. To calculate morphological variation along the geographic distribution of each species, we used a multivariate spatial analysis (spatial principal component analysis – sPCA), with the function *multispati* from the package *adespatial* (Dray et al. 2018), which maximizes the product of variance and spatial autocorrelation. In order to produce maps of morphological variation, we created a grid with cells of one degree latitude x longitude (ca. 111 km^2) for each species and extracted the lagged scores from each cell to generate a matrix where the geographic grid cells are the rows and the columns are the species. If multiple samples of the same species were found in the same cell, we averaged their lagged score to obtain a single value for that particular cell.

Results

After filtering, we obtained an average of 4 million reads from each sample of the *M. lemniscatus* complex, which resulted in 24,000 (outgroups included) and 26,000 (outgroups excluded) loci per sample, on average. For *M. surinamensis* we obtained an average of 1.7 million reads per sample which resulted in 15,000 (outgroups included) and 16,000 (outgroups excluded) loci per sample, on average.

The maximum likelihood trees recovered for the *M. lemniscatus* complex using both RAxML (Fig. 31) and IQ-TREE (Fig. 32) included three major clades that appear congruent with three recognized sub-species: *M. lemniscatus diutius*, *M. lemniscatus lemniscatus* and *M. lemniscatus carvalhoi*. The three groups are spatially structured with one clade (attributed herein to *M. lemniscatus diutius*) occurring in the Amazon, another clade (attributed herein to *M. lemniscatus lemniscatus*) occurring in the Cerrado and Amazon, and a third clade (attributed herein to *M. lemniscatus carvalhoi*) occurring in the Cerrado and Atlantic Forest (Fig 33 and Fig. 34). In both phylogenetic analyses *M. filiformis* is recovered as the sister clade of *M. lemniscatus lemniscatus*, however, fastStructure analysis suggests that *M. filiformis* might have been originated from hybridization among the three subspecies of *M. lemniscatus* (Fig. 33 and Fig 34). The best k selected by fastStructure was 3, which corresponds to the same major clades that define the subspecies (Fig. 34). Also of note, three sampled paratypes of *M. potyguara,* were recovered nested within *M. l. carvalhoi* (see taxonomic remarks at the end of this chapter).

The phylogenetic relationships recovered from maximum likelihood analysis of *Micrurus surinamensis* showed much shallower structure, with two major clades: one west of Araguaia/Tocantins rivers, distributed throughout the Amazon basin, and another clade east of Araguaia/Tocantins rivers occurring in areas of influence of the Cerrado and Caatinga biomes.

These two clades were recovered by RAxML, IQtree and fastStrucutre analyses (Fig. 35 and Fig. 36). Both eastern and western clades have a contact zone south of the lower Amazon river (Fig 37 sites k,l,m and Fig 38).

The coalescent tree obtained with SNAPP showed some topological incongruences with RAxML and IQtree trees. The coalescent tree placed *M. carvalhoi* as the sister taxon of the other species of the *M. lemniscatus* complex but with a low posterior probability (i.e., PP=0.54; Fig. 39). Our estimate of the age of the most recent common ancestor of *Micruroides* and *Micrurus* was ~34.83 Mya (95% Highest Posterior Densisity - HPD 26.22-42.37 Mya). The divergence time of *M. surinamensis* was around 10.37 Mya (95% HPD 7.99-12.86 Mya). The most recent common ancestor of *M. hemprichii* and the *M. lemniscatus* is estimated to occur around 9.38 Mya (95% HPD 7.26-11.54 Mya). According to SNAPP estimates the most recent common ancestor of the *M. lemniscatus* occurred around 6.97 Mya (95% HPD 5.06-9.23 Mya). *M. l. diutius* separated from *M. l. lemniscatus* + *M. filiformis* around 5.59 Mya (95% HPD 3.68-7.48 Mya), and *M. filiformis* which nested within the *M. lemniscatus* complex, diverged from *M. l. lemniscatus* approximately 3.91 Mya (95% HPD 2.14-5.91 Mya).

For the *M. lemniscatus* complex, niche modeling analyses were conducted using the following bioclimatic layers after removal of autocorrelated layers: "bio2", "bio3", "bio8", "bio15", "bio18" and "bio19". We obtained a good accuracy (AUC training = 0.80, AUC test = 0.73). The most important variable for modeling the potential distribution of the *M. lemniscatus* complex was “bio2” which is the mean Diurnal Range. (Mean of monthly, max temp - min temp). Three discontinuous areas of high niche suitability were predicted for the *M. lemniscatus* complex during the LGM. One area is situated in the border between Venezuela and Colombia, a second one at the northern part of Brazil bordering Suriname, Guyana and Venezuela and the

third situated at Northeast and Central Brazil (Fig. 40, left panel). As temperature got warmer, suitable areas for *M. lemniscatus* expanded, increasing the connections between these three areas (Fig. 40, right panel).

The variables retained, after removal of autocorrelated layers, for our niche modeling analysis of *M. surinamensis* model were: "bio2", "bio3", "bio5", "bio13", "bio15", "bio18" and "bio19". We obtained a good accuracy with the niche modeling (AUC training = 0.83, AUC test = 0.77). The most important variable for modeling the potential distribution of *M. surinamensis* was “Bio13” which is the precipitation of the wettest month. During the LGM, a major gap in niche suitability occurred for *M. surinamensis* in the middle of the Amazon basin (Fig. 41, left panel) separating two highly suitable regions. One area is situated at the northern edge of South America, extending from longitude -45º to -55º and another area at the border between Bolivia and Brazil. The present day modeling indicated that the gap in niche suitability was reduced and predicted for most of the Amazon basin (Fig 41, right panel)

Morphologically, both *M. lemniscatus* complex and *M. surinamensis* can be separated in distinct groups that are geographically clustered. The first two spatial principal components (sPCA1 and sPCA2) capture most of the variation for both groups (Fig. 42, and 43). The first sPCA1 separate *M. lemniscatus* complex in three groups: the first group occurring in the tropical forests of the Amazon basin, marked by an intermediate number of bands, with an intermediate length of white and red bands (compared to the other groups) (Fig 44 and Table 7). A second group occured in central Brazil, inhabiting tropical savannahs and grasslands, extending from -3° to 25° of latitude, marked by the presence of a high number of bands with short red and white bands (Fig 44 and Table 7). Finally, a third group included populations in the northeast Brazil, with fewer bands and the largest red and white band lengths (Fig 44 and Table 7). The sPCA2

separated *M. lemniscatus* in two groups: southeast Brazil with small internal and external black bands and northwest Brazil with large internal and external black bands (Fig 44 and Table 7).

Like the *Micrurus lemniscatus* complex, geographically clustered morphological groups were identified in *M. surinamensis*. sPCA1 divides *M. surinamensis* in two groups: one distributed at the western part of the Amazon floodplain, extending at the areas of the Guaporé/Mamoré influence, characterized by larger white bands (Fig 45 and Table 8) and a second group, under the influence of Tocantins/Araguaia rivers, with smaller white bands (Fig 45 and Table 8). sPCA2 seems to separate *M. surinamensis* in a West-East gradient of number of bands, with specimens in the East possessing a large number of bands specially between Xingu and Tocantins/Araguaia rivers (Fig 45 and Table 8).

Discussion

Micrurus lemniscatus and *M. surinamensis* are two widespread clades occurring throughout South America. Despite being closely related phylogenetically, the two clades show unique patterns of evolution. *M. lemniscatus* is clearly a species complex with *M. l. diutius* positioned as a sister clade of ((*M. filiformes* + *M. l. carvalhoi*) + *M. l. lemniscatus*), while *M. surinamensis* is clearly a single species with a more recent intraspecific differentiation and/or high levels of gene flow.

Micrurus surinamensis is the only species of the genus *Micrurus* that is adapted to an aquatic lifestyle (Passos and Fernandes 2005; Olamendi-Portugal et al. 2008; Morais et al. 2016). The importance of the amount of water present in the environment for the distribution of *M. surinmanesis* is demonstrated by our Maxent analysis. Previous estimates have shown that the split between *M. surinamensis* and its sister clade, *M. lemniscatus* + *M. hemprichii* occurred

roughly 11.75 million years ago (Zheng and Wiens 2016), during the middle Miocene. This previous finding is in accordance with our estimative recovered by our divergence time analysis. During the middle Miocene, the Pebas mega-wetland in western Amazonia began to develop. This wetland was comprised of many shallow lakes that resulted in the fragmentation of the rainforest (Hoorn et al. 2010). This Miocene fragmentation of the landscape coincided with an increase in diversity in several clades, including aquatic species (Hoorn et al. 2010). Selection to live in a flooded landscape during the middle Miocene, combined with fragmentation of the landscape, were probably key factors in the origin of *M. surinamensis*. The Andes were continuously uplifted during the late Miocene by tectonic forces, changing the Pebas system into a transcontinental river (*Acre* system) (Hoorn et al. 2010). The flowing waters towards the Amazon mouth during the latest Miocene likely helped *M. surinamensis* to colonize the eastern part of the Amazon. West to East colonization of the Amazon basin might explain the morphological clinal geographic structure that we found with individuals with wider white bands in the West and smaller bands in the East (Fig. 45). During the beginning of the last glacial cycles, many parts of South America experienced drier and cold conditions, but the core of Amazonia remained buffered from this process, except at the peripheral parts of the Amazonia and parts of the East lowland (Colinvaux et al. 2000). We found that suitable areas for *M. surinamensis* during the LGM were not at the core of the Amazon, which would be expected for a species adapted to forested environments. Instead, our results point to two highly suitable areas for *M. surinamensis* at the periphery of Amazonia, one at the Amazon mouth and other to the south, near what is currently the Pantanal (Fig. 41). The north-south division during the LGM might have contributed to the current population structure found as it is consistent with the geographic distribution of the recovered clades (Fig. 37 and Fig 38). During the Pliocene, *M.*

surinamensis probably colonized a large part of the Amazon basin, whereas during the LGM north and south populations became isolated, and further differentiated near the Tocantins/Araguaia rivers. Individuals from the Tocantins/Araguaia area are morphologically different (Nelson Jorge da Silva personal communication, Fig 37 and Fig 45), being usually smaller and having an increased number of bands (Fig 45). The flow of the Tocantins-Araguaia rivers from South to North, as opposed to a flow from West to East like the Amazon river, seems to be a strong barrier isolating populations from the Tocantins/Araguaia and populations of the Amazon. The direction of the Araguaia River implies that most of the admixture between North and South populations would occur near to the Amazon mouth, a pattern confirmed by our FastStrucure analysis, which shows that admixture between this southeastern and central clade decreases as one moves upstream along the Amazon River (Fig 38).

While *M. surinamensis* has a recent diversification history and an apparent rapid capacity for colonizing new areas in an aquatic matrix, species of the *M. lemniscatus* complex seems to have a deeper history of differentiation influenced by more intricate biogeographic process. The most recent common ancestor of the *M. lemniscatus* complex and *M.hemprichii* lived around 10.29 Mya according to Zheng et. al,(Zheng and Wiens) and 9.38 Mya according to our analysis, during the late Miocene and the formation of the Acre System. The formation of this system probably isolated populations that would later become what we know today as *M. hemprichii* in the north of the Acre system, and a population in the south that would become the *M. lemniscatus* complex. Ancestral populations of the *M. lemniscatus* complex possibly colonized vast areas of the Atlantic forest via the Southeast – Northwest route (SE-NW) that connected these two biomes since the middle and late Miocene (Ledo and Colli 2017). Populations that stayed in the Amazon would later become *M. l. diutius*. Major shifts in the Brazilian shield

during the Pliocene (Colli 2005) would impact the populations dispersed from Amazonia probably separating populations in this area and latter originating *M. l lemniscatus* and *M. l carvalhoi*. The separation between ancestral populations of *M. l lemniscatus, M. l. carvalhoi* and *M. l.* diutius, was enhanced by reduced habitat suitability at SE-NW and NE connections between the Atlantic forest and Amazonia. *M. l. lemniscatus* probably later colonized the Amazon by one of the connections between the Atlantic forest and the Amazonia. This pattern of recolonization is in accordance with our tree topology, and might explain why *M. l. diutius* and *M. l. lemniscatus* are syntopic. The scenario described above for the diversification of the *M. lemniscatus* complex reflects the topology recovered by our maximum likelihood analysis, which uses more loci and has a greater support.

It is worth to noting that both species also have some biogeographic similarities. *M. surinamensis*, *M. l. lemniscatus* and *M. l. diutius* populations seem to be structured by the Amazon river, in a North-South pattern. The Amazon River is a major biogeographic barrier for many organisms (Ribas et al. 2012) but not insurmountable (Nazareno et al. 2017) for populations of the genus *Micrurus*. Additionally, populations of *M. l. lemniscatus* and *M. surinamensis* show a clear genetic and morphological signature of isolation near the Araguaia river, a stable area that is an area of endemicity for other taxa (Brown and Gifford 2002).

Taxonomic remarks

The *Micrurus lemniscatus* complex, has a complicated taxonomic history, with the division into numerous subspecies, and descriptions of several new species in recent years. The lack of clear distinctive diagnostic traits between taxa of the *M. lemniscatus* complex, lead scientist and curators to make (non-intentional) erroneous identification of specimens. This fact is intensified

by the lack of a clear phylogeny of the complex including distribution-wide sampling. Simple and straightforward analyses can illustrate how difficult the identification of specimens might be: the individuals described as *M. potyguara* (Pires et al. 2014b) UFPB 4358/UFPB 4361 (paratypes) and UFPB4359 (holotype) are nested within the putative *M. lemniscatus carvalhoi* clade. Even more surprising is that another paratype UFPB 4355 is nested within the *M. ibiboboca* clade (results not presented here). In a recent study of the *Micrurus lemniscatus* complex (Terribile et al. 2018), we noticed some misidentifications of specimens compared to our phylogeny. For example individuals MPEG22054, MPEG20083, MPEG23544, identified as *M. lemniscatus lemniscatus*, all fall within the putative *Micrurus lemniscatus diutius* clade. It should be noted that we do not address the validity of taxonomic assignations and subspecies included in this study. However, we note that the present work could be used as a guide to reevaluate the morphological characters used during the descriptions, in order to identify good morphological traits (if any exist) to separate the species of the *M. lemniscatus* complex.

In conclusion, our results show that the evolution of *Micrurus* species and populations in South America followed different histories but some similarities were observed. Although we provide robust assignment tests, in an unprecedented scale for the group, we acknowledge that our proposed biogeographic scenarios for the evolution of the *M. surinamensis* and *M. lemniscatus* complexes still deserves further investigation. The Miocene and its geomorphological dynamics were fundamental for the diversification of the *M. surinamensis* and the *M. lemniscatus* complex with profound impacts on the origin of new species and populations subdivisions.

LIST OF REFERENCES

Akcali, C. K. and D. W. Pfennig. 2014. Rapid evolution of mimicry following local model extinction. Biol Letters 10:20140304.

Akcali, C. K. and D. W. Pfennig. 2017. Geographic variation in mimetic precision among different species of coral snake mimics. J. Evol. Biol. 30:1420-1428.

Akima, H. and A. Gebhardt. 2016. akima: Interpolation of Irregularly and Regularly Spaced Data. R package version 0.6-2. https://CRAN.R-project.org/package=akima.

Aljanabi, S. M. and I. Martinez. 1997. Universal and rapid salt-extraction of high quality genomic DNA for PCR-based techniques. Nucleic Acids Res 25:4692-4693.

Allen, W. L., R. Baddeley, N. E. Scott-Samuel, and I. C. Cuthill. 2013. The evolution and function of pattern diversity in snakes. Behav Ecol 24:1237-1250.

Apanius, V. 1998. Ontogeny of Immune Function *in* J. M. Starck , and R. E. Ricklefs eds. Avian Growth and Development. Oxford University Press, New York.

Arbuckle, K. and M. P. Speed. 2015. Antipredator defenses predict diversification rates. Proceedings of the National Academy of Sciences 112:13597-13602.

Aubier, T. G. and T. N. Sherratt. 2015. Diversity in Müllerian mimicry: The optimal predator sampling strategy explains both local and regional polymorphism in prey. Evolution 69:2831-2845.

Balogh, A. C. V., G. Gamberale-Stille, and O. Leimar. 2008. Learning and the mimicry spectrum: from quasi-Bates to super-Muller. Animal Behaviour 76:1591-1599.

Bates, H. W. 1862. Contributions to an insect fauna of the Amazon Valley (Lepidoptera: Heliconidae). Transactions of the Linnean Society of London 23:495-566.

Bayona-Vásquez, N. J., T. C. Glenn, T. J. Kieran, T. W. Pierson, S. L. Hoffberg, P. A. Scott, K. E. Bentley, J. W. Finger, S. Louha, N. Troendle, P. Díaz-Jaimes, R. Mauricio, and B. C. Faircloth. 2019. Adapterama III: Quadruple-indexed, double/triple-enzyme RADseq libraries (2RAD/3RAD). bioRxiv:205799.

Beaulieu, J. M., B. C. O'Meara, and M. J. Donoghue. 2013. Identifying Hidden Rate Changes in the Evolution of a Binary Morphological Character: The Evolution of Plant Habit in Campanulid Angiosperms. Syst Biol 62:725-737.

Benjamini, Y. and H. Yosef. 1995. Controlling the False Discovery Rate: A Practical and Powerful Approach to Multiple Testing. Journal of the Royal Statistical Society 57:289-300.

Bernardo, P. H., F. A. MacHado, R. W. Murphy, and H. Zaher. 2012. Redescription and Morphological Variation of *Oxyrhopus clathratus* Duméril, Bibron and Duméril, 1854 (Serpentes: Dipsadidae: Xenodontinae). South American Journal of Herpetology 7:134-148.

Biro, P. A. and J. A. Stamps. 2008. Are animal personality traits linked to life-history productivity? Trends Ecol Evol 23:361-368.

Bivand, R. 2002. Spatial econometrics functions in R: Classes and methods. Journal of Geographical Systems 4:405-421.

Bivand, R. and N. Lewin-Koh. 2017. maptools: Tools for Reading and Handling Spatial Objects. R package version 0.9-2. https://CRAN.R-project.org/package=maptools.

Bocak, L. and T. Yagi. 2010. Evolution of Mimicry Patterns in Metriorrhynchus (Coleoptera: Lycidae): The History of Dispersal and Speciation in Southeast Asia. Evolution 64:39-52.

Bollback, J. 2006. SIMMAP: Stochastic character mapping of discrete traits on phylogenies. BMC Bioinformatics 7:88.

Bosque, R. J., B. P. Noonan, and G. R. Colli. 2016. Geographical coincidence and mimicry between harmless snakes (Colubridae: *Oxyrhopus*) and harmful models (Elapidae: *Micrurus*). Global Ecology and Biogeography 25:218-226.

Brodie, E. D. 1992. Correlational selection for color pattern and antipredator behavior in the garter snake *Thamnophis ordinoides*. Evolution 46:1284-1298.

Brodie, E. D. 1993. Differential avoidance of coral snake banded patterns by free-ranging avian predators in Costa Rica. Evolution 47:227-235.

Brodie, E. D. and F. J. Janzen. 1995. Experimental studies of coral snake mimicry: generalized avoidance of ringed snake patterns by free-ranging avian predators. Functional Ecology 9:186-190.

Brown, K. S. and D. R. Gifford. 2002. Lepidoptera in the Cerrado landscape and the conservation of vegetation, soil, and topographical mosaics. Pp. 201-222 *in* P. S. Oliveira, and R. J. Marquis, eds. The Cerrados of Brazil: Ecology and Natural History of a Neotropical Savanna. Columbia University Press, New York.

Brown, M. E. 1996. Assessing body condition in birds. Pp. 67-135 *in* N. V., and K. E.D., eds. Current Ornithology. Springer, Boston, MA.

Brunsdon, C. and H. Chen. 2014. GISTools: Some further GIS capabilities for R. R package version 0.7-4. https://CRAN.R-project.org/package=GISTools.

Bryant, D., R. Bouckaert, J. Felsenstein, N. A. Rosenberg, and A. RoyChoudhury. 2012. Inferring Species Trees Directly from Biallelic Genetic Markers: Bypassing Gene Trees in a Full Coalescent Analysis. Mol Biol Evol 29:1917-1932.

Buasso, C. M., G. C. Leynaud, and F. B. Cruz. 2006. Predation on snakes of Argentina: effects of coloration and ring pattern on coral and false coral snakes. Studies on Neotropical Fauna and Environment 41:183-188.

Bucaretchi, F., E. M. De Capitani, R. J. Vieira, C. K. Rodrigues, M. Zannin, N. J. d. Silva Jr., L. L. Casais-e-Silva, and S. Hyslop. 2016. Coral snake bites (Micrurus spp.) in Brazil: a review of literature reports. Clinical Toxicology 54:222-234.

Bustard, H. R. 1969. Defensive Behavior and Locomotion of the Pacific Boa, Candoia aspera, with a Brief Review of Head Concealment in Snakes. Herpetologica 25:164-170.

Calhim, S. and R. Montgomerie. 2015. Testis asymmetry in birds: the influences of sexual and natural selection. J Avian Biol 46:175-185.

Campbell, J. A. and W. W. Lamar. 2004. The venomous reptiles of the Western Hemisphere. Volume 1. Comstock Publishing Associates.

Colinvaux, P. A., P. E. De Oliveira, and M. B. Bush. 2000. Amazonian and neotropical plant communities on glacial time-scales: The failure of the aridity and refuge hypotheses. Quaternary Science Reviews 19:141-169.

Colli, G. R. 2005. As origens e a diversificação da herpetofauna do Cerrado. Pp. 247-264 *in* A. Scariot, J. C. Sousa-Silva, and J. M. Felfili, eds. Cerrado: Ecologia, Biodiversidade e Conservação. Ministério do Meio Ambiente Brasília.

Cox, C. L. and A. R. Davis Rabosky. 2013. Spatial and temporal drivers of phenotypic diversity in polymorphic snakes. Am Nat 182:E40-57.

Cuthill, I. C., W. L. Allen, K. Arbuckle, B. Caspers, G. Chaplin, M. E. Hauber, G. E. Hill, N. G. Jablonski, C. D. Jiggins, A. Kelber, J. Mappes, J. Marshall, R. Merrill, D. Osorio, R. Prum, N. W. Roberts, A. Roulin, H. M. Rowland, T. N. Sherratt, J. Skelhorn, M. P.

Speed, M. Stevens, M. C. Stoddard, D. Stuart-Fox, L. Talas, E. Tibbetts, and T. Caro. 2017. The biology of color. Science 357:eaan0221.

Cuthill, I. C. and A. T. D. Bennett. 1993. Mimicry and the eye of the beholder. Proceedings of the Royal Society of London Series B-Biological Sciences 253:203-204.

Cuthill, I. C., M. Stevens, A. M. M. Windsor, and H. J. Walker. 2006. The effects of pattern symmetry on detection of disruptive and background-matching coloration. Behav Ecol 17:828-832.

Davis Rabosky, A. R., C. L. Cox, and D. L. Rabosky. 2016a. Unlinked Mendelian inheritance of red and black pigmentation in snakes: Implications for Batesian mimicry. Evolution 70:944-953.

Davis Rabosky, A. R., C. L. Cox, D. L. Rabosky, P. O. Title, I. A. Holmes, A. Feldman, and J. A. McGuire. 2016b. Coral snakes predict the evolution of mimicry across New World snakes. Nat Commun 7.

de Almeida, P. C. R., A. L. C. Prudente, F. F. Curcio, and M. T. U. Rodrigues. 2016. Biologia e história natural da cobras-corais *in* N. J. d. Silva Jr, ed. As cobras-corais do Brasil: bioloogia, taxonomia, venenos e envenenamentos PUC, Goiânia, Brazil

de Reviers, M. and J. B. Williams. 1984. Testis development and production of spermatozoa in the cockerel (*Gallus domesticus*). Pp. 183-202 *in* F. J. Cunningham, L. P. E., and D. Hewitt, eds. Reproductive Biology of Poultry. British Poultry Science, Ltd, Harlow, UK.

Dray, S., D. Bauman, G. Blanchet, D. Borcard, S. Clappe, G. Guenard, T. Jombart, G. Larocque, P. Legendre, N. Madi, and H. H. Wagner. 2018. adespatial: Multivariate Multiscale Spatial Analysis. R package version 0.3-2. https://CRAN.R-project.org/package=adespatial.

Dray, S. and A.-B. Dufour. 2007. The ade4 Package: Implementing the Duality Diagram for Ecologists. Journal of Statistical Software 22:20.

Drent, P. J., K. v. Oers, and A. J. v. Noordwijk. 2003. Realized heritability of personalities in the great tit (*Parus major*). Proceedings of the Royal Society of London. Series B: Biological Sciences 270:45-51.

Dunnington, D. 2017. prettymapr: Scale Bar, North Arrow, and Pretty Margins in R. R package version 0.2.2. https://CRAN.R-project.org/package=prettymapr.

DuVal, E. H., H. W. Greene, and K. L. Manno. 2006. Laughing falcon (*Herpetotheres cachinnans*) predation on coral snakes (*Micrurus nigrocinctus*). Biotropica 38:566-568.

Edmunds, M. 2000. Why are there good and poor mimics? Biological Journal of the Linnean Society 70:459-466.

Ellers, J., C. L. Boggs, and J. Mallet. 2003. The evolution of wing color: male mate choice opposes adaptive wing color divergence in *Colias butterflies*. Evolution 57:1100-1106.

Endler, J. A. 1992. Signals, Signal Conditions, and the Direction of Evolution. The American Naturalist 139:S125-S153.

English, S., T. W. Fawcett, A. D. Higginson, P. C. Trimmer, and T. Uller. 2016. Adaptive Use of Information during Growth Can Explain Long-Term Effects of Early Life Experiences. The American Naturalist 187:620-632.

Exnerová, A., K. H. Svádová, E. Fučíková, P. Drent, and P. Štys. 2010. Personality matters: individual variation in reactions of naive bird predators to aposematic prey. Proceedings of the Royal Society B: Biological Sciences 277:723-728.

Feitosa, D. T., P. P. Passo, and A. L. d. C. Prudente. 2007. Taxonomic status and geographic variation of the slender coralsnake Micrurus filiformis (Guenther, 1859) (Serpentes, Elapidae). South American Journal of Herpetology 2:149-156.

Feitosa, D. T., N. J. d. Silva Jr., M. G. Pires, H. Zaher, and A. L. da Costa Prudente. 2015. A new species of monadal coral snake of the genus *Micrurus* (Serpentes, Elapidae) from western Amazon. Zootaxa 3974:538-554.

FitzJohn, R. G. 2012. Diversitree: comparative phylogenetic analyses of diversification in R. Methods in Ecology and Evolution 3:1084-1092.

Forsman, A. and S. Merilaita. 1999. Fearful symmetry: pattern size and asymmetry affects aposematic signal efficacy. Evol Ecol 13:131-140.

França, F. G. R. 2008. O mimetismo das serpentes corais em ambientes campestres, savânicos e florestais da América do Sul. Tese de Doutorado. Pp. 153. Ecologia. Universidade de Brasília, Brasília.

Francis, R. M. 2017. pophelper: an R package and web app to analyse and visualize population structure. Mol Ecol Resour 17:27-32.

Fritz, S. A. and A. Purvis. 2010. Selectivity in Mammalian Extinction Risk and Threat Types: a New Measure of Phylogenetic Signal Strength in Binary Traits

Selectividad en el Riesgo de Extinción y Tipos de Amenaza en Mamíferos: una Nueva Medida de la Intensidad de la Señal Filogenética en Atributos Binarios. Conserv Biol 24:1042-1051.

Garamszegi, L. s. Z. 2014. Modern Phylogenetic Comparative Methods and Their Application in Evolutionary Biology. Springer, Seville, Spain.

Goerlich, V. C., D. Nätt, M. Elfwing, B. Macdonald, and P. Jensen. 2012. Transgenerational effects of early experience on behavioral, hormonal and gene expression responses to acute stress in the precocial chicken. Hormones and Behavior 61:711-718.

Goslee, S. C. and D. L. Urban. 2007. The ecodist Package for Dissimilarity-based Analysis of Ecological Data. 2007 22:19.

Gray, D. A. 1996. Carotenoids and Sexual Dichromatism in North American Passerine Birds. The American Naturalist 148:453-480.

Greenberg, R. and C. Mettke-hofmann. 2001. Ecological Aspects of Neophobia and Neophilia in Birds. Pp. 119-178 *in* V. Nolan, Jr., and C. Thompson, eds. Current Ornithology. Springer US.

Greene, H. W. and R. W. McDiarmid. 1981. Coral snake mimicry: does It occur? Science 213:1207-1212.

Ham, A. D., E. Ihalainen, L. Lindstrom, and J. Mappes. 2006. Does colour matter? The importance of colour in avoidance learning, memorability and generalisation. Behavioral Ecology and Sociobiology 60:482-491.

Harper, G. R. and D. W. Pfennig. 2007. Mimicry on the edge: why do mimics vary in resemblance to their model in different parts of their geographical range? Proceedings of the Royal Society B-Biological Sciences 274:1955-1961.

Harper, G. R. and D. W. Pfennig. 2008. Selection overrides gene flow to break down maladaptive mimicry. Nature 451:1103-1107.

Hart, N. S. 2001. The Visual Ecology of Avian Photoreceptors. Progress in Retinal and Eye Research 20:675-703.

Hawlena, D., R. Boochnik, Z. Abramsky, and A. Bouskila. 2006. Blue tail and striped body: why do lizards change their infant costume when growing up? Behav Ecol 17:889-896.

Hijmans, R. J. 2017. geosphere: Spherical Trigonometry. R package version 1.5-7. https://CRAN.R-project.org/package=geosphere.

Hijmans, R. J. 2019. raster: Geographic Data Analysis and Modeling. R package version 2.8-19. https://CRAN.R-project.org/package=raster.

Hines, H. M. and P. H. Williams. 2012. Mimetic colour pattern evolution in the highly polymorphic *Bombus trifasciatus* (Hymenoptera: Apidae) species complex and its comimics. Zoological Journal of the Linnean Society 166:805-826.

Hinman, K. E., H. L. Throop, K. L. Adams, A. J. Dake, K. K. McLauchlan, and M. J. McKone. 1997. Predation by free-ranging birds on partial coral snake mimics: the importance of ring width and color. Evolution 51:1011-1014.

Hoekstra, H. E. 2006. Genetics, development and evolution of adaptive pigmentation in vertebrates. Heredity 97:222-234.

Hoorn, C., G. R. Bogotá-A, M. Romero-Baez, E. I. Lammertsma, S. G. A. Flantua, E. L. Dantas, R. Dino, D. A. do Carmo, and F. Chemale. 2017. The Amazon at sea: Onset and stages of the Amazon River from a marine record, with special reference to Neogene plant turnover in the drainage basin. Global and Planetary Change 153:51-65.

Hoorn, C. and F. Wesselingh. 2010. Amazonia - Landscape and Species Evolution: a look into the past. Blackwell Publishing Ltd.

Hoorn, C., F. P. Wesselingh, H. ter Steege, M. A. Bermudez, A. Mora, J. Sevink, I. Sanmartín, A. Sanchez-Meseguer, C. L. Anderson, J. P. Figueiredo, C. Jaramillo, D. Riff, F. R. Negri, H. Hooghiemstra, J. Lundberg, T. Stadler, T. Särkinen, and A. Antonelli. 2010.

Amazonia Through Time: Andean Uplift, Climate Change, Landscape Evolution, and Biodiversity. Science 330:927-931.

Hotová Svádová, K., A. Exnerová, M. Kopečková, and P. Štys. 2013. How Do Predators Learn to Recognize a Mimetic Complex: Experiments with Naive Great Tits and Aposematic Heteroptera. Ethology 119:814-830.

Houde, A. E. 1997. Sex, color, and mate choice in guppies. Princeton University, Princeton, New Jersey.

Ingalls, V. 1993. Startle and Habituation Responses of Blue Jays (Cyanocitta cristata) in a Laboratory Simulation of Anti-Predator Defenses of Catocala Moths (Lepidoptera: Noctuidae). Behaviour 126:77-96.

Jiggins, C. D., R. Mallarino, K. R. Willmott, and E. Bermingham. 2006. The phylogenetic pattern of speciation and wing pattern change in neotropical Ithomia butterflies (Lepidoptera : Nymphalidae). Evolution 60:1454-1466.

John, J. L. 1994. The avian spleen: a neglected organ. Q Rev Biol 69:327-351.

Jowers, M. J., J. L. Garcia Mudarra, S. P. Charles, and J. C. Murphy. 2019. Phylogeography of West Indies Coral snakes (*Micrurus*): Island colonisation and banding patterns. Zool Scr 48:263-276.

Kapan, D. D. 2001. Three-butterfly system provides a field test of mullerian mimicry. Nature 409:338-340.

Kassambara, A., M. Kosinski, P. Biecek, and S. Fabian. 2018. Drawing Survival Curves using 'ggplot2' version 0.4.2.

Kazemi, B., G. Gamberale-Stille, Birgitta S. Tullberg, and O. Leimar. 2014. Stimulus Salience as an Explanation for Imperfect Mimicry. Curr Biol 24:965-969.

Kikuchi, D. W. and D. W. Pfennig. 2010. Predator Cognition Permits Imperfect Coral Snake Mimicry. American Naturalist 176:830-834.

Kikuchi, D. W. and D. W. Pfennig. 2013. Imperfect Mimicry and the Limits of Natural Selection. Q Rev Biol 88:297-315.

Kikuchi, D. W., B. M. Seymoure, and D. W. Pfennig. 2014. Mimicry's palette: widespread use of conserved pigments in the aposematic signals of snakes. Evol Dev 16:61-67.

Kraemer, A. C. and D. C. Adams. 2014. Predator perception of batesian mimicry and conspicuousness in a salamander. Evolution 68:1197-1206.

Kurvers, R. H. J. M., H. H. T. Prins, S. E. van Wieren, K. van Oers, B. A. Nolet, and R. C. Ydenberg. 2010. The effect of personality on social foraging: shy barnacle geese scrounge more. Proceedings of the Royal Society B: Biological Sciences 277:601-608.

Lawrence, J. P., B. Rojas, A. Fouquet, J. Mappes, A. Blanchette, R. A. Saporito, R. J. Bosque, E. A. Courtois, and B. P. Noonan. 2019. Weak warning signals can persist in the absence of gene flow. Proceedings of the National Academy of Sciences 116:19037-19045.

Leaché, A. D., B. L. Banbury, J. Felsenstein, A. n.-M. de Oca, and A. Stamatakis. 2015. Short Tree, Long Tree, Right Tree, Wrong Tree: New Acquisition Bias Corrections for Inferring SNP Phylogenies. Syst Biol 64:1032-1047.

Ledo, R. M. D. and G. R. Colli. 2017. The historical connections between the Amazon and the Atlantic Forest revisited. J Biogeogr 44:2551-2563.

Lee, M. S. Y., K. L. Sanders, B. King, and A. Palci. 2016. Diversification rates and phenotypic evolution in venomous snakes (Elapidae). Royal Society Open Science 3:150277.

Lewis, P. O. 2001. A Likelihood Approach to Estimating Phylogeny from Discrete Morphological Character Data. Syst Biol 50:913-925.

Leynaud, G. C., G. J. Reati, and E. H. Bucher. 2008. Annual activity patterns of snakes from central Argentina (Cordoba province). Studies on Neotropical Fauna and Environment 43:19-24.

Lichtenstein, J. L. L., C. M. Wright, L. P. Luscuskie, G. A. Montgomery, N. Pinter-Wollman, and J. N. Pruitt. 2017. Participation in cooperative prey capture and the benefits gained from it are associated with individual personality. Curr Zool 63:561-567.

Lindstrom, L., R. V. Alatalo, and J. Mappes. 1997. Imperfect Batesian mimicry - The effects of the frequency and the distastefulness of the model. Proceedings of the Royal Society of London Series B-Biological Sciences 264:149-153.

Lindstrom, L., R. V. Alatalo, and J. Mappes. 1999. Reactions of hand-reared and wild-caught predators toward warningly colored, gregarious, and conspicuous prey. Behav Ecol 10:317-322.

Lindström, L., R. V. Alatalo, J. Mappes, M. Riipi, and L. Vertainen. 1999. Can aposematic signals evolve by gradual change? Nature 397:249.

Lomonte, B., P. Rey-Suárez, J. Fernández, M. Sasa, D. Pla, N. Vargas, M. Bénard-Valle, L. Sanz, C. Corrêa-Netto, V. Núñez, A. Alape-Girón, A. Alagón, J. M. Gutiérrez, and J. J. Calvete. 2016. Venoms of Micrurus coral snakes: Evolutionary trends in compositional patterns emerging from proteomic analyses. Toxicon 122:7-25.

Lynch, J. D. 2009. Snakes of the genus *Oxyrhopus* (Colubridae: Squamata) in Colombia: taxonomy and geographic variation. Papéis Avulsos de Zoologia (São Paulo) 49:319-337.

Macedonia, J. M., D. L. Clark, R. G. Riley, and D. J. Kemp. 2013. Species recognition of color and motion signals in Anolis grahami: evidence from responses to lizard robots. Behav Ecol 24:846-852.

Maddison, W. P., P. E. Midford, and S. P. Otto. 2007. Estimating a binary character's effect on speciation and extinction. Syst Biol 56:701-710.

Mallet, J. and M. Joron. 1999. Evolution of diversity in warning color and mimicry: polymorphisms, shifting balance, and speciation. Annual Review of Ecology and Systematics 30:201-233.

Mappes, J. and R. V. Alatalo. 1997. Batesian mimicry and signal accuracy. Evolution 51:2050-2053.

Margalida, A., J. J. Negro, and I. Galván. 2008. Melanin-based color variation in the Bearded Vulture suggests a thermoregulatory function. Comparative Biochemistry and Physiology Part A: Molecular & Integrative Physiology 149:87-91.

Marples, N. M. and P. M. Brakefield. 1995. Genetic variation for the rate of recruitment of novel insect prey into the diet of a bird. Biological Journal of the Linnean Society 55:17-27.

Marques, O. A. V. 2002. Natural history of the coral snake Micrurus decoratus (Elapidae) from the Atlantic Forest in southeast Brazil, with comments on possible mimicry. Amphibia-Reptilia 23:228-232.

McCue, M. D. 2006. Cost of Producing Venom in Three North American Pitviper Species. Copeia 2006:818-825.

Michaux, J. R., R. Libois, and M. G. Filippucci. 2005. So close and so different: comparative phylogeography of two small mammal species, the Yellow-necked fieldmouse (*Apodemus flavicollis*) and the Woodmouse (*Apodemus sylvaticus*) in the Western Palearctic region. Heredity 94:52-63.

Molina-Venegas, R. and M. Á. Rodríguez. 2017. Revisiting phylogenetic signal; strong or negligible impacts of polytomies and branch length information? Bmc Evol Biol 17:53.

Møller, A. P. 1994. Directional selection on directional asymmetry: testes size and secondary sexual characters in birds. Proceedings of the Royal Society of London. Series B: Biological Sciences 258:147-151.

Moore, D. F. 2016. Applied Survival Analysis Using R. Springer International Publishing, Switzerland.

Morais, D. H., R. W. Ávila, R. A. Kawashita-Ribeiro, and M. A. d. Carvalho. 2016. Squamata, Elapidae, *Micrurus surinamensis* (Cuvier, 1817): new records and distribution map in the state of Mato Grosso, Brazil, with notes on diet and activity period. Check List 7:350-351.

Müller, F. 1878. Über die vortheile der mimicry bei schmetterlingen. Zoologischer Anzeiger 1:54-55.

Naimi, B., N. A. S. Hamm, T. A. Groen, A. K. Skidmore, and A. G. Toxopeus. 2014. Where is positional uncertainty a problem for species distribution modelling? Ecography 37:191-203.

Nazareno, A. G., C. W. Dick, and L. G. Lohmann. 2017. Wide but not impermeable: Testing the riverine barrier hypothesis for an Amazonian plant species. Mol Ecol 26:3636-3648.

Nguyen, L.-T., H. A. Schmidt, A. von Haeseler, and B. Q. Minh. 2014. IQ-TREE: A Fast and Effective Stochastic Algorithm for Estimating Maximum-Likelihood Phylogenies. Mol Biol Evol 32:268-274.

Olamendi-Portugal, T., C. V. F. Batista, R. Restano-Cassulini, V. Pando, O. Villa-Hernandez, A. Zavaleta-Martínez-Vargas, M. C. Salas-Arruz, R. C. R. de la Vega, B. Becerril, and L. D. Possani. 2008. Proteomic analysis of the venom from the fish eating coral snake Micrurus surinamensis: Novel toxins, their function and phylogeny. Proteomics 8:1919-1932.

Olsson, M., D. Stuart-Fox, and C. Ballen. 2013. Genetics and evolution of colour patterns in reptiles. Seminars in Cell & Developmental Biology 24:529-541.

Pagel, M. 1999. Inferring the historical patterns of biological evolution. Nature 401:877-884.

Passos, P. and D. S. Fernandes. 2005. Variation and taxonomic status of the aquatic coral snake Micrurus surinamensis (Cuvier, 1817) (Serpentes: Elapidae). Zootaxa 953:1-14.

Pekar, S., M. Jarab, L. Fromhage, and M. E. Herberstein. 2011. Is the Evolution of Inaccurate Mimicry a Result of Selection by a Suite of Predators? A Case Study Using Myrmecomorphic Spiders. American Naturalist 178:124-134.

Peterson, B. K., J. N. Weber, E. H. Kay, H. S. Fisher, and H. E. Hoekstra. 2012. Double Digest RADseq: An Inexpensive Method for De Novo SNP Discovery and Genotyping in Model and Non-Model Species. PLOS ONE 7:e37135.

Pfennig, D. W., C. K. Akcali, and D. W. Kikuchi. 2015. Batesian mimicry promotes pre- and postmating isolation in a snake mimicry complex. Evolution 69:1085-1090.

Pfennig, D. W., G. R. Harper, A. F. Brumo, W. R. Harcombe, and K. S. Pfennig. 2007. Population differences in predation on Batesian mimics in allopatry with their model: selection against mimics is strongest when they are common. Behavioral Ecology and Sociobiology 61:505-511.

Phillips, S. J., R. P. Anderson, and R. E. Schapire. 2006. Maximum entropy modeling of species geographic distributions. Ecol Model 190:231-259.

Pires, M. G., N. J. d. Silva Jr., D. T. Feitosa, A. L. d. C. Prudente, G. A. P. Filho, and H. Zaher. 2014a. A new species of triadal coral snake of the genus *Micrurus* Wagler, 1824 (Serpentes: Elapidae) from northeastern Brazil. 2014 3811:16.

Pires, M. G., N. J. d. Silva Jr., D. T. Feitosa, A. L. d. C. Prudente, G. A. P. Filho, and H. Zaher. 2014b. A new species of triadal coral snake of the genus *Micrurus* Wagler, 1824 (Serpentes: Elapidae) from northeastern Brazil. Zootaxa 3811:16.

Pravossoudovitch, K., F. Cury, S. G. Young, and A. J. Elliot. 2014. Is red the colour of danger? Testing an implicit red–danger association. Ergonomics 57:503-510.

Protas, M. E. and N. H. Patel. 2008. Evolution of Coloration Patterns. Annu Rev Cell Dev Bi 24:425-446.

Pryke, S. R. 2009. Is red an innate or learned signal of aggression and intimidation? Animal Behaviour 78:393-398.

Przeczek, K., C. Mueller, and S. M. Vamosi. 2008. The evolution of aposematism is accompanied by increased diversification. Integrative Zoology 3:149-156.

Pyron, R. A. and F. T. Burbrink. 2013. Early origin of viviparity and multiple reversions to oviparity in squamate reptiles. Ecol Lett.

Pyron, R. A., F. T. Burbrink, G. R. Colli, A. N. M. de Oca, L. J. Vitt, C. A. Kuczynski, and J. J. Wiens. 2011. The phylogeny of advanced snakes (Colubroidea), with discovery of a new subfamily and comparison of support methods for likelihood trees. Molecular Phylogenetics and Evolution 58:329-342.

Pyron, R. A., F. T. Burbrink, and J. J. Wiens. 2013. A phylogeny and revised classification of Squamata, including 4161 species of lizards and snakes. Bmc Evol Biol 13.

R Core Team. 2017. R: A Language and Environment for Statistical Computing. R Foundation for Statistical Computing, Vienna, Austria.

R Core Team. 2018. R: A Language and Environment for Statistical Computing. R Foundation for Statistical Computing, Vienna, Austria.

R Hackathon et al. 2019. phylobase: Base Package for Phylogenetic Structures and Comparative Data. R package version 0.8.6.

Raj, A., M. Stephens, and J. K. Pritchard. 2014. fastSTRUCTURE: Variational Inference of Population Structure in Large SNP Data Sets. Genetics 197:573.

Rangel, T. F., N. R. Edwards, P. B. Holden, J. A. F. Diniz-Filho, W. D. Gosling, M. T. P. Coelho, F. A. S. Cassemiro, C. Rahbek, and R. K. Colwell. 2018. Modeling the ecology and evolution of biodiversity: Biogeographical cradles, museums, and graves. Science 361:eaar5452.

Revell, L. J. 2012. phytools: an R package for phylogenetic comparative biology (and other things). Methods in Ecology and Evolution 3:217-223.

Revell, L. J. 2013. Two new graphical methods for mapping trait evolution on phylogenies. Methods in Ecology and Evolution 4:754-759.

Ribas, C. C., A. Aleixo, A. C. R. Nogueira, C. Y. Miyaki, and J. Cracraft. 2012. A palaeobiogeographic model for biotic diversification within Amazonia over the past three million years. Proceedings of the Royal Society B: Biological Sciences 279:681-689.

Rowe, C. and T. Guilford. 2000. Aposematism: to be red or dead. Trends Ecol Evol 15:261-262.

Roze, J. A. 1996. Coral Snakes of the Americas: Biology, Identification, and Venoms. Krieger Publishing Company, Malabar.

Roze, J. A. and A. Bernal-Carlo. 1987. Las serpientes corales venenosas del genero Leptomicrurus (Serpentes, Elapidae) de Suramerica con descripcion de una nueva subespecie. Museo Regionale di Scienze Naturali Bollettino (Turin) 5:573-608.

Rull, V. 2008. Speciation timing and neotropical biodiversity: the Tertiary–Quaternary debate in the light of molecular phylogenetic evidence. Mol Ecol 17:2722-2729.

Ruxton, G. D., T. N. Sherratt, and M. P. Speed. 2004. Avoiding Attack: The Evolutionary Ecology of Crypsis, Warning Signals and Mimicry. Oxford University Press, Oxford.

Sanders, K. L., A. Malhotra, and R. S. Thorpe. 2006. Evidence for a Mullerian mimetic radiation in Asian pitvipers. Proceedings of the Royal Society B-Biological Sciences 273:1135-1141.

Santos, J. C., M. Baquero, C. Barrio-Amorós, L. A. Coloma, L. K. Erdtmann, A. P. Lima, and D. C. Cannatella. 2014. Aposematism increases acoustic diversification and speciation in poison frogs. Proceedings of the Royal Society B: Biological Sciences 281:20141761.

Savage, J. M. and J. B. Slowinski. 1992. The colouration of the venomous coral snakes (family Elapidae) and their mimics (families Aniliidae and Colubridae). Biological Journal of the Linnean Society 45:235-254.

Sazima, I. and A. S. Abe. 1991. Habits of 5 Brazilian Snakes with Coral-Snake Pattern, Including a Summary of Defensive Tactics. Studies on Neotropical Fauna and Environment 26:159-164.

Schall, J. J. and E. R. Pianka. 1980. Evolution of Escape Behavior Diversity. The American Naturalist 115:551-566.

Schmidt, K. P. 1952. The surinam coral snake. Fieldiana Zoology 34:25-34.

Sherratt, T. N. 2002. The evolution of imperfect mimicry. Behav Ecol 13:821-826.

Sherratt, T. N. 2008. The evolution of Müllerian mimicry. Die Naturwissenschaften 95:681-695.

Sherwin, C. M., C. M. Heyes, and C. J. Nicol. 2002. Social learning influences the preferences of domestic hens for novel food. Animal Behaviour 63:933-942.

Silva Jr., N. J. d., M. G. Pires, and D. T. Feitosa. 2016. Diversidade das cobras-corais do Brasil Pp. 81-167 *in* N. J. d. S. Júnior, ed. As cobras corais do Brasil: biologia, taxonomia, venenos e PUC Goiás, Goiânia.

Silva Jr., N. J. d. and J. C. Sites. 2001. Phylogeny of South American triad coral snakes (Elapidae : *Micrurus*) based on molecular characters. Herpetologica 57:1-22.

Silva Jr., N. J. d. and J. W. Sites, Jr. 1999. Revision of the *Micrurus frontalis* complex (Serpentes: Elapidae). Herpetol. Monogr. 13:142-194.

Skelhorn, J. and G. D. Ruxton. 2010. Mimicking multiple models: polyphenetic masqueraders gain additional benefits from crypsis. Behav Ecol 22:60-65.

Slagsvold, T. and K. L. Wiebe. 2011. Social learning in birds and its role in shaping a foraging niche. Philosophical Transactions of the Royal Society B: Biological Sciences 366:969-977.

Slowinski, J. B. 1995. A phylogenetic analysis of the New World coral snakes (Elapidae: *Leptomicrurus, Micruroides*, and *Micrurus*) based on allozymic and morphological characters. Journal of Herpetology 29:325-338.

Smith, S. M. 1975. Innate recognition of coral snake pattern by a possible avian predator. Science 187:759-760.

Smith, S. M. 1976. Predatory behaviour of young turquoise-browed motmots, *Eumomota superciliosa*. Behaviour 56:309-320.

Speed, M. P. 2000. Warning signals, receiver psychology and predator memory. Animal Behaviour 60:269-278.

Speed, M. P. and J. R. G. Turner. 1999. Learning and memory in mimicry: II. Do we understand the mimicry spectrum? Biological Journal of the Linnean Society 67:281-312.

Stamatakis, A. 2014. RAxML version 8: a tool for phylogenetic analysis and post-analysis of large phylogenies. Bioinformatics 30:1312-1313.

Strarace, F. 2013. Serpents et Amphisbènes de Guyane Française, Matoury, French Guyana.

Svádová, K., A. Exnerová, P. Štys, E. Landová, J. Valenta, A. Fučíková, and R. Socha. 2009. Role of different colours of aposematic insects in learning, memory and generalization of naïve bird predators. Animal Behaviour 77:327-336.

Symula, R., R. Schulte, and K. Summers. 2001. Molecular phylogenetic evidence for a mimetic radiation in Peruvian poison frogs supports a Müllerian mimicry hypothesis. Proceedings of the Royal Society of London. Series B: Biological Sciences 268:2415-2421.

Terribile, L. C., D. T. Feitosa, M. G. Pires, P. C. R. de Almeida, G. de Oliveira, J. A. F. Diniz-Filho, and N. J. d. Silva Jr. 2018. Reducing Wallacean shortfalls for the coralsnakes of the Micrurus lemniscatus species complex: Present and future distributions under a changing climate. PLOS ONE 13:e0205164.

Therneau, T. M. 2015. A Package for Survival Analysis in S.

Thorogood, R., H. Kokko, and J. Mappes. 2017. Social transmission of avoidance among predators facilitates the spread of novel prey. Nature Ecology & Evolution 2:254-261.

Titcomb, G. C., D. W. Kikuchi, and D. W. Pfennig. 2014. More than mimicry? Evaluating scope for flicker-fusion as a defensive strategy in coral snake mimics. Curr Zool 60:123-130.

Toews, D. P. L., N. R. Hofmeister, and S. A. Taylor. 2017. The Evolution and Genetics of Carotenoid Processing in Animals. Trends in Genetics 33:171-182.

Turner, J. R. G. 1988. The Evolution of Mimicry: A Solution to the Problem of Punctuated Equilibrium. The American Naturalist 131:S42-S66.

Uetz, P. and J. Hošek. 2019. The Reptile Database, http://www.reptile-database.org, accessed Jan 8, 2014.

Vamosi, S. M. 2005. On the role of enemies in divergence and diversification of prey: a review and synthesis. Canadian Journal of Zoology 83:894-910.

Wesselingh, F. P., C. Hoorn, S. B. Kroonenberg, A. Antonelli, J. G. Lundberg, H. B. Vonhof, and H. Hooghiemstra. 2011. On the Origin of Amazonian Landscapes and Biodiversity: A Synthesis *in* C. Hoorn, and F. P. Wesselingh, eds. Amazonia: Landscape and Species Evolution. Blackwell Publishing Ltd.

Wiens, J. J., R. A. Pyron, and D. S. Moen. 2011. Phylogenetic origins of local-scale diversity patterns and the causes of Amazonian megadiversity. Ecol Lett 14:643-652.

Williams, P. 2007. The distribution of bumblebee colour patterns worldwide: possible significance for thermoregulation, crypsis, and warning mimicry. Biological Journal of the Linnean Society 92:97-118.

Zaher, H. and U. Caramaschi. 1992. Sur le statut taxinomique d'*Oxyrhopus trigeminus* et *O. guibei* (Serpentes, Xenodontinae). Bulletin du Museum National d'Histoire Naturelle Section A Zoologie Biologie et Ecologie Animales 14:805-827.

Zaher, H., F. G. Grazziotin, J. E. Cadle, R. W. Murphy, J. C. de Moura-Leite, and S. L. Bonatto. 2009. Molecular phylogeny of advanced snakes (Serpentes, Caenophidia) with an emphasis on South American xenodontines: a revised classification and descriptions of new taxa. Papéis Avulsos de Zoologia (São Paulo) 49:115-153.

Zaher, H., F. G. Grazziotin, A. L. C. Prudente, and J. Silva, Nelson Jorge 2016. Origem e Evolução dos Elapídeos e das cobras-corais do Novo Mundo. . Pp. 24-45 *in* N. J. d. Silva

Jr, ed. As cobras-corais do Brasil: biologia, taxonomia, venenos e envenenamentos. . PUC, Goiânia.

Zaher, H., R. W. Murphy, J. C. Arredondo, R. Graboski, P. R. Machado-Filho, K. Mahlow, G. G. Montingelli, A. B. Quadros, N. L. Orlov, M. Wilkinson, Y.-P. Zhang, and F. G. Grazziotin. 2019. Large-scale molecular phylogeny, morphology, divergence-time estimation, and the fossil record of advanced caenophidian snakes (Squamata: Serpentes). PLOS ONE 14:e0216148.

Zheng, Y. and J. J. Wiens. 2016. Combining phylogenomic and supermatrix approaches, and a time-calibrated phylogeny for squamate reptiles (lizards and snakes) based on 52 genes and 4162 species. Molecular Phylogenetics and Evolution 94:537-547.

Zizka, A. 2019. Big data suggest migration and bioregion connectivity as crucial for the evolution of Neotropical biodiversity. Frontiers of Biogeography 11.

APPENDICES

Appendix A: Tables

Table 1. sPCA loadings of all morphological variables for the first three Spatial Principal Components axis (sPCAa).

	sPCAa1	**sPCAa2**	**sPCAa3**
Number of red bands	-0.607	-0.259	0.092
Proportion of external black band length	0.450	0.249	0.780
Proportion of internal black band length	0.582	-0.350	-0.416
Proportion of white band length	-0.127	0.851	-0.310
Proportion of red band length	0.271	0.154	-0.340

Table 2. Morphological variables of 5 species of the genus *Micrurus*. Length variables in centimeters.

	M. brasiliensis	***M. frontalis***	***M. ibiboboca***	***M. lemniscatus***	***M. surinamensis***
Total length (min - max)	21.21 -110.37	22.12 -132.26	21.62 -144.25	16.51 - 155.46	24.08 - 127.71
External black band length (min - max)	0.24 - 1.90	0.18 -1.93	0.23 – 2.829	0.32 - 6.47	0.212 – 2.55
Internal black band length (min -max)	0.25 - 2.65	0.07 - 2.67	0.33 – 3.50	0.26 – 3.98	0.68 – 6.46
Red band length (min - max)	0.336 - 4.50	0.30 -5.97	0.21 - 8.16	0.122 - 6.31	0.29 - 7.26
White bands length (min - max)	0.16 - 2.02	0.19 - 1.90	0.12 - 1.66	0.163 - 4.41	0.10 – 1.57
Number of black bands (min - max)	18 - 45	29 - 53	21 - 46	24 - 59	20 - 37
Number of red bands (min - max)	9 -15	9 - 17	6 - 15	0 - 19	6 -10
Number of white bands (min - max)	19 - 30	19 - 39	14 - 30	2 - 38	13 - 23

Table 3. t tests comparing lagged scores of the first axis of the SPCA using one degree cells. First values correspond were a pair of species overlap in their distribution. Second values correspond were they do not show overlap in their distribution. Upper diagonal showing t values, lower diagonal showing p values.

	M. brasiliensis	***M. frontalis***	***M. ibiboboca***	***M. lemniscatus***	***M. surinamensis***
M. surinamensis	t_3 =0.80; t_{13}= 5.33	t_4=0.01; t_{89} =18.3	t_2= 0.99; t_{92}= 5.16	t_{50}= 0.31; t_{79}=-5.55	----------
M. lemniscatus	t_4= 0.04; t_{14}= 2.11	t_{26}= -0.01; t_{98}=10.11	t_{21}= 0.87; t_{93}= -0.29	----------	p= 0.75; p<<0.001
M. ibiboboca	t_4= 0.03; t_{13}= 1.76	t_2= -0.16; t_{75}=10.50	----------	p= 0.87; p = 0.77	p= 0.43; p<<0.001
M. frontalis	t_2= 0.81; t_{13}= 4.58	----------	p= 0.89; p<< 0.001	p= 0.99; p<<0.001	p= 0.99; p<<0.001
M. brasiliensis	----------	p= 0.50; p<< 0.001	p= 0.99; p = 0.10	p= 0.96; p= 0.05	p= 0.47; p<<0.001

Table 4. Mantel test results using PCA scores of the first principal component. Upper diagonal showing rMatel values, lower diagonal showing p values.

	M. brasiliensis	***M. frontalis***	***M. ibiboboca***	***M. lemniscatus***	***M. surinamensis***
M. surinamensis	r= 0.193	r= 0.127	r= 0.263	r= -0.007	----------
M. lemniscatus	r= 0.101	r= 0.165	r= 0.167	----------	p= 0.881
M. ibiboboca	r= 0.290	r= 0.263	----------	p= 0.001	p= 0.794
M. frontalis	r= 0.241	----------	p= 0.002	p= 0.002	p= 0.217
M. brasiliensis	----------	p= 0.002	p= 0.002	p= 0.002	p= 0.035

Table 5. PCA loadings of all morphological variables for the first three Principal Components axis (PCA1,2,3) for the mid-portion of the body of *M. brasiliensis*, *M. frontalis, M. lemniscatus* and *M. surinamensis* and *Oxyrhopus guibei*. Values in parenthesis represent the proportion of variance explained by each component.

	PCA1(0.53)	**PCA2**(0.19)	**PCA3**(0.15)
Number of triads	-0.573	0.026	0.081
External black band length	0.477	-0.163	-0.196
Internal black band length	0.511	0.118	-0.450
White band length	0.359	-0.465	0.754
Red band length	0.231	0.862	0.429

Table 6. PCA loadings of all morphological variables for the first three Principal Components axis (PCA1,2,3) measurements of the body bands closest to the head (neck) of the body of *M. brasiliensis*, *M. frontalis, M. lemniscatus* and *M. surinamensis* and *Oxyrhopus guibei*. Values in parenthesis represent the proportion of variance explained by each component.

	PCA1(0.47)	**PCA2**(0.18)	**PCA3**(0.17)
Number of triads	-0.598	0.007	0.171
External black band length	0.414	-0.015	-0.164
Internal black band length	0.546	-0.264	-0.306
White band length	0.297	0.888	0.276
Red band length	0.290	-0.375	0.880

Table 7. sPCA loadings of all morphological variables for the first two Spatial Principal Components axis (sPCAa) of *Micrurus lemniscatus* complex.

	sPCA1	sPCA2
Number of bands	-0.592	0.235
Red band length	0.411	0.327
External black band length	0.090	-0.557
Internal black band length	0.278	-0.627
White band length	0.628	0.365

Table 8. sPCA loadings of all morphological variables for the first two Spatial Principal Componnts axis (sPCAa) of *Micrurus surinamensis*.

	sPCA1	sPCA2
Number of bands	-0.002	0.895
Red band length	0.229	-0.246
External black band length	0.428	0.211
Internal black band length	-0.341	-0.263
White band length	0.804	-0.152

Appendix B: figures

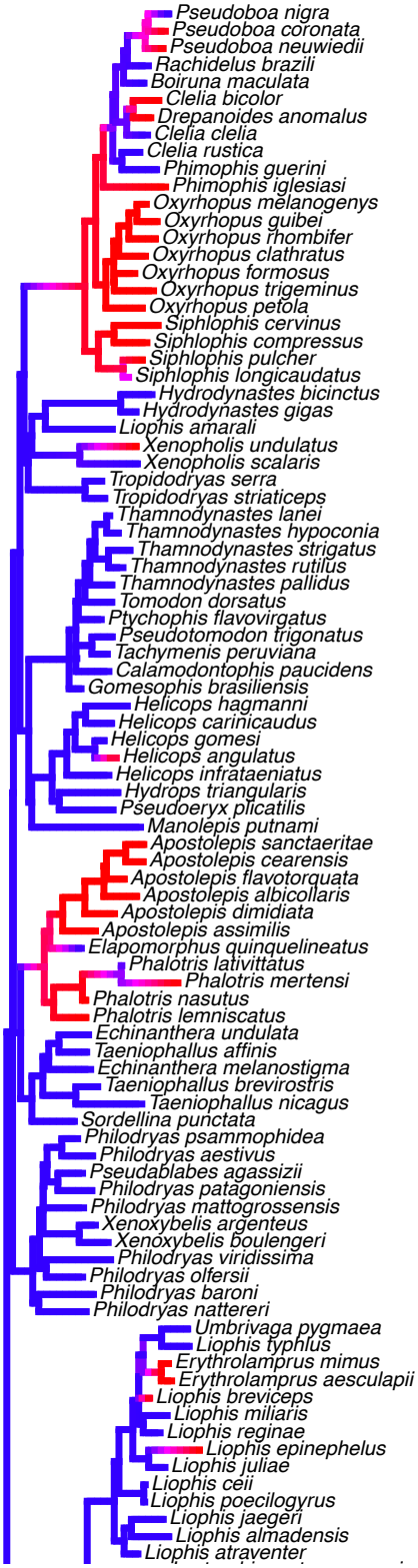

Continue on next page

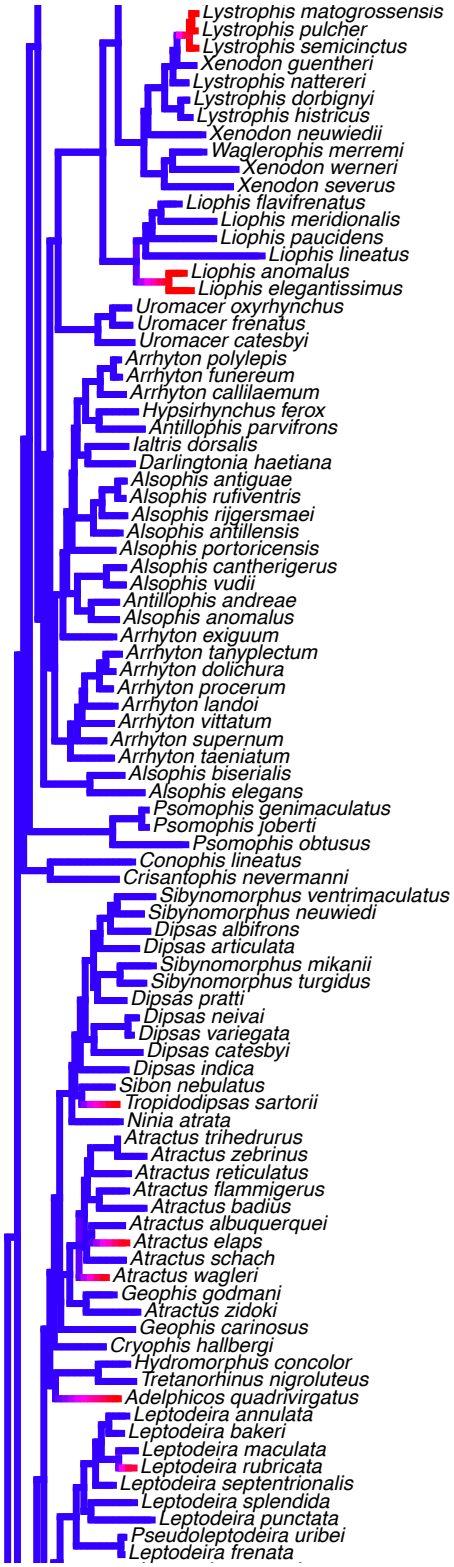

Continue on next page

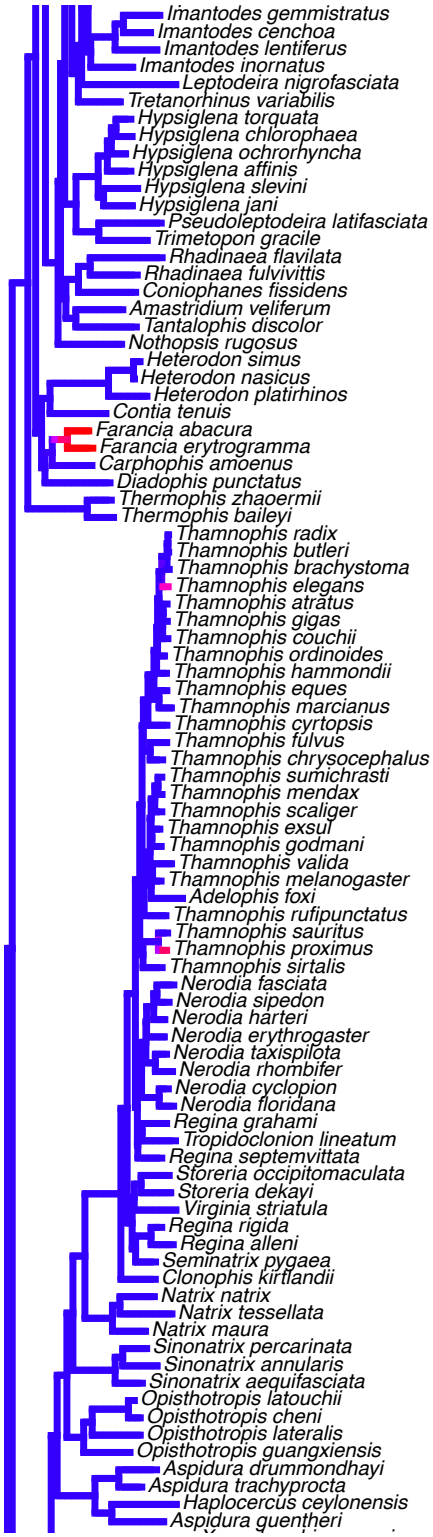

Continue on next page

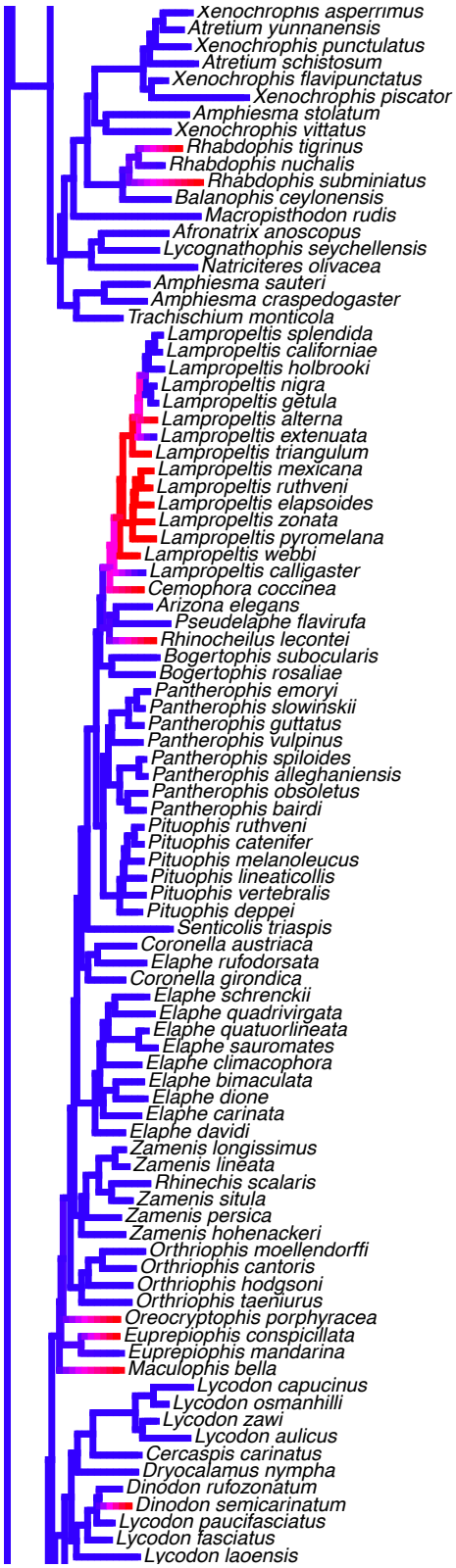

Continue on next page

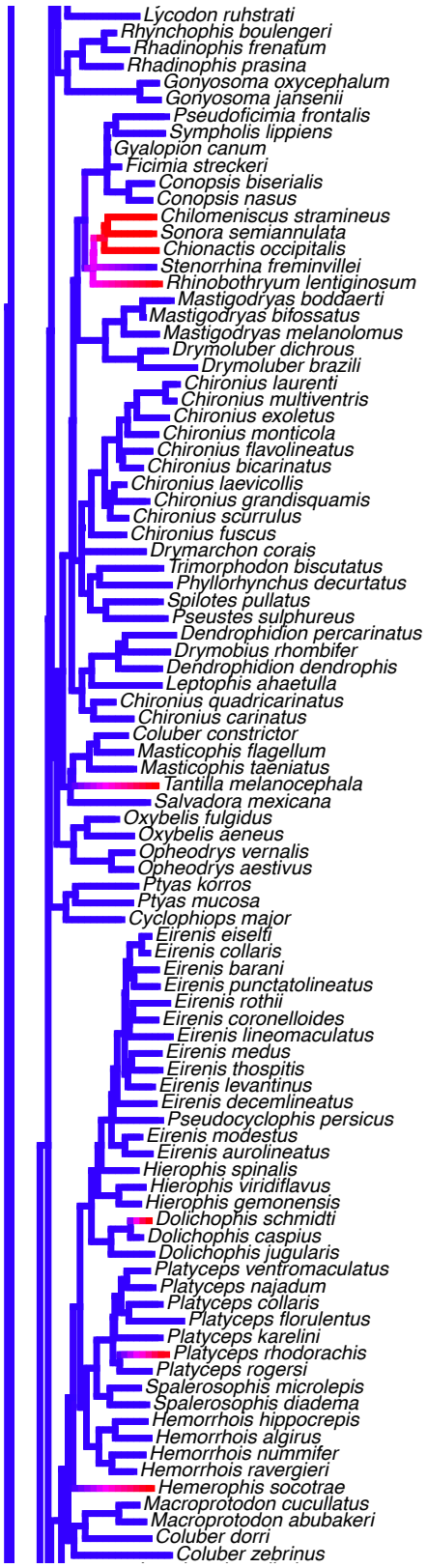

Continue on next page

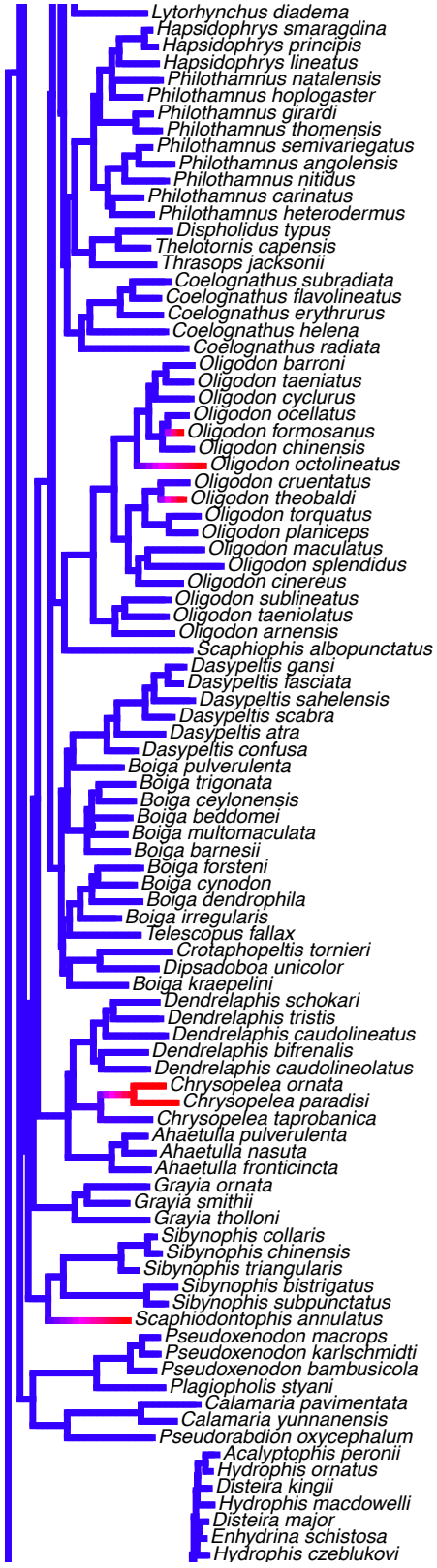

Continue on next page

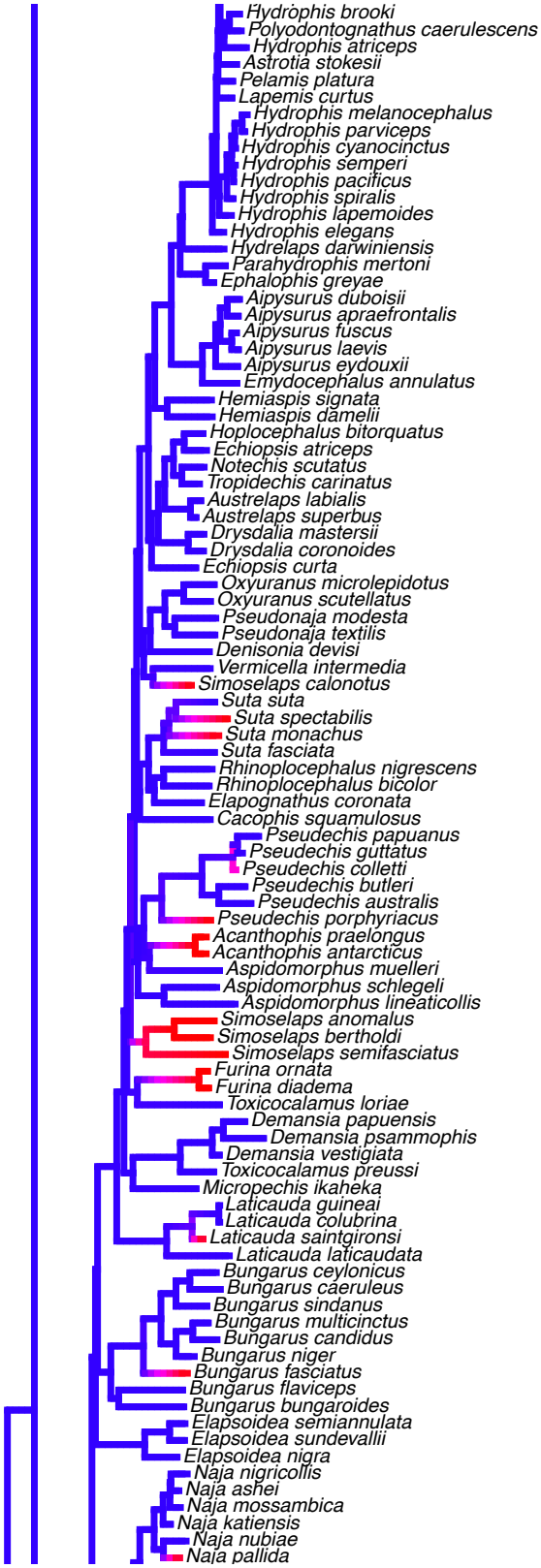

Continue on next page

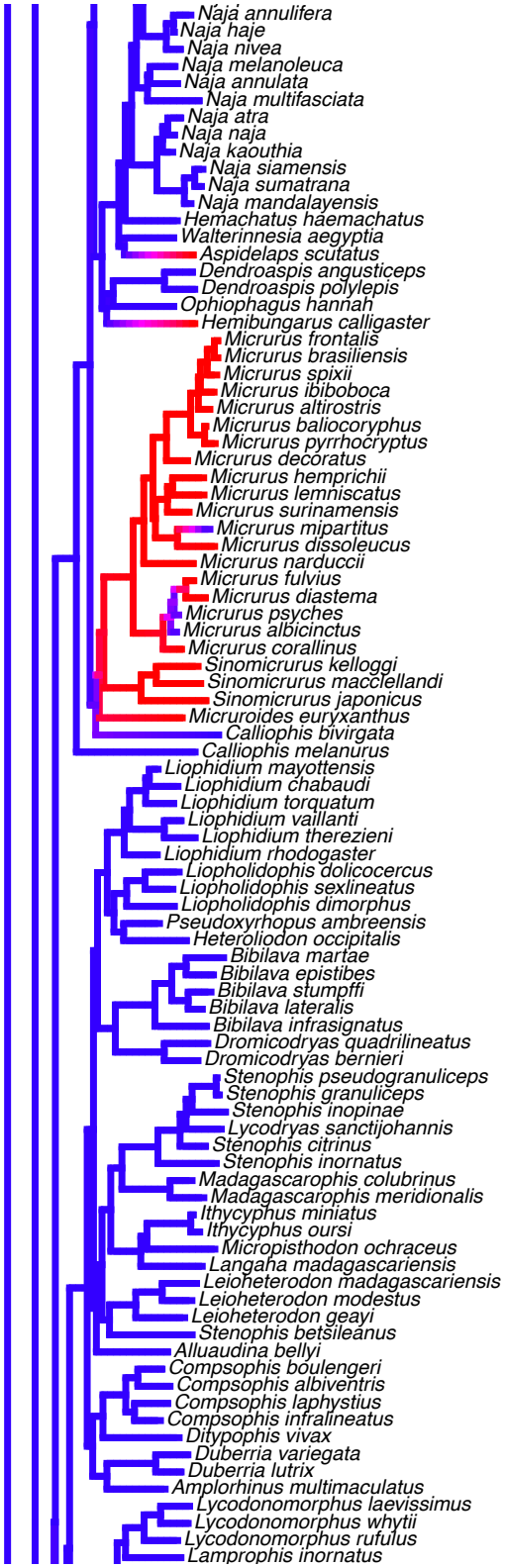

Continue on next page

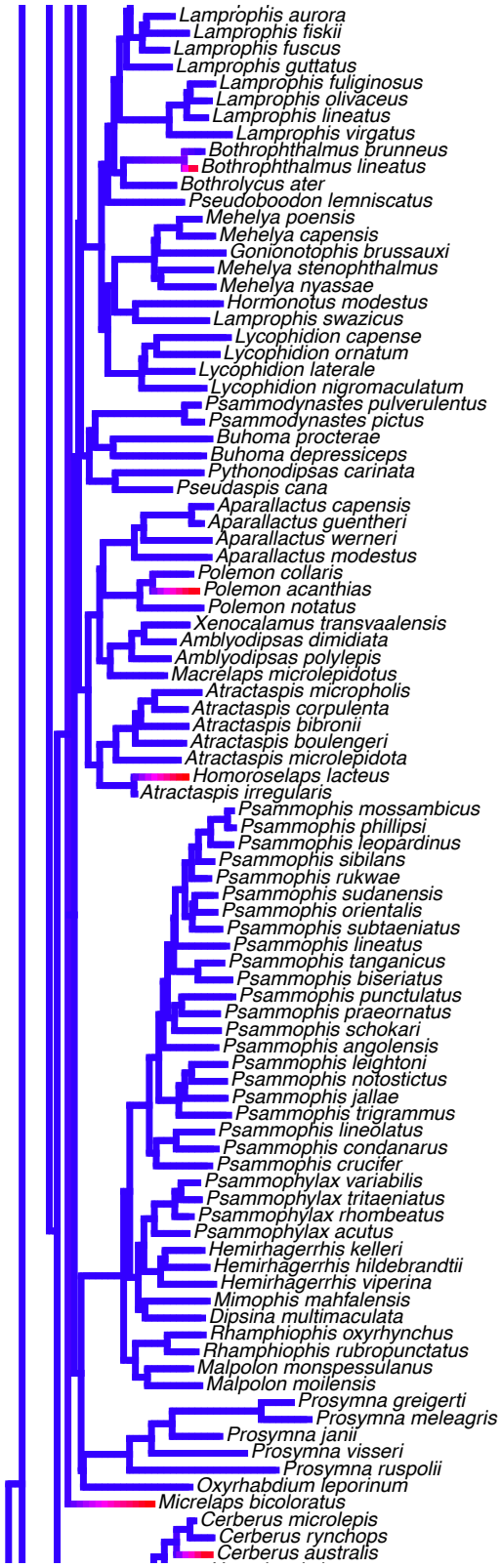

Continue on next page

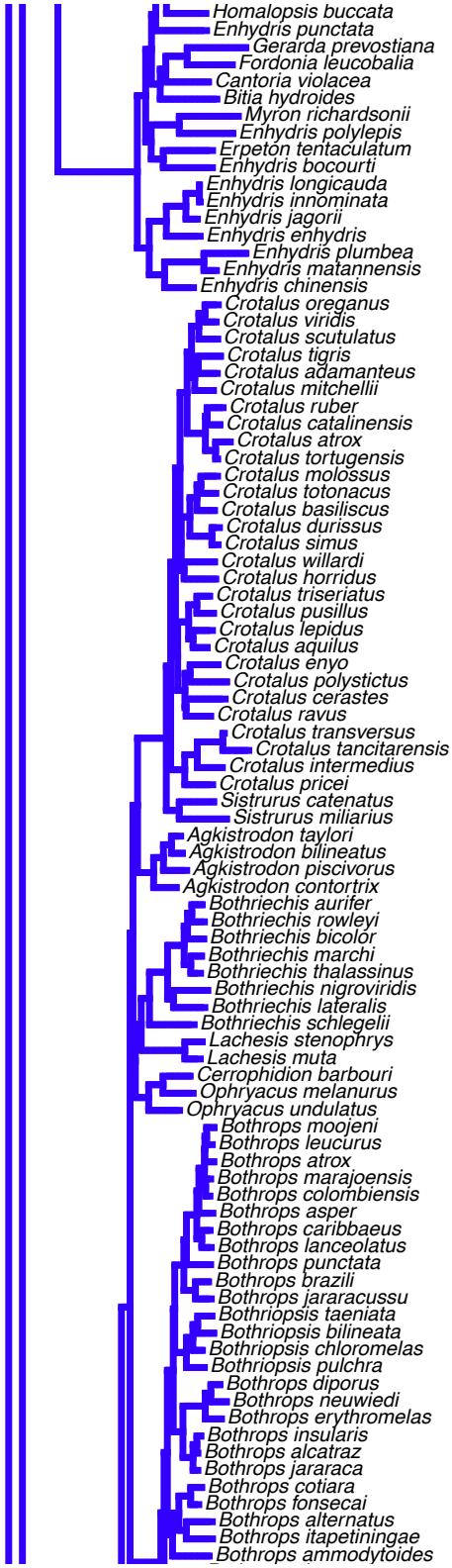

Continue on next page

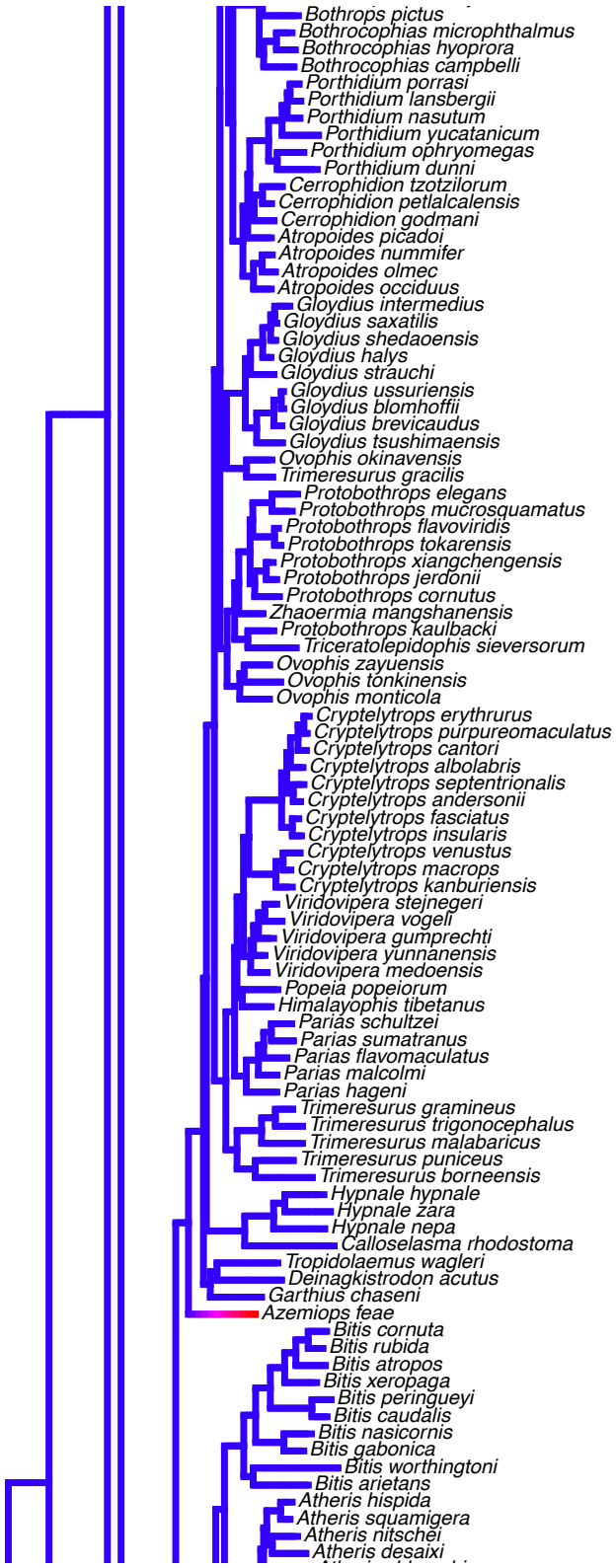

Continue on next page

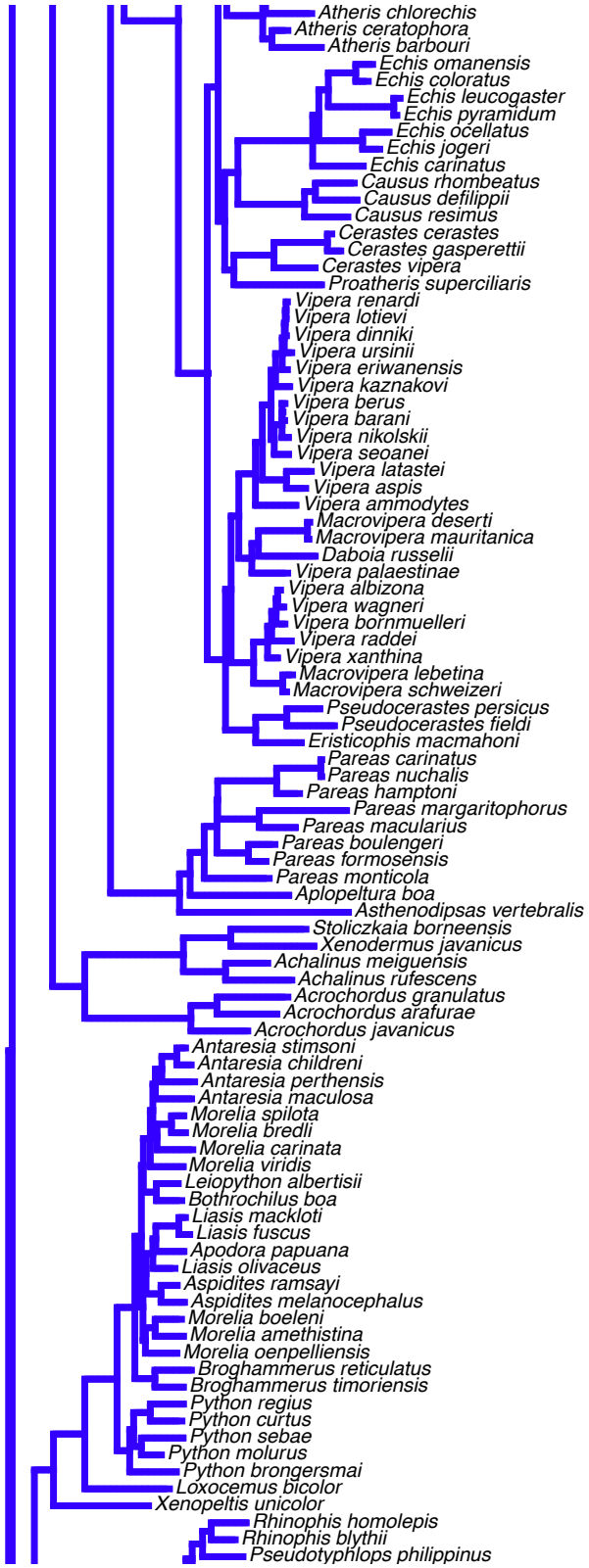

Continue on next page

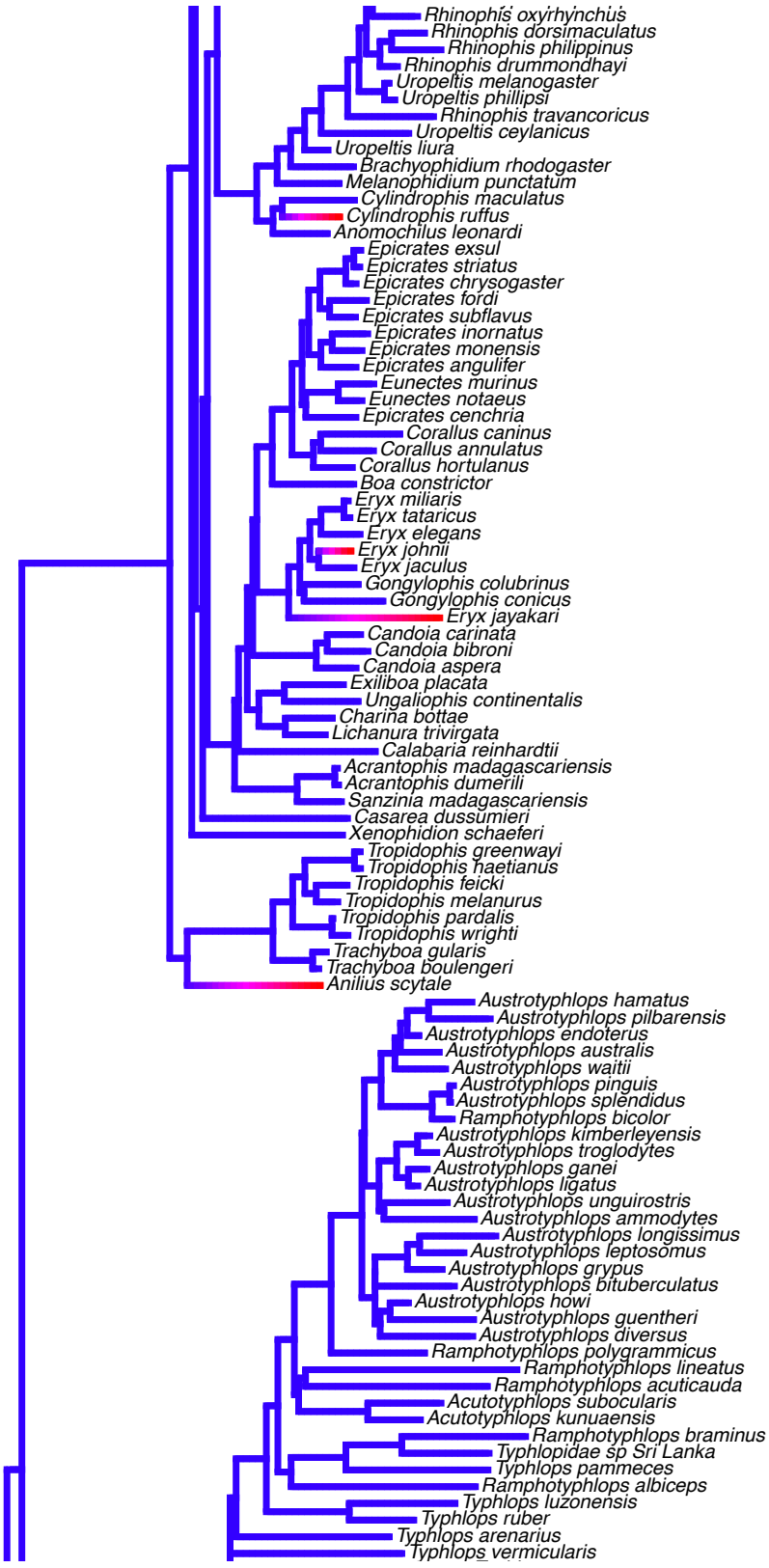

Continue on next page

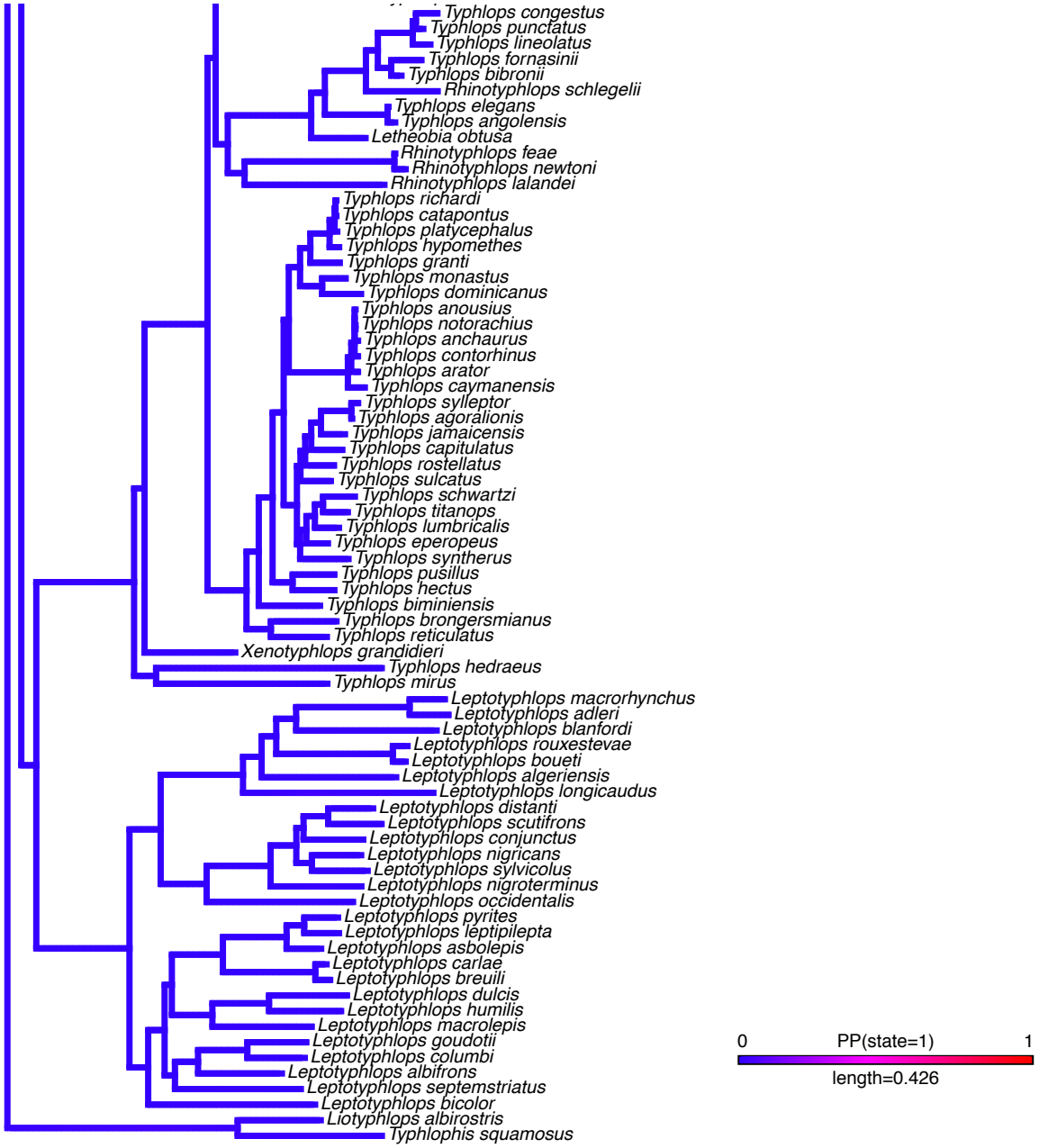

Figure 1. Stochastic character map probability of the presence of red coloration (in red) or the absence of red coloration (in blue). Phylogeny based on Pyron et al 2013.

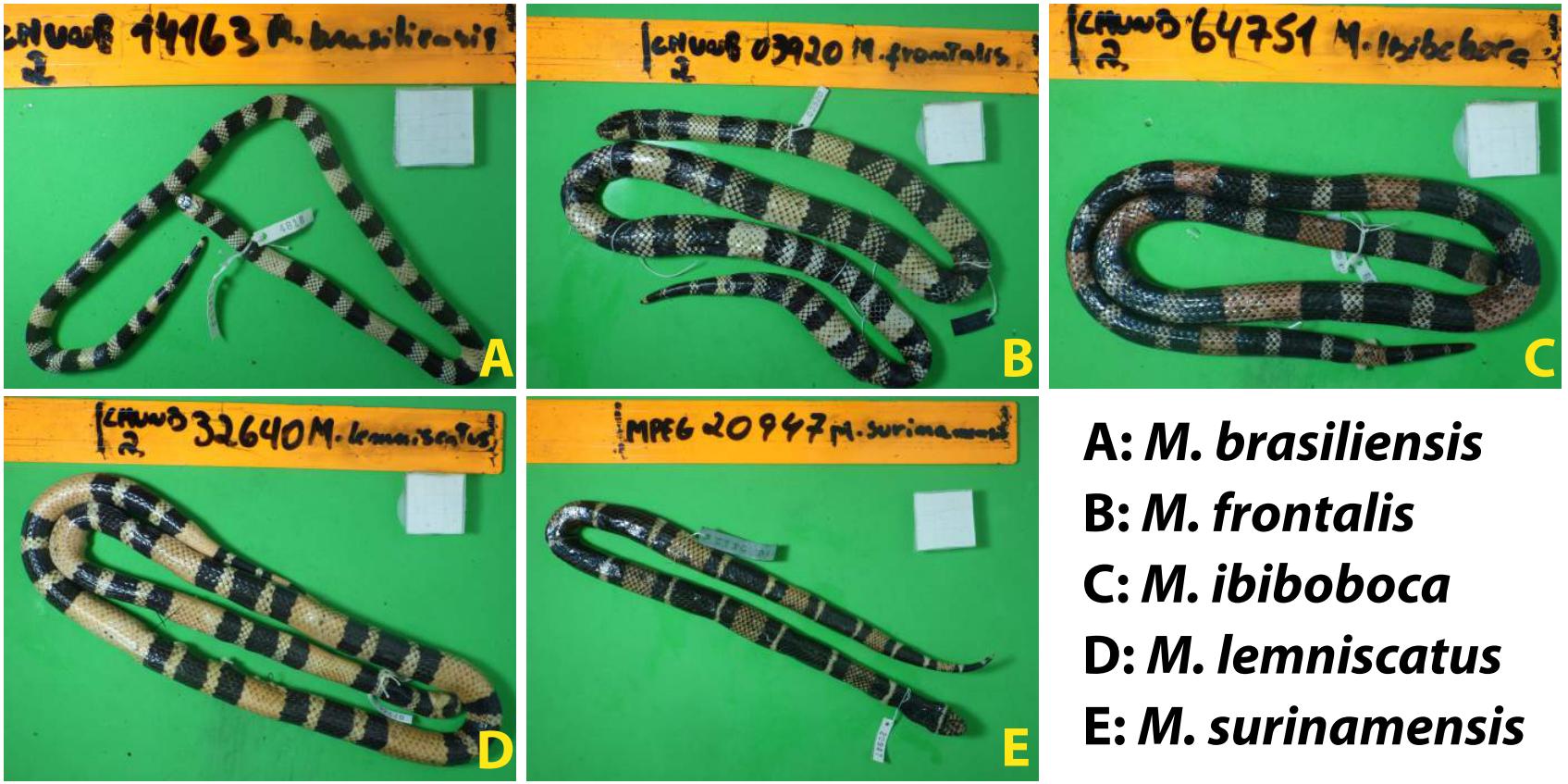

Figure 2. Example of photographs used to take morphological measurements of coral snakes. A: *Micrurus brasiliensis*; B: *M. frontalis*; C: *M. ibiboboca*; D: *M. lemniscatus*; E: *M. surinamensis*.

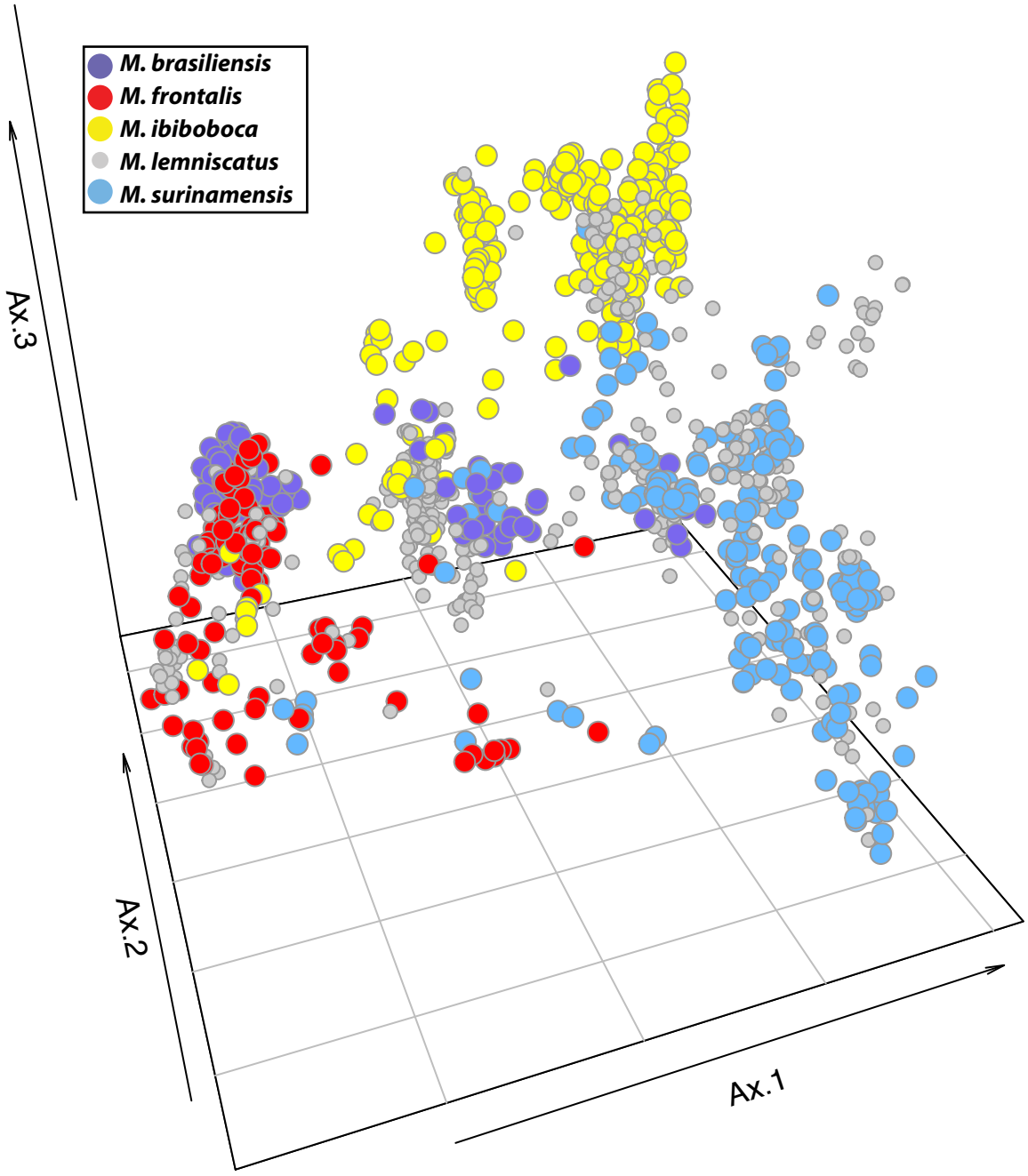

Figure 3. Three-dimensional scatterplot displaying the first three axes of the spatial principal components analysis (sPCA). Each dot represents a lagged (i.e., spatially weighted) score resulting from sPCA of morphological variables of five species of the genus *Micrurus*.

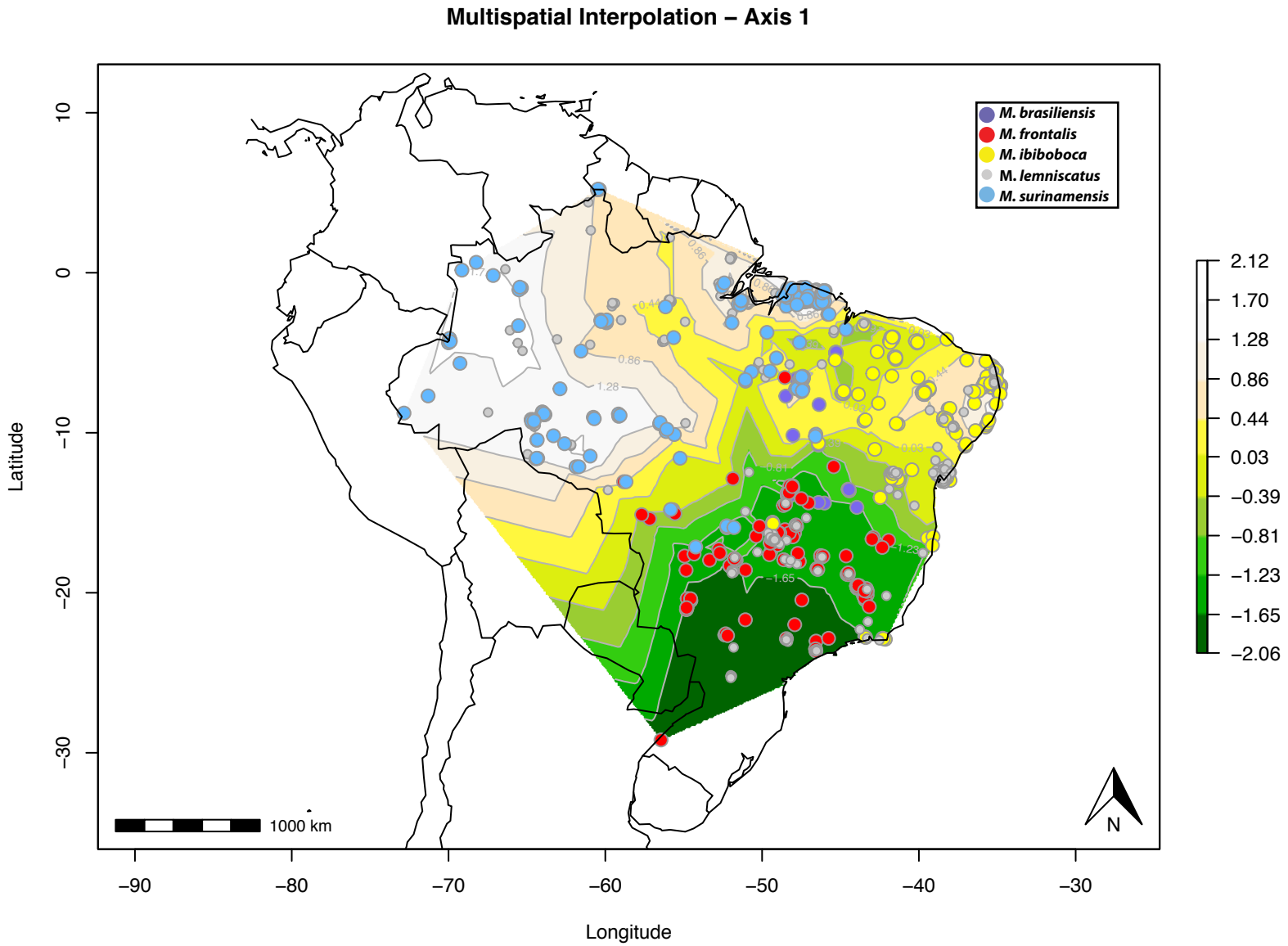

Figure 4. Spatial interpolation of the first sPCA axis. Colored dots represent the five different *Micrurus* species. Background color, ranging from green (negative values) to white (positive values), represents interpolated lagged scores based on sPCA of Micrurus morphological variables.

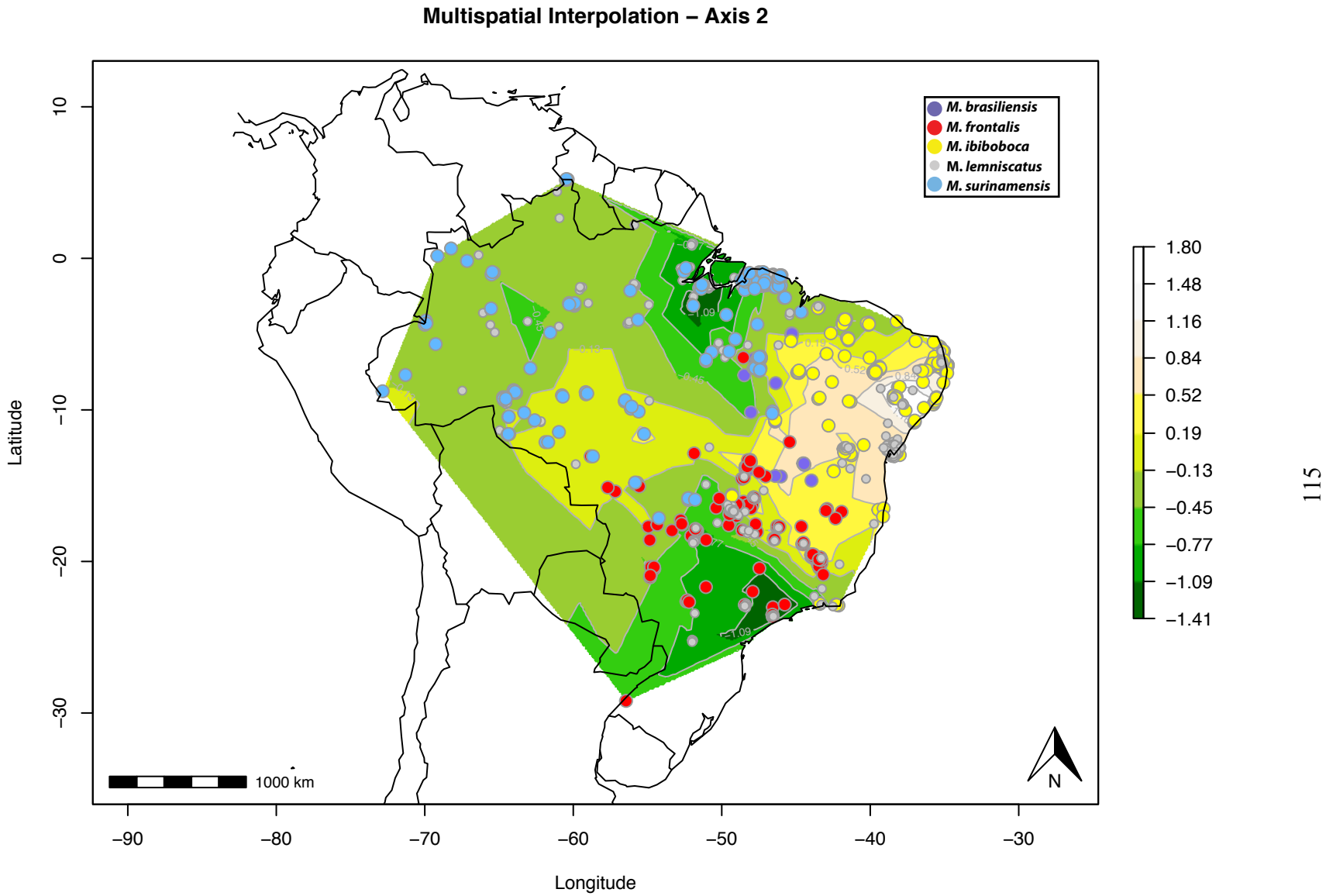

Figure 5. Spatial interpolation of the second sPCA axis. Colored dots represent the five different *Micrurus* species. Background color, ranging from green (negative values) to white (positive values), represents interpolated lagged scores based on sPCA of Micrurus morphological variables.

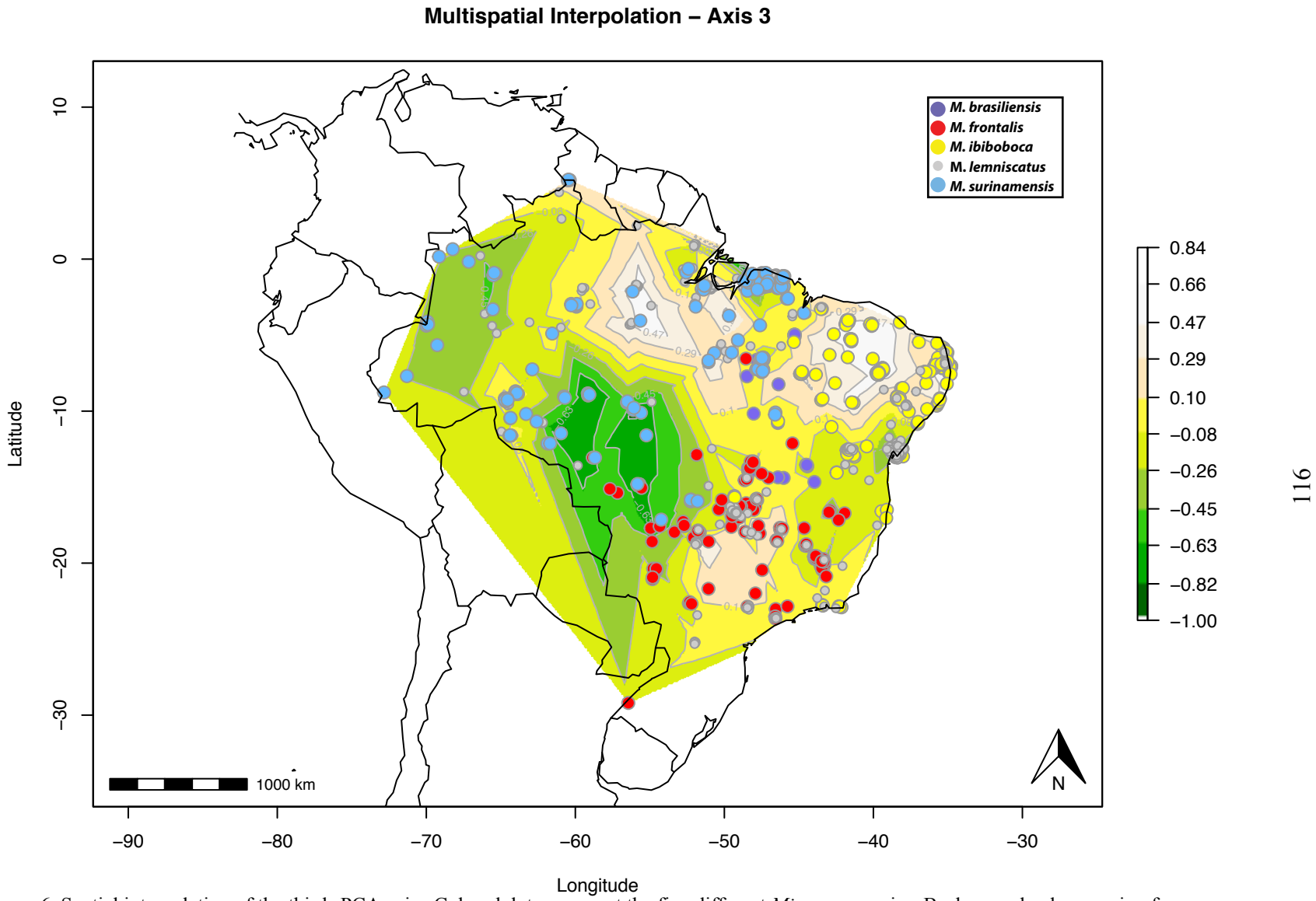

Figure 6. Spatial interpolation of the third sPCA axis. Colored dots represent the five different *Micrurus* species. Background color, ranging from green (negative values) to white (positive values), represents interpolated lagged scores based on sPCA of Micrurus morphological variables.

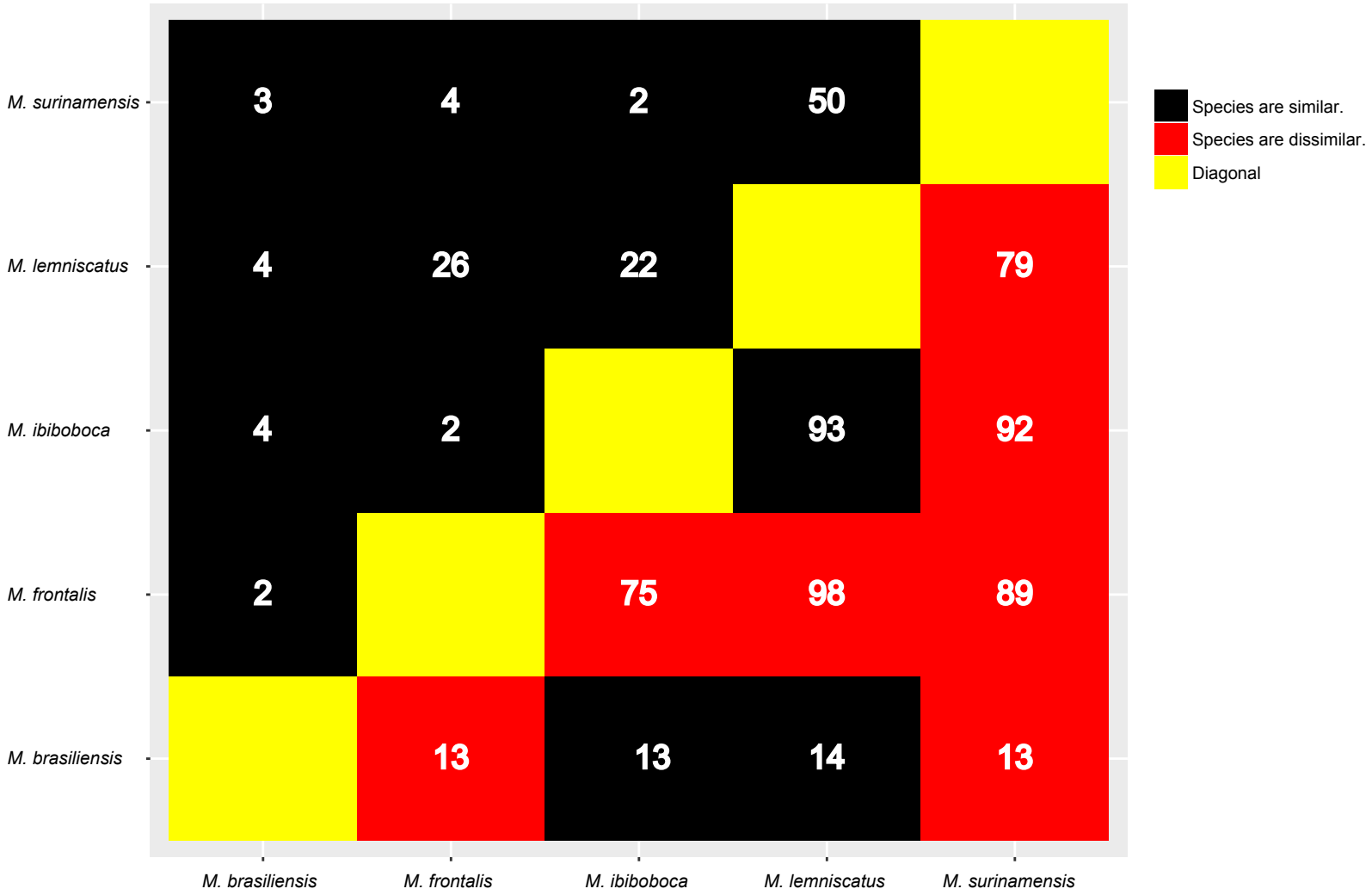

Figure 7. t tests comparing mean lagged scores (first axis) using a grid of size one degree of latitude by one degree of longitude. The upper diagonal shows the number of grid cells where pairs of species overlap. The lower diagonal shows the number of cells where there is no distributional overlap among pairs of species. Values inside each square represent degrees of freedom. Squares are shaded based upon whether a pair of species is similar (black; $p>0.05$) or dissimilar (red; $p<0.05$).

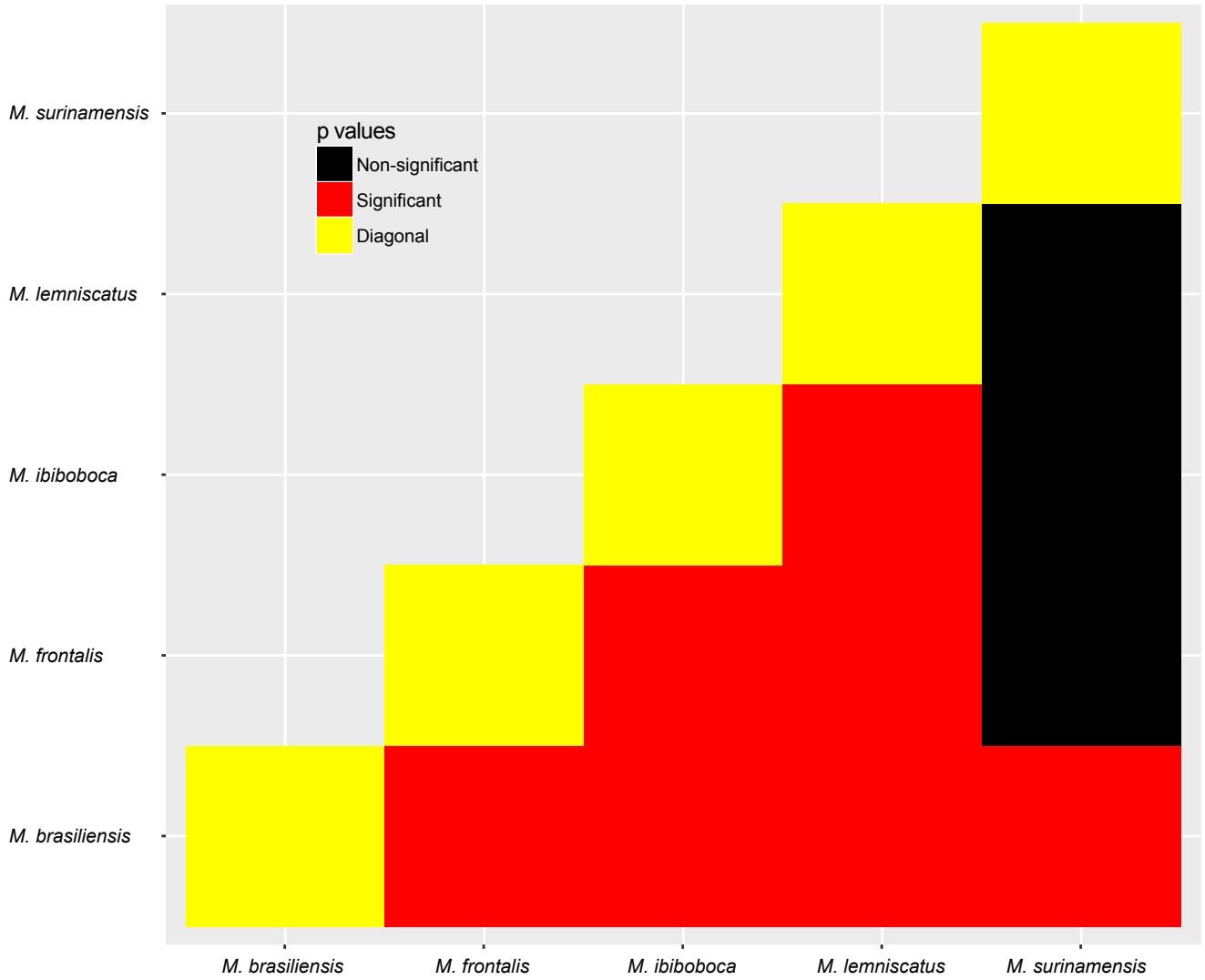

Figure 8. Mantel test results using scores of the first axis of PCA. Red squares: p<0.05; black squares p>0.05.

Figure 9. Photograph of an individual of *Oxyrhopus guibei* from Brasília-DF, Brazil (Photo: Guarino Rinaldi Colli)

Figure 10. Specimen of *Oxyrhopus guibei* showing the morphological variables of this study. Measurements near the head (neck) - A: red band length, B: first black band length, C: first white band length, D: second black band length, E: second white band F: third black band length. Measurements at the mid-portion of the body - G: red band length, H: first black band length, I: first white band length, J: second black band length, K: second white band L: third black band length. M: mismatch length. Numbers: triads count. *: example of triad with mismatch. **: example of triad without mismatch.

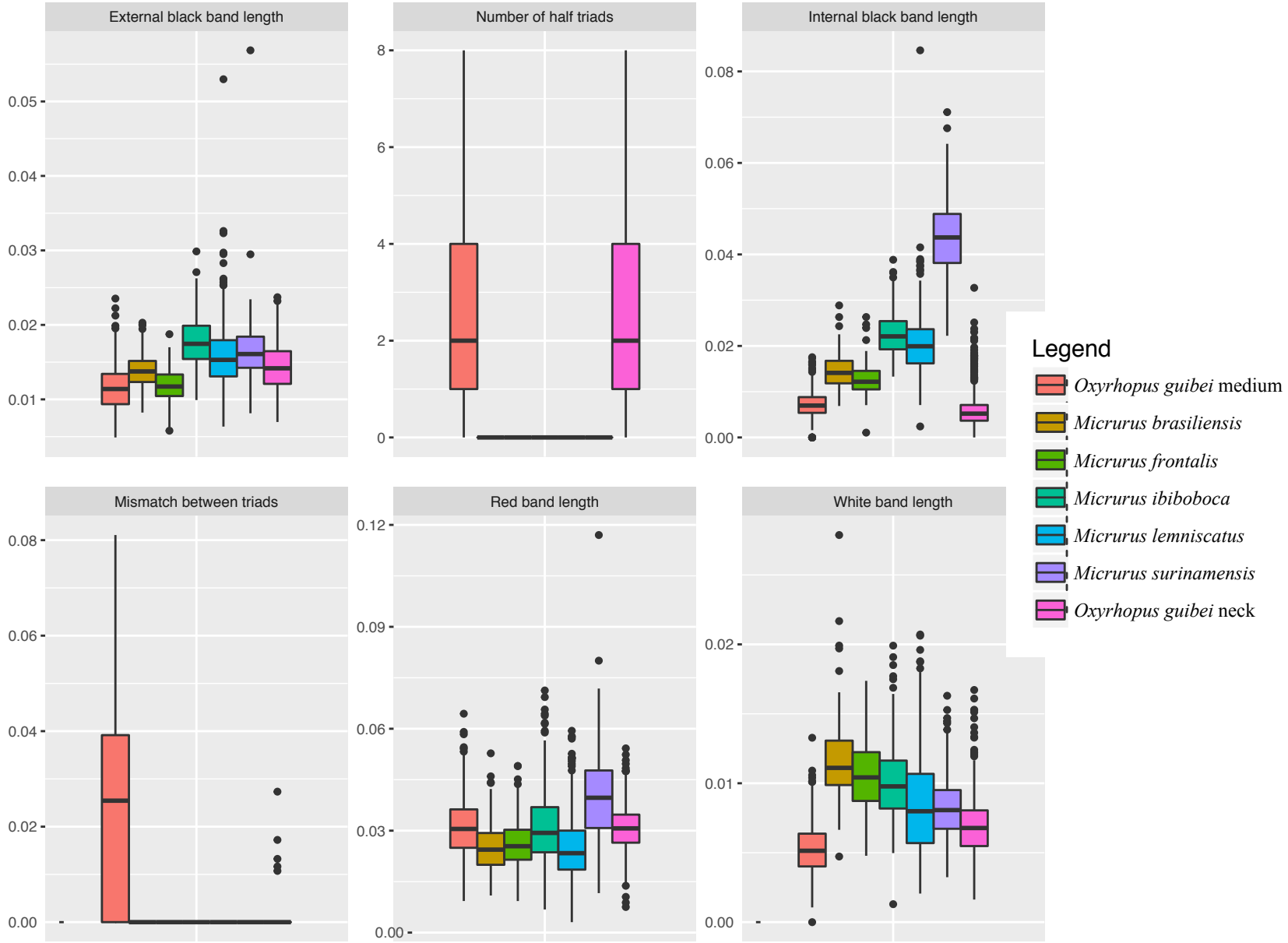

Figure 11. Boxplots displaying the variation of morphological variables on *Oxyrhopus guibei* and *Micrurus* species.

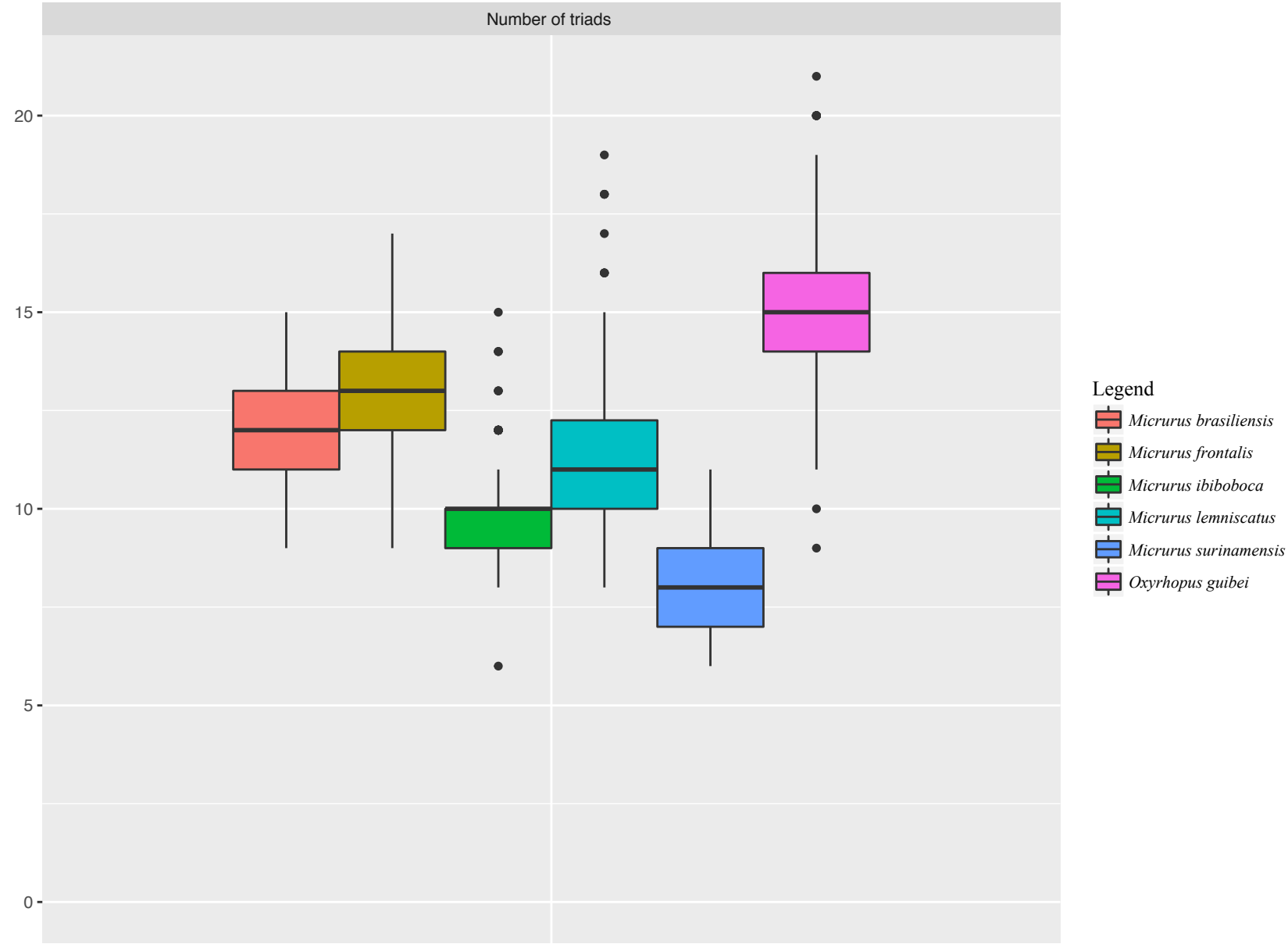

Figure 12. Boxplots displaying the variation of number of triads on *Oxyrhopus guibei* and *Micrurus* species.

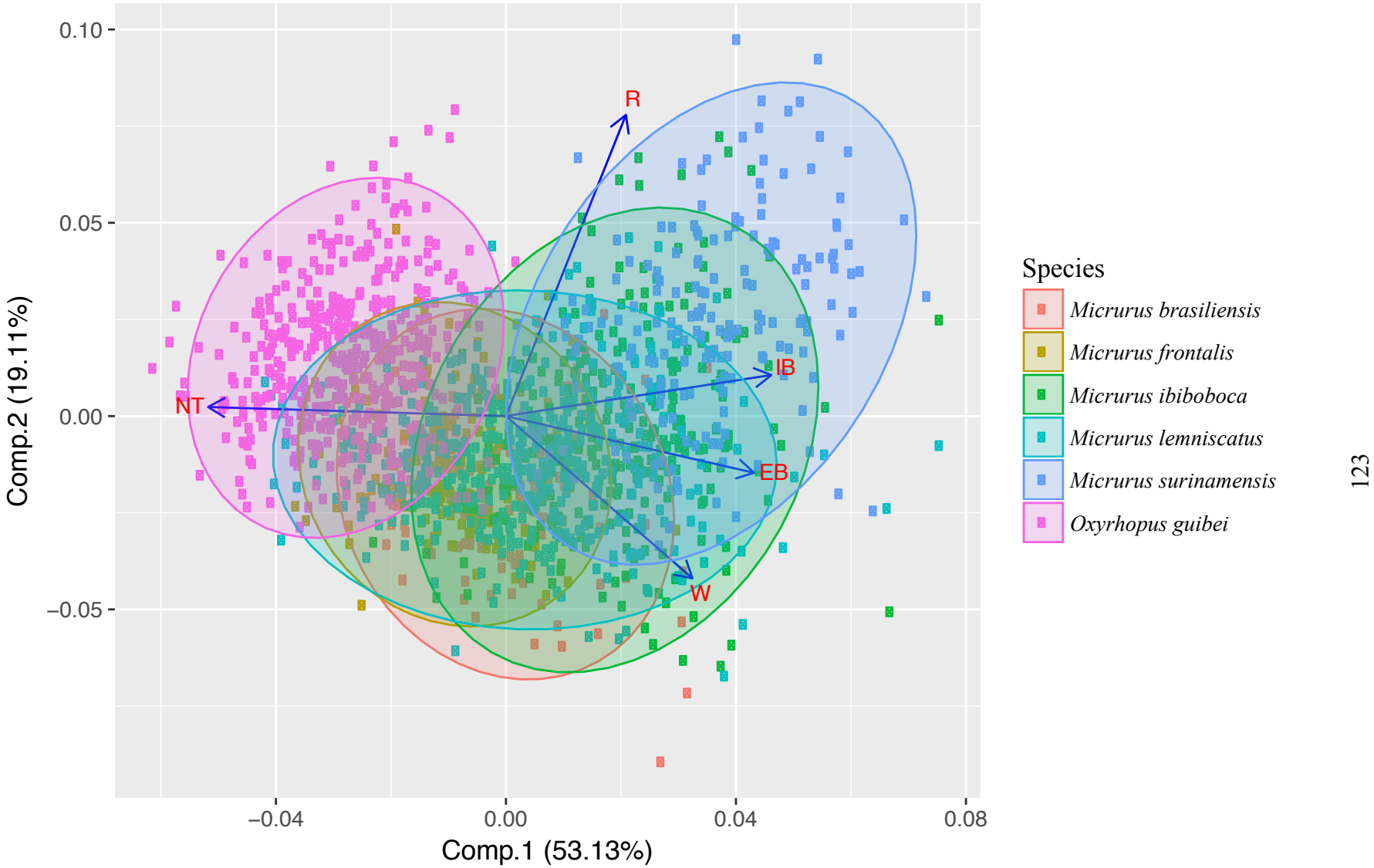

Figure 13. Principal component analysis (axis 1 and 2) of Morfological variables of the mid-portion of the body of *Oxyrhopus guibei* and *Micrurus brasiliensis, M. frontalis, M. lemniscatus* and *M. surinamensis*. Values in parenthesis represent the proportion of variance explained by each component. NT: number of triads, EB: external black band length, IB: internal black band length W: white band length R: red band length.

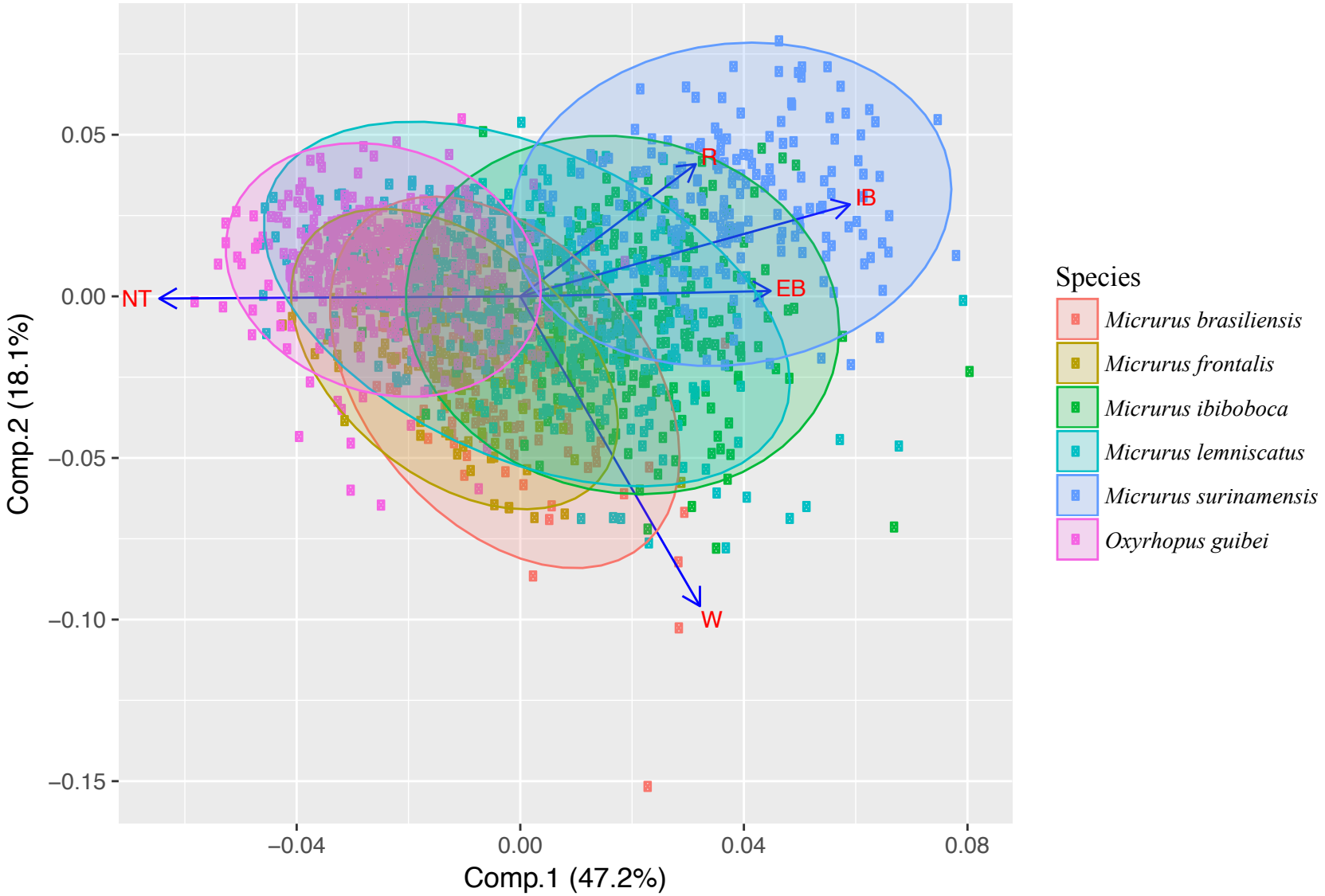

Figure 14. Principal component analysis (axis 1 and 2) of Morfological variables of the body bands closest to the head (neck) of *Oxyrhopus guibei* and *Micrurus brasiliensis, M. frontalis, M. lemniscatus* and *M. surinamensis*. Values in parenthesis represent the proportion of variance explained by each component. NT: number of triads, EB: external black band length, IB: internal black band length W: white band length R: red band length.

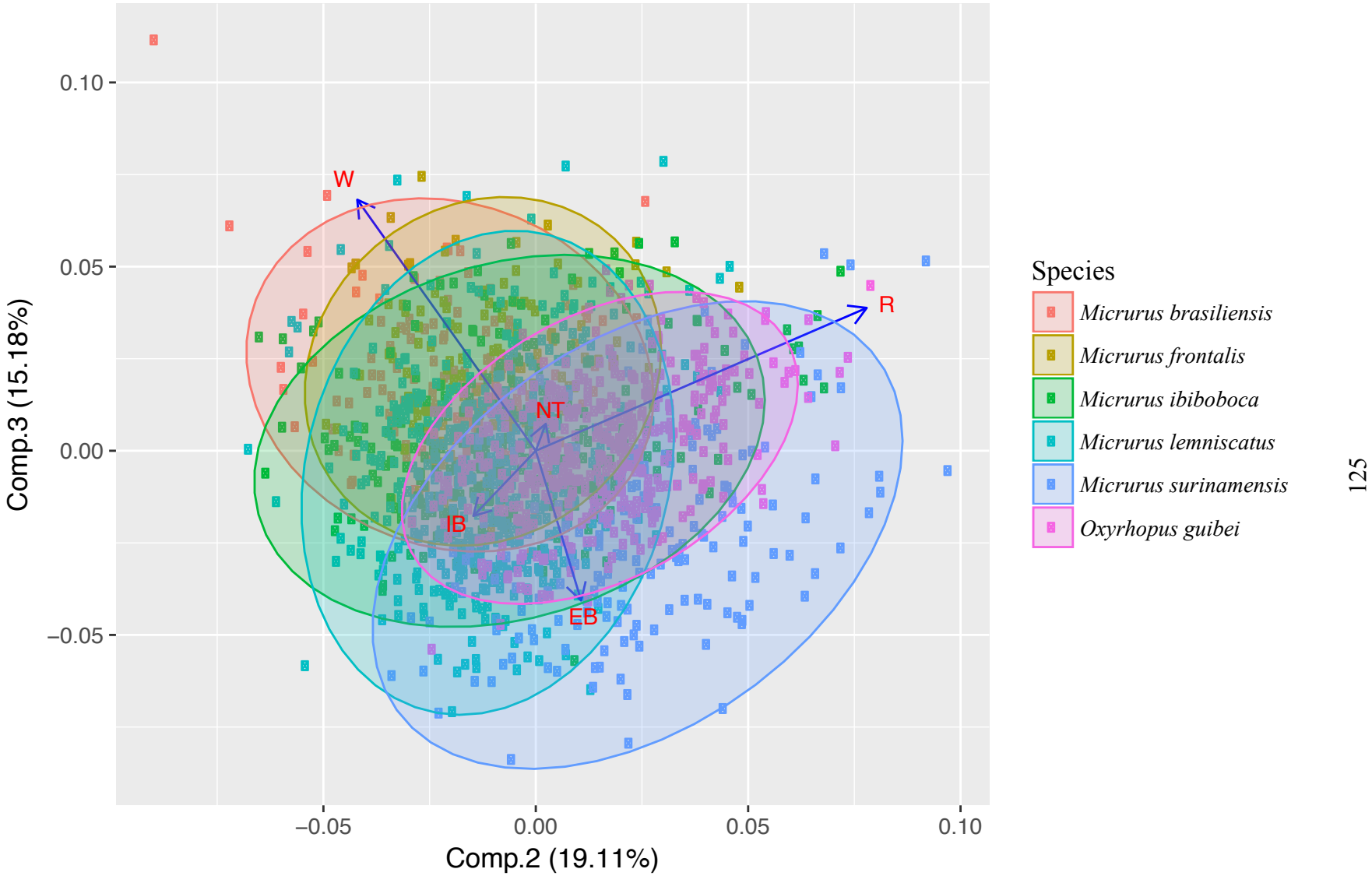

Figure 15. Principal component analysis (axis 2 and 3) of Morfological variables of the mid-portion of the body of *Oxyrhopus guibei* and *Micrurus brasiliensis, M. frontalis, M. lemniscatus* and *M. surinamensis*. Values in parenthesis represent the proportion of variance explained by each component. NT: number of triads, EB: external black band length, IB: internal black band length W: white band length R: red band length.

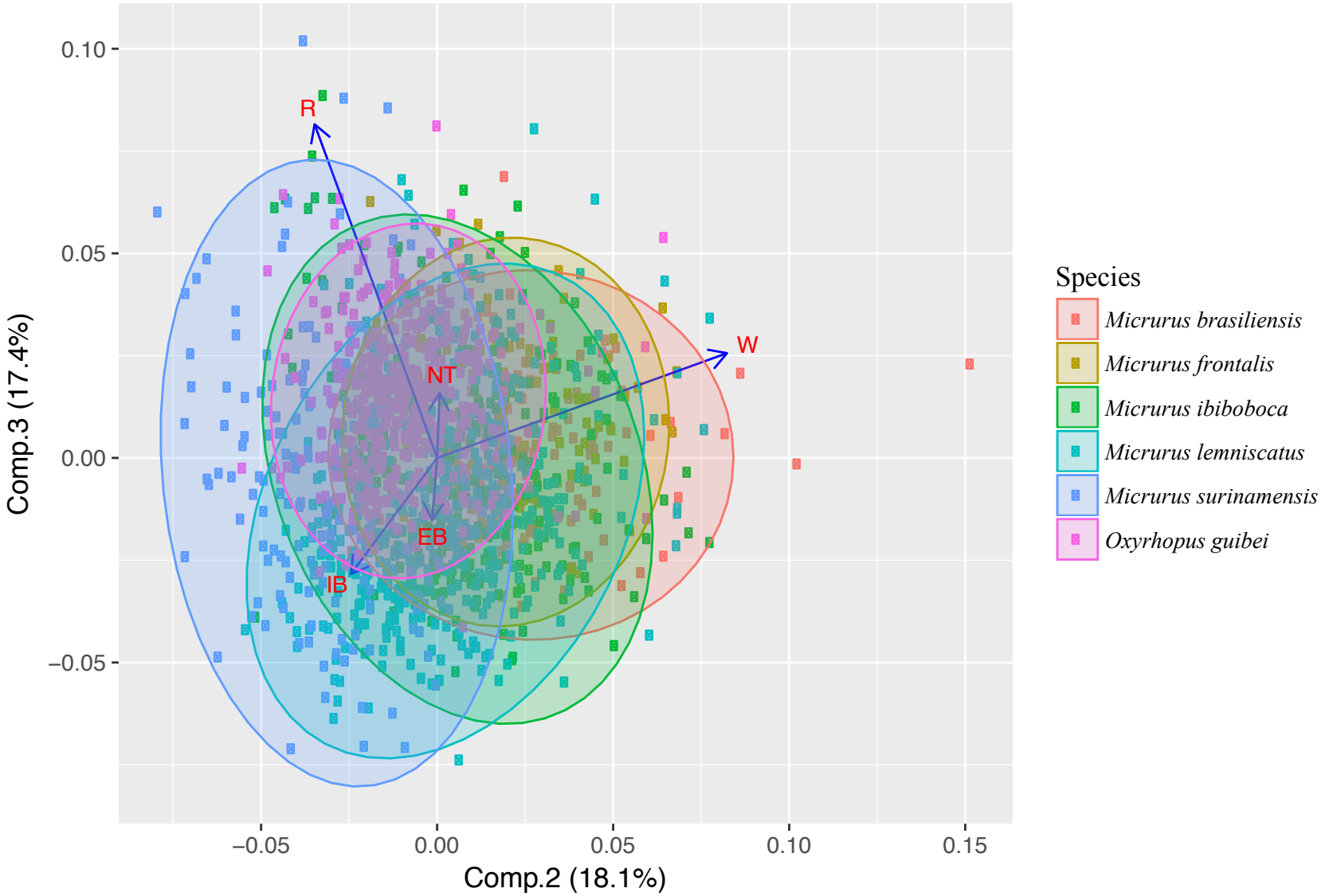

Figure 16. Principal component analysis (axis 2 and 3) of Morfological variables of the body bands closest to the head (neck) of *Oxyrhopus guibei* and *Micrurus brasiliensis, M. frontalis, M. lemniscatus* and *M. surinamensis*. Values in parenthesis represent the proportion of variance explained by each component. NT: number of triads, EB: external black band length, IB: internal black band length W: white band length R: red band length.

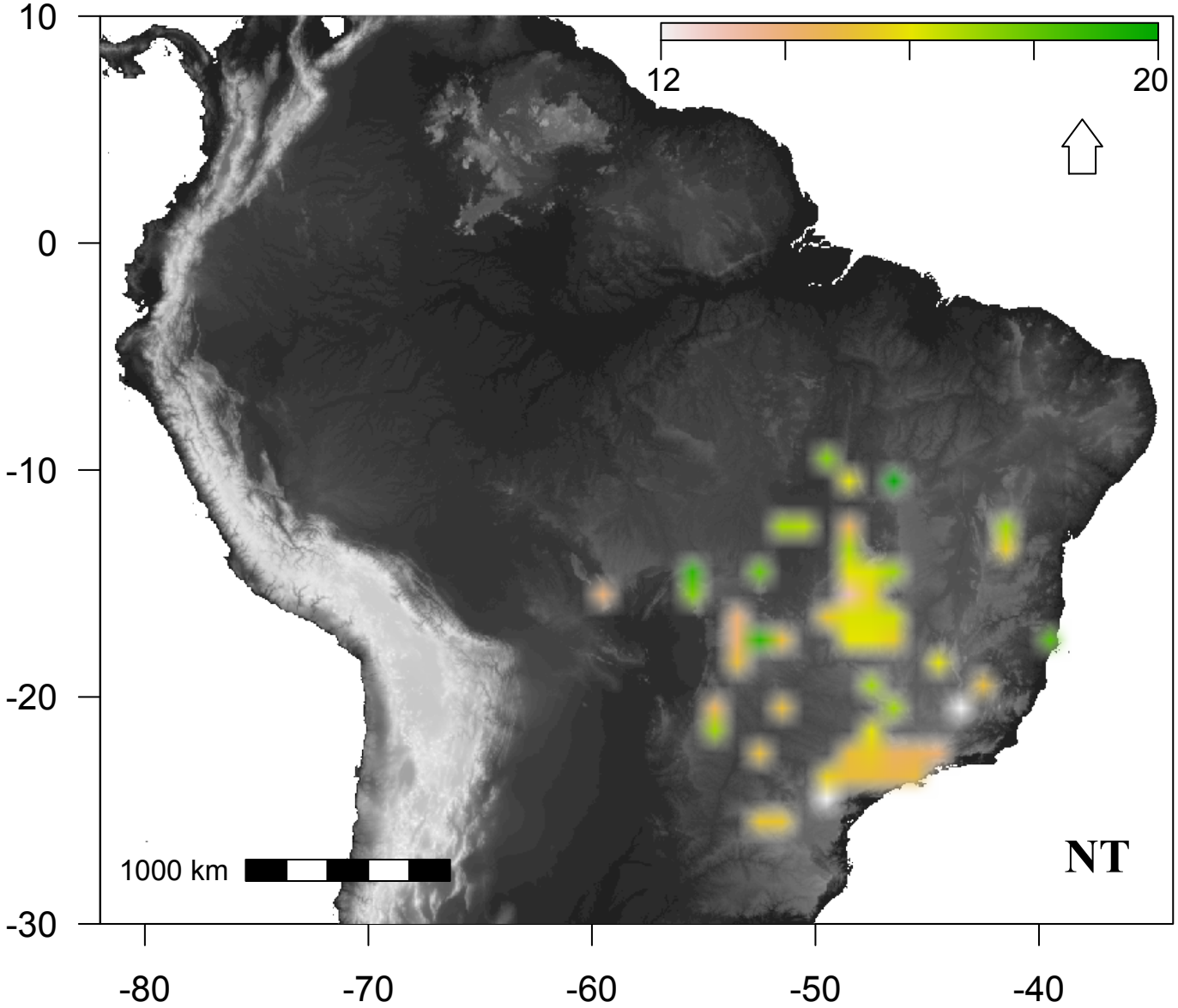

Figure 17. Map displaying the variation on number of triads (NT) in *Oxyrhopus guibei* on 1 degree cells. Each cell represents the average of number of triads per cell. Gray scale represents an altitudinal gradient (darker colors = lower altitude).

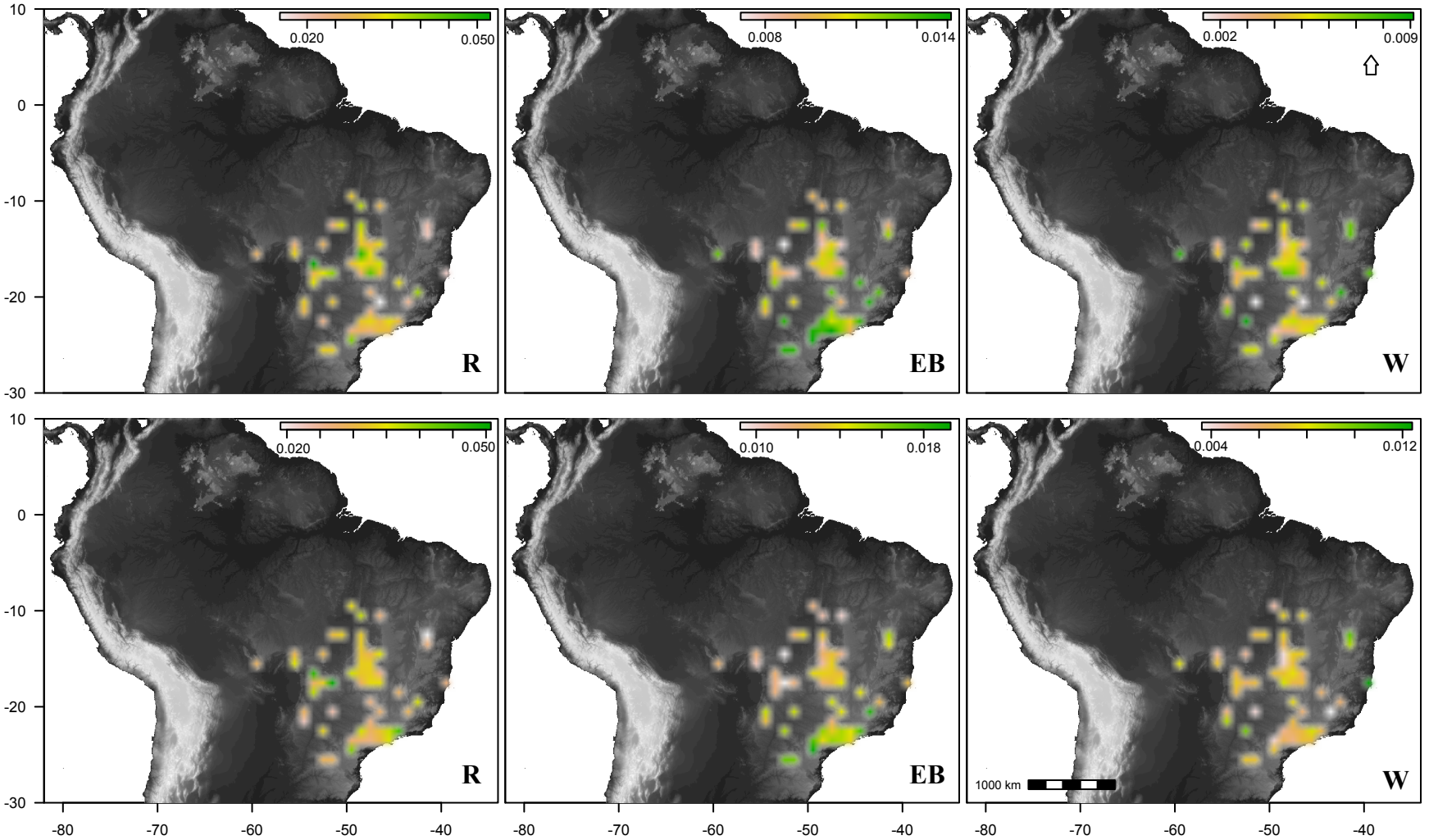

Figure 18. Maps displaying the morphological variation of *Oxyrhopus guibei* on 1 degree cells. Each cell represents the average of the value measured for each morphological variable. Top row are variables of the mid-portion of the body bottom row are variables measured of the body bands closest to the head (neck). R: red band length, EB: external black band length, W: white band length. Gray scale represents an altitudinal gradient (darker colors = lower altitude)

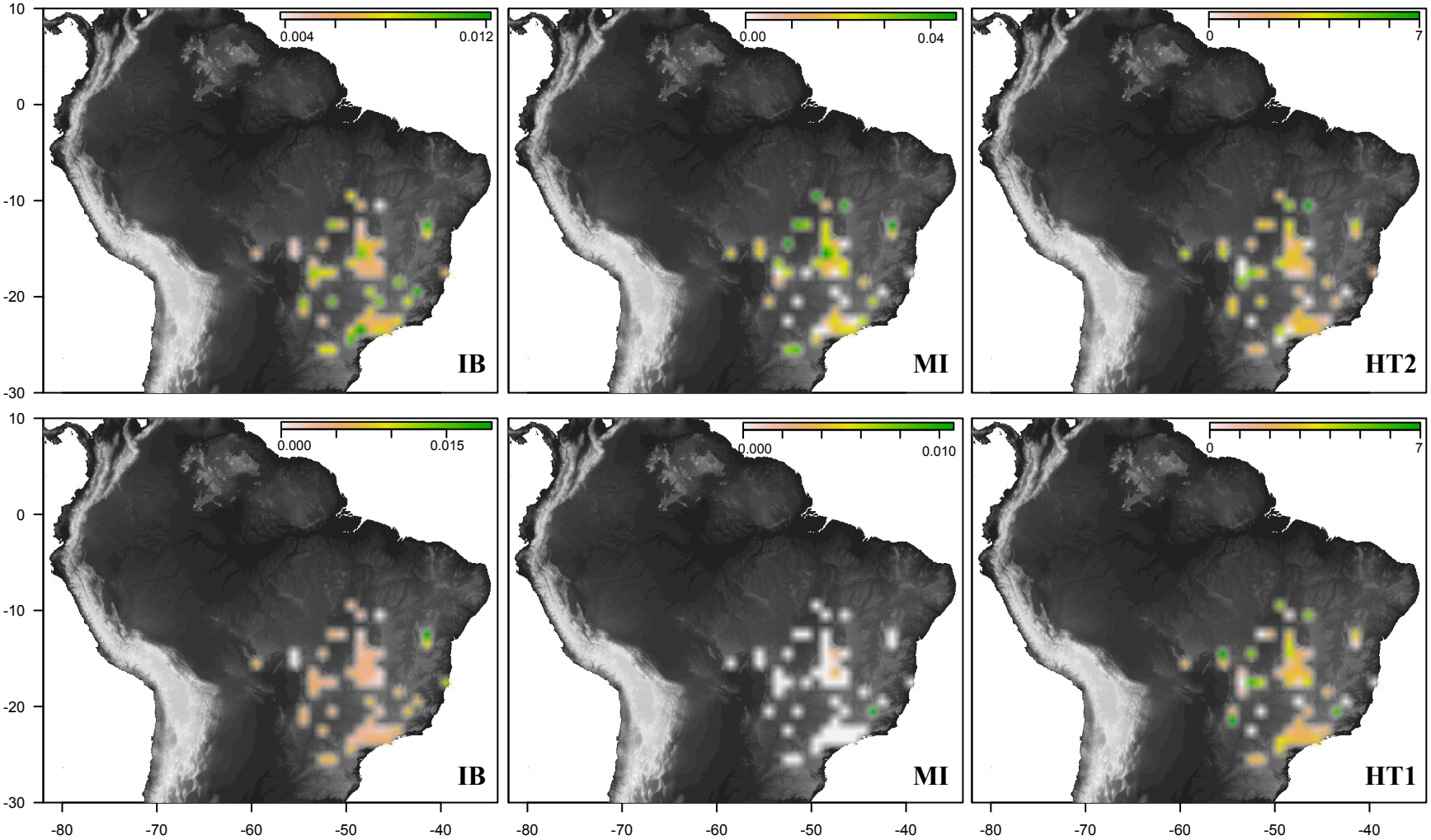

Figure 19. Maps displaying the morphological variation of *Oxyrhopus guibei* on 1 degree cells. Each cell represents the average of the value measured for each morphological variable. Top row are variables of the mid-portion of the body bottom row are variables measured of the body bands closest to the head (neck). IB: internal black band length, MI: mismatch between triads. HT2: number of half triads on the second half of the body, HT1: number of half triads on the first part of the body. Gray scale represents an altitudinal gradient (darker colors = lower altitude).

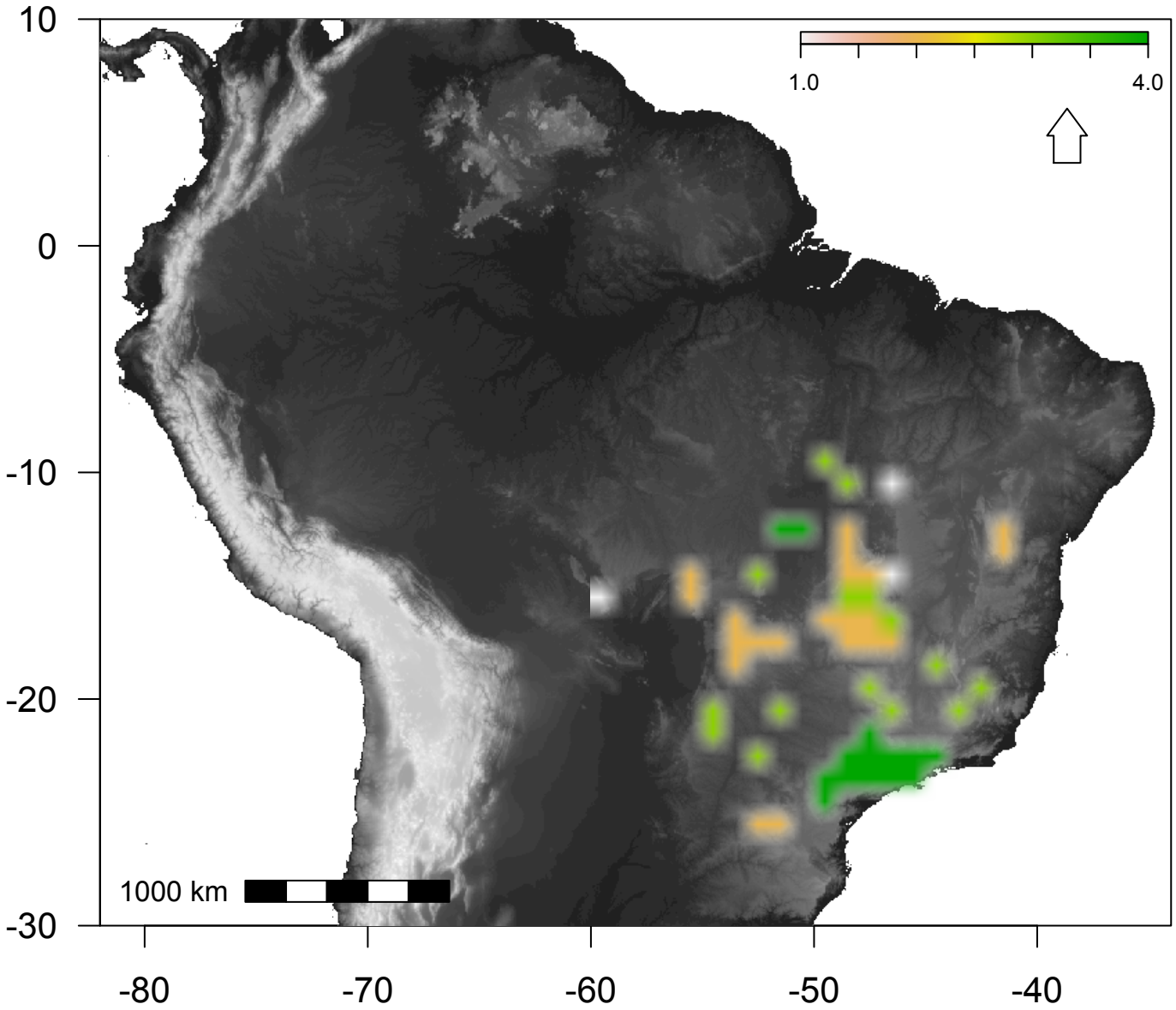

Figure 20. Maps displaying the number of species richness of *Micrurus* based on Bosque et al, 2016 on 1 degree cells.

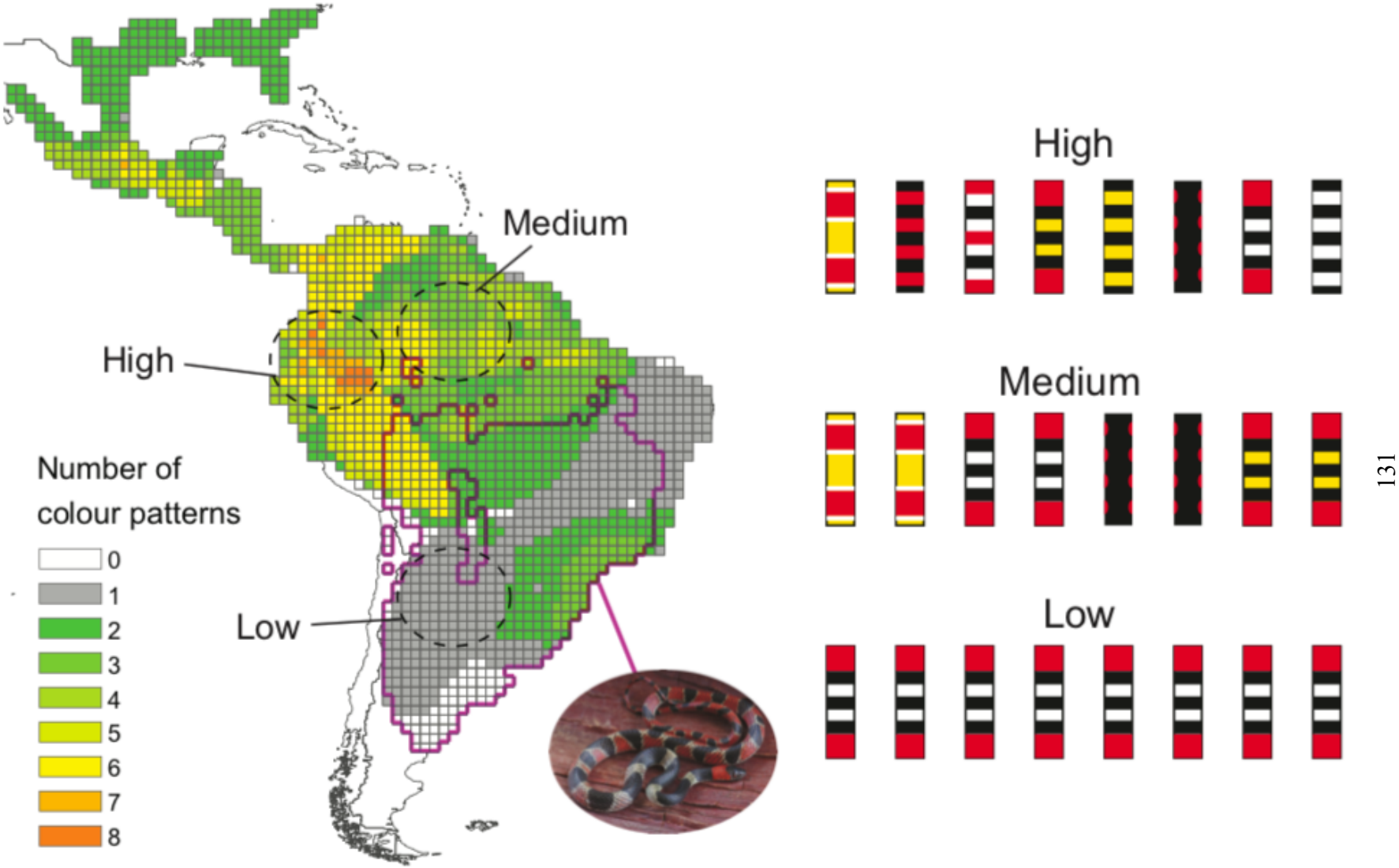

Figure 21. Map with one-degree cells showing *Micrurus* color pattern richness. To the right are patterns used in the exposure phase. In pink the distribution of *Oxyrhopus rhombifer*. Map based on data from Bosque et al, 2016.

Figure 22. Bird feeders used during the experiment. Colors of the feeders are based on coloration of coral snakes of the genus Micrurus (model) and its mimic *Oxyrhopus rhombifer* (aposematic-imperfect). High, medium and low represent the number of color pattern richness that birds were exposed prior to test with a brown or/and aposematic-imperfect feeder.

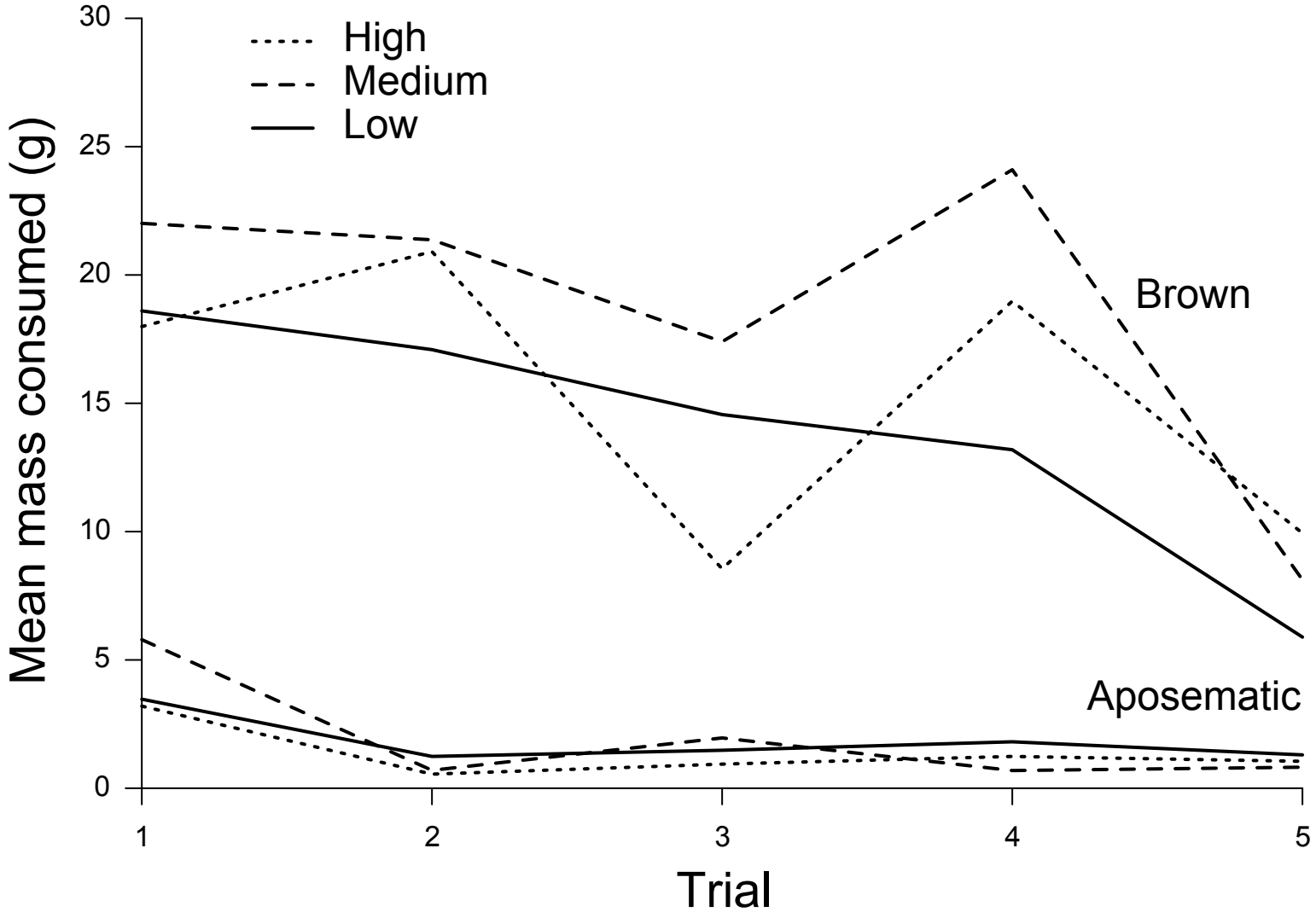

Figure 23. Bird food mass eaten by chickens after 10 min (rounds 1-5) of exposure. Top lines show feeders with brown coloration. Bottom lines show aposematic feeders (*Micrurus* patterns). High: 8 aposematic patterns; medium: 4 aposematic patterns; low: 1 aposematic pattern.

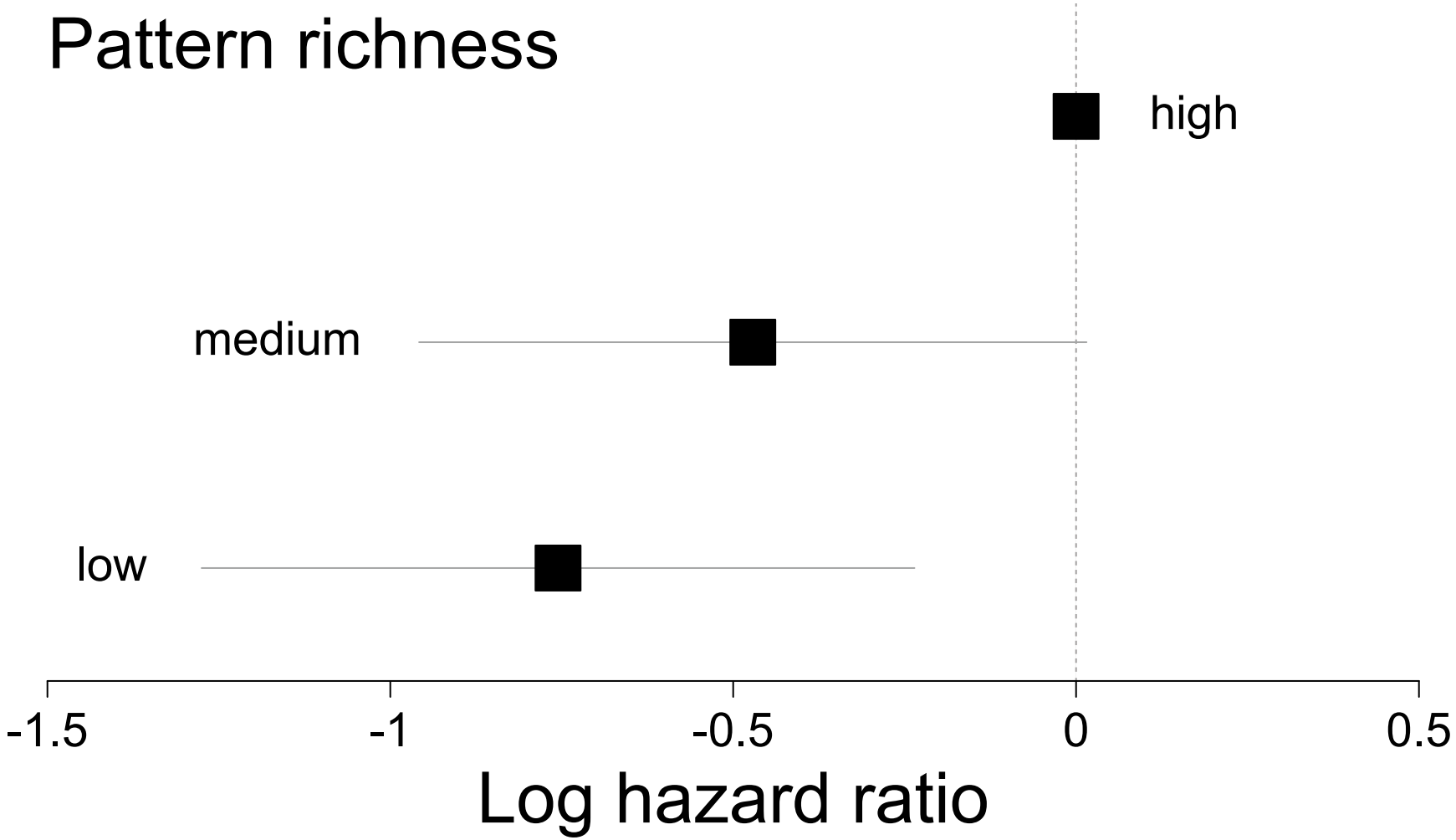

Figure 24. Survival analysis modeling hesitation time for chicks exposed as a group to different coral snake pattern richness to peck at feeders painted with non-aposematic (brown) or aposematic-imperfect patterns as a function of pattern richness. Graphs depict log hazard ratios estimated by a Cox proportional hazards model having high color pattern richness as reference compared to log hazard ratio of medium and low pattern richness; horizontal bar represents 95% confidence interval.

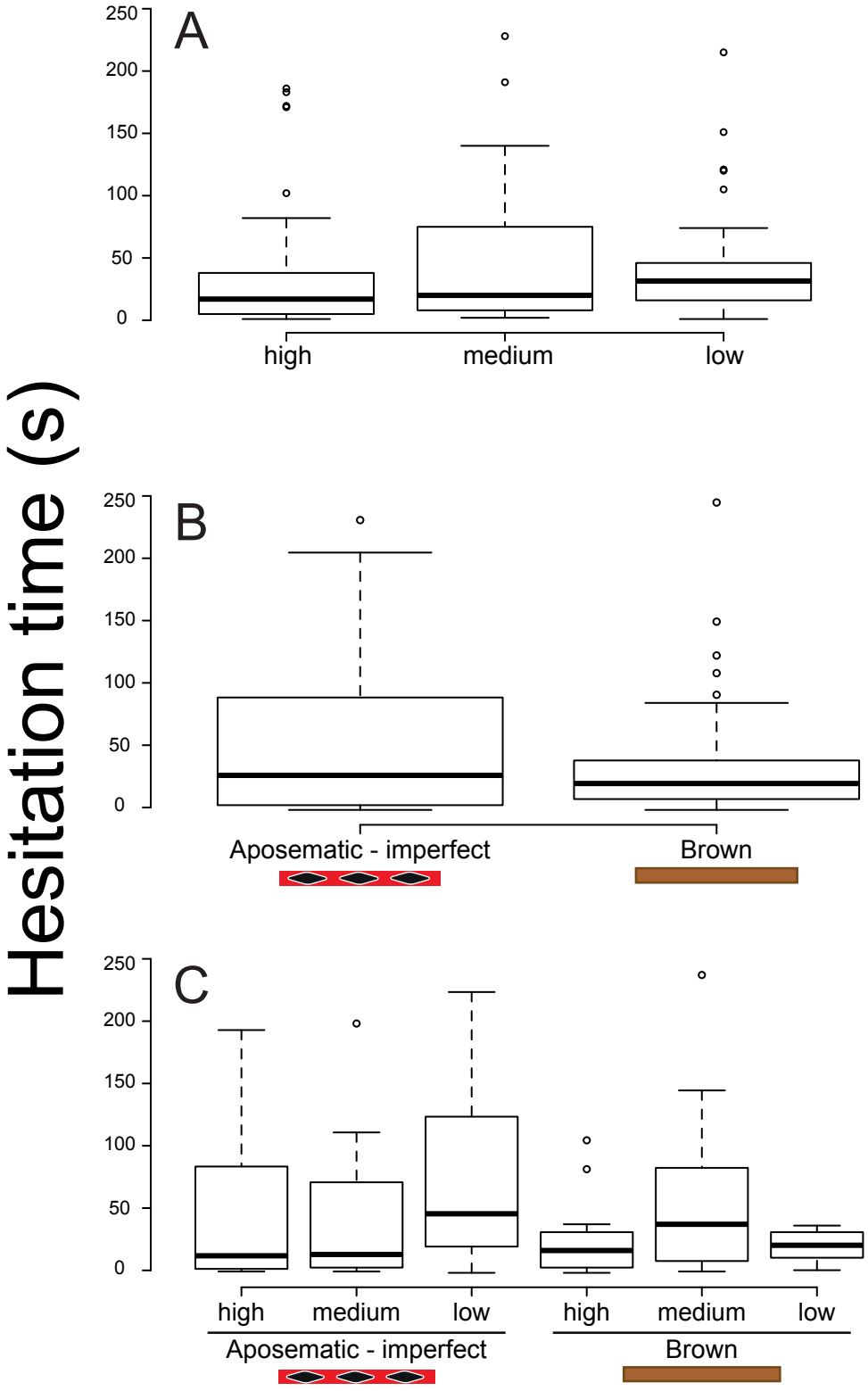

Figure 25. Hesitation time for chicks exposed as a group to different coral snake pattern richness to peck on feeders painted with non-aposematic (brown) or aposematic-imperfect patterns. A – hesitation time comparing color pattern rich- ness. B - hesitation time compar- ing non-aposematic imperfect versus brown feeder. C hesitation time comparing A & B.

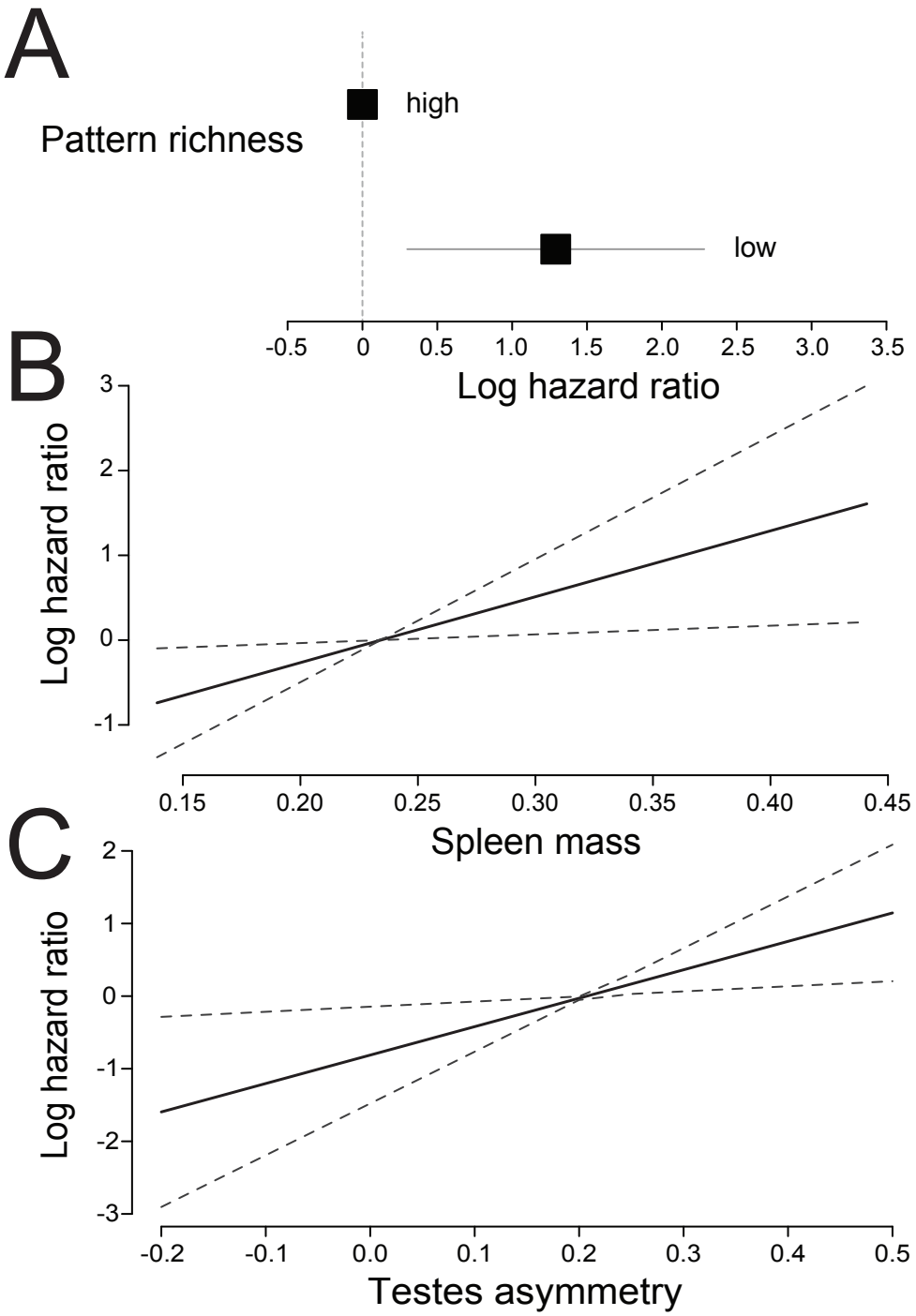

Figure 26. Survival analysis modeling hesitation time for chicks individually exposed to different coral snake pattern richness to peck on feeders painted with non-aposematic (brown) and aposematic-imperfect patterns as a function of pattern richness, spleen mass, and testes asymmetry. Graphs depict log hazard ratios estimated by a Cox proportional hazards model as a function of the three predictors. A: log hazard ratio reference (high color pattern richness) compared to log hazard ratio of low pattern richness; horizontal bar represents 95% confidence interval. B: linear fit of the log hazard ratio as a function of spleen mass; dashed line represents 95% confidence interval. C: linear fit of the log hazard ratio as a function of testes asymmetry; dashed line represents 95% confidence interval.

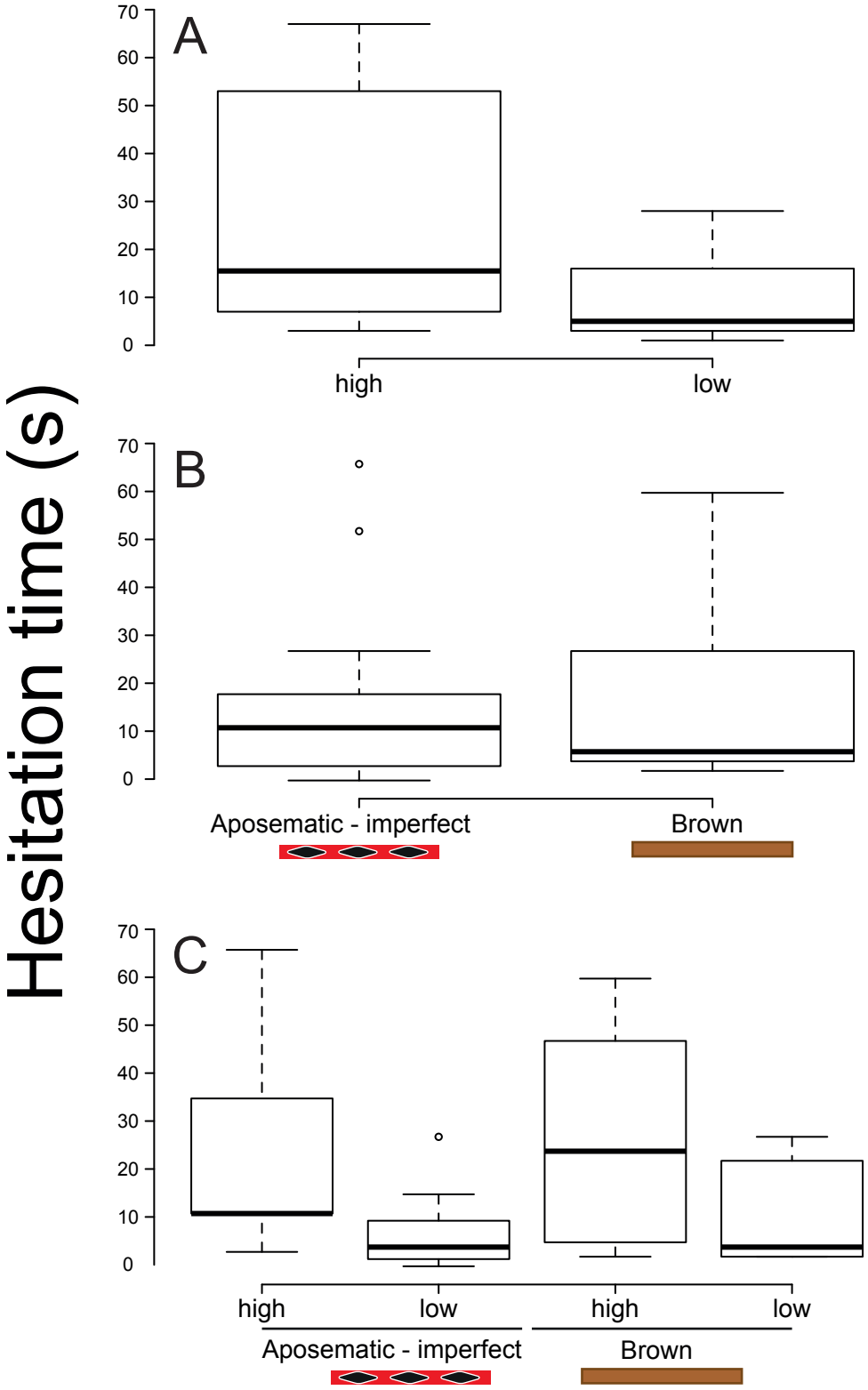

Figure 27. Hesitation time for chicks individually exposed to different coral snake pattern richness to peck on feeders painted with non-aposematic (brown) and aposematic-imperfect patterns. A – hesitation time comparing color pattern richness. B - hesitation time comparing non-aposematic imperfect versus brown feeder. C hesitation time comparing A & B.

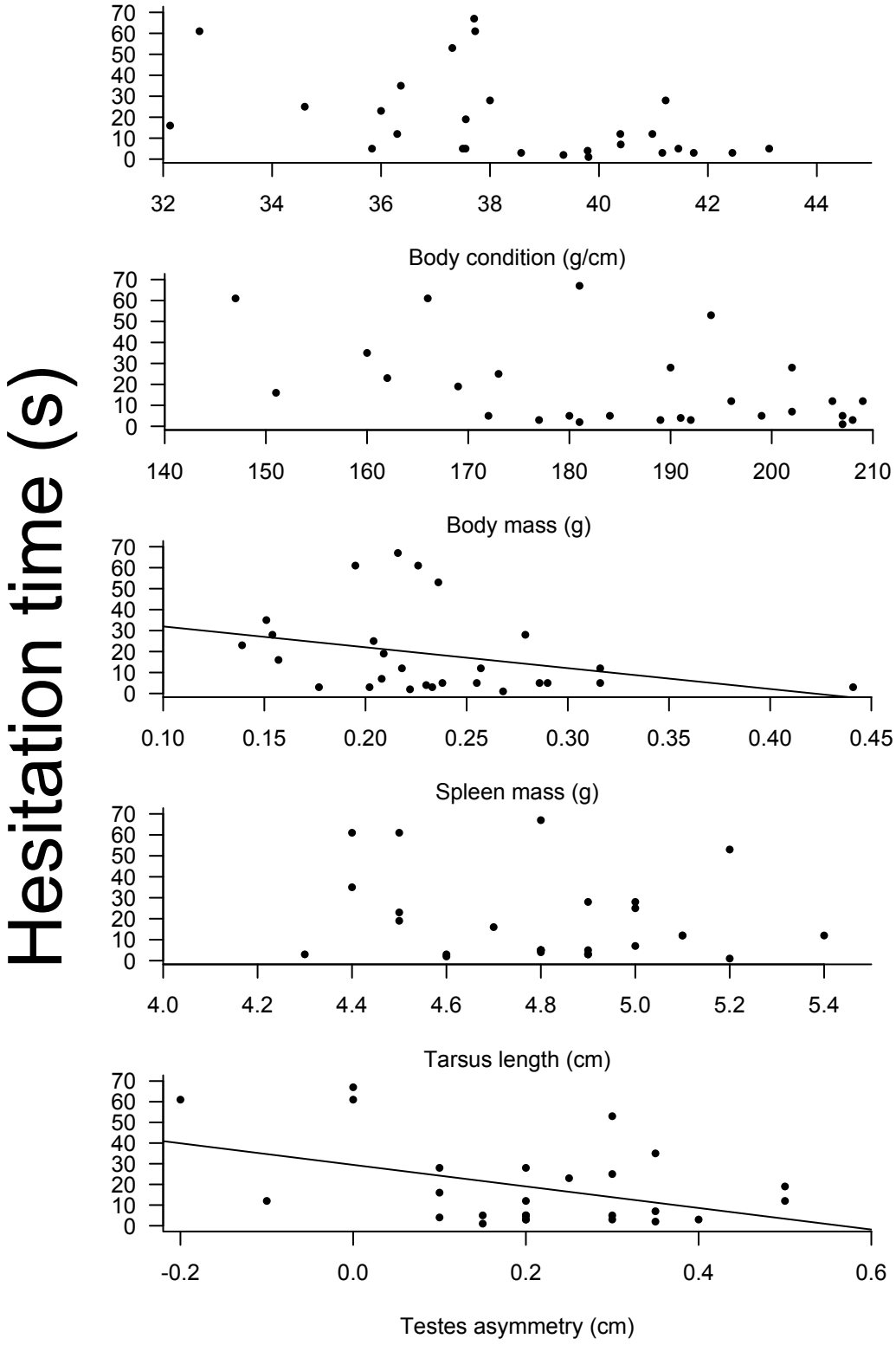

Figure 28. Hesitation time and morphological measurements for chicks individually exposed to different coral snake pattern richness to peck on feeders painted with non-aposematic (brown) and aposematic-imperfect patterns.

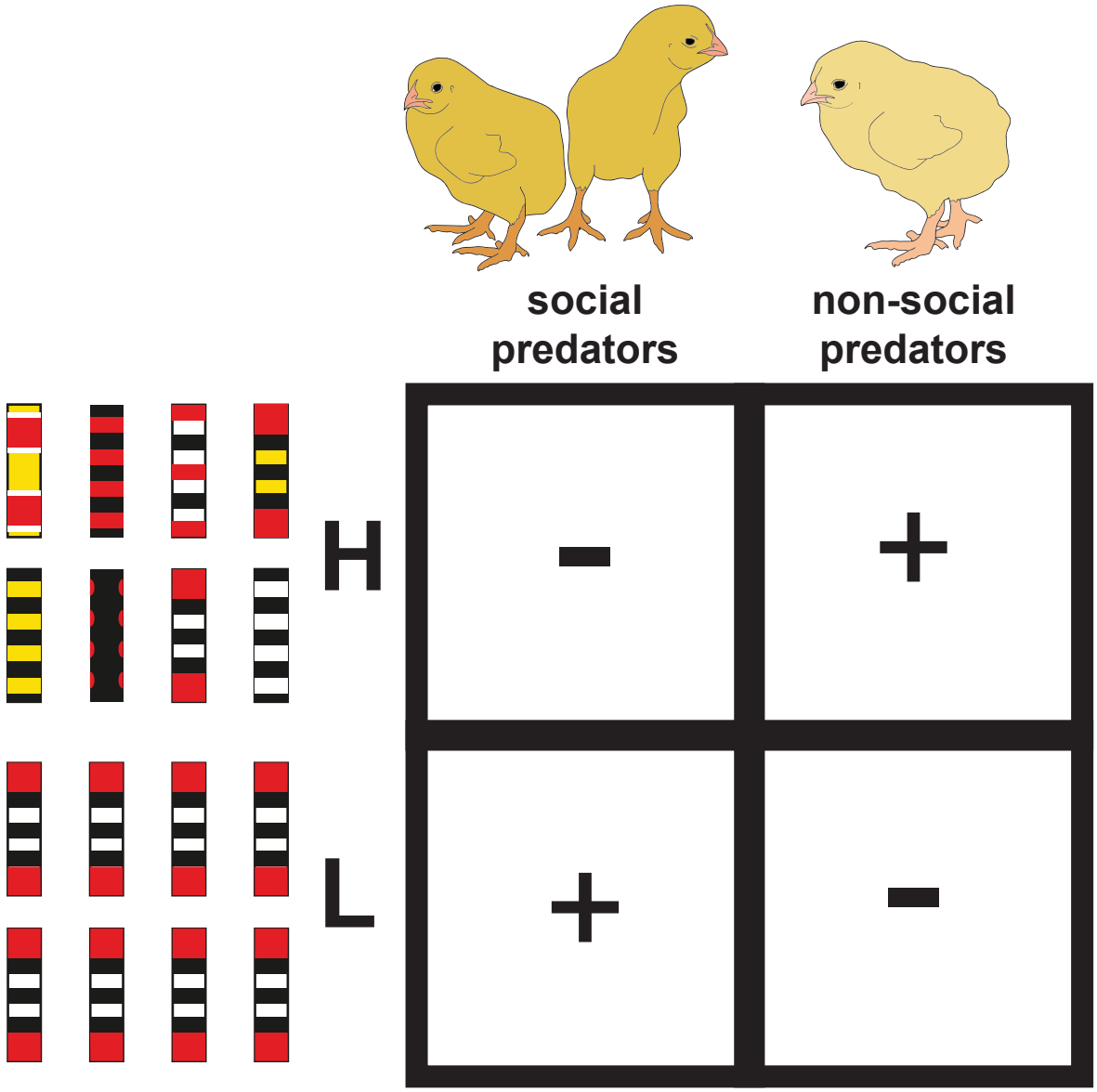

Figure 29. Diagram showing the effect of social and non-social predators on the evolution of mimicry/color pattern diversity. In areas of high model color diversity (H) new color patterns can be favored (+) by reduced predation pressure as a result of higher attack hesitation of non-social predators and disfavored (-) by lower attack hesitation of social predators. In areas of low pattern diversity (L) new color patterns can be favored (+) by reduced predation pressure as a result of higher attack hesitation of social predators and disfavored (-) by lower attack hesitation of non-social predators.

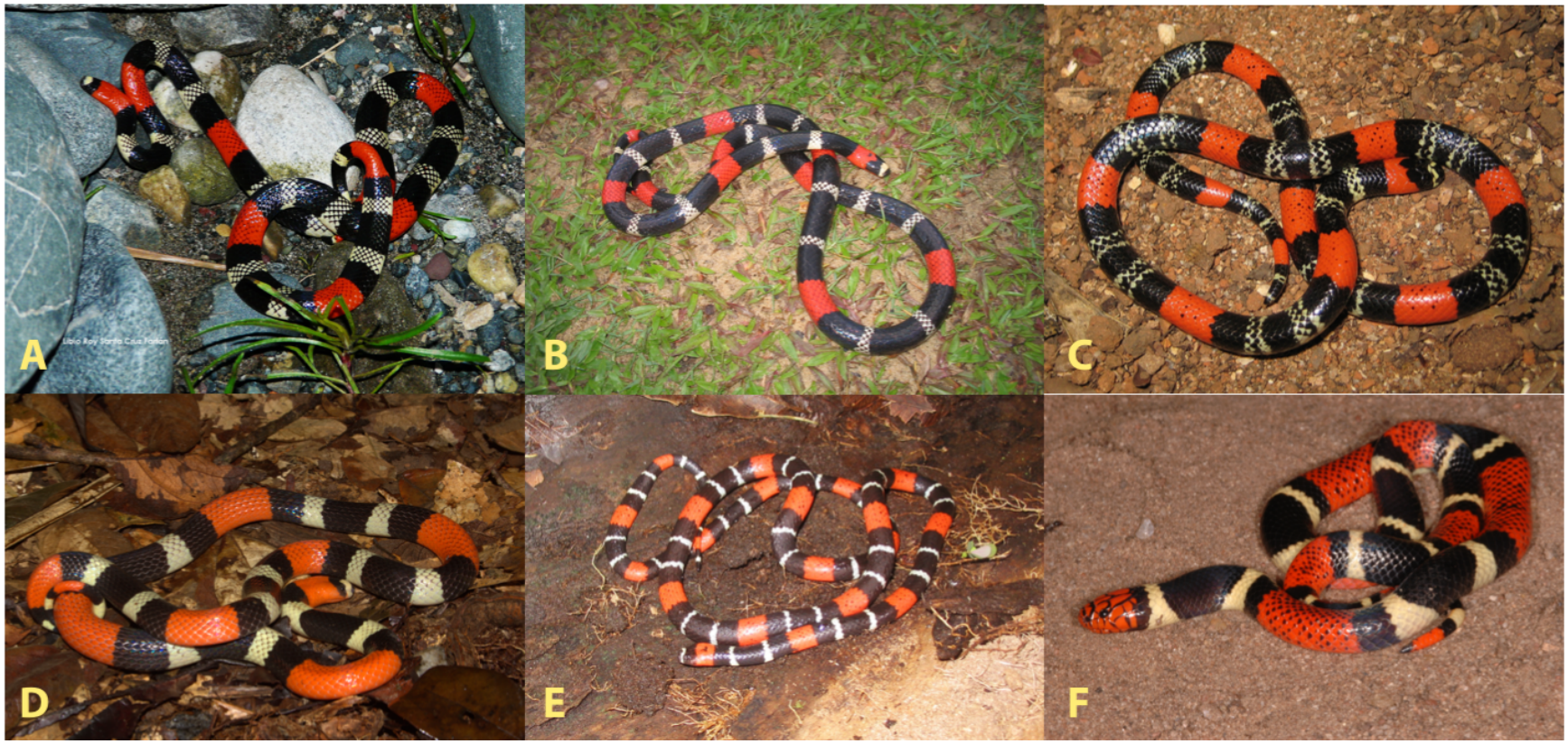

Figure 30. Photographs of species of the genus *Micrurus*. A: *M. lemniscatus lemniscatus*, Madre de Dios, Peru (photo by Roy Libio Santa Cruz). B: *M. lemniscatus lemniscatus*, Letícia, Colômbia (photo by Jairo Maldonado) C: *M. lemniscatus carvalhoi*, Santa Cruz do Rio Pardo, São Paulo, Brazil (photo by Nelson Jorge da Silva Júnior). D: *M. lemniscatus diutius*, Paracou, French Guyana (photo by Antoine Fouquet). E: *M. filiformis*, Santa Barbara do Pará, Pará Brazil (photo by Ulisses Galatti). F: *M. surinamensis*, Goiás Brazil (photo by Nelson Jorge da Silva Júnior).

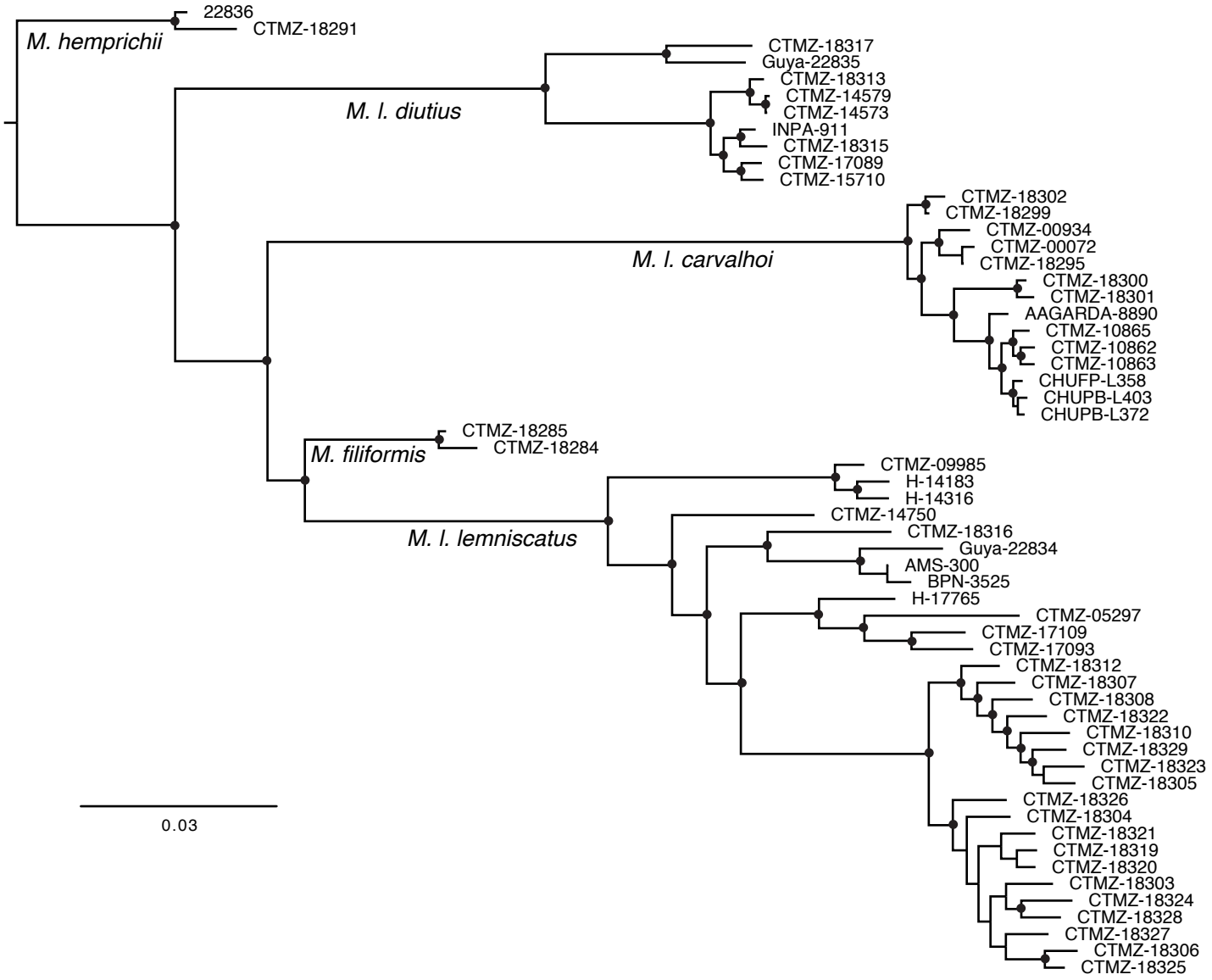

Figure 31. Maximum likelihood tree for the *Micrurus lemniscatus* complex using the software RAxML. Circles represent nodes with bootstrap values with support ≥ 75%.

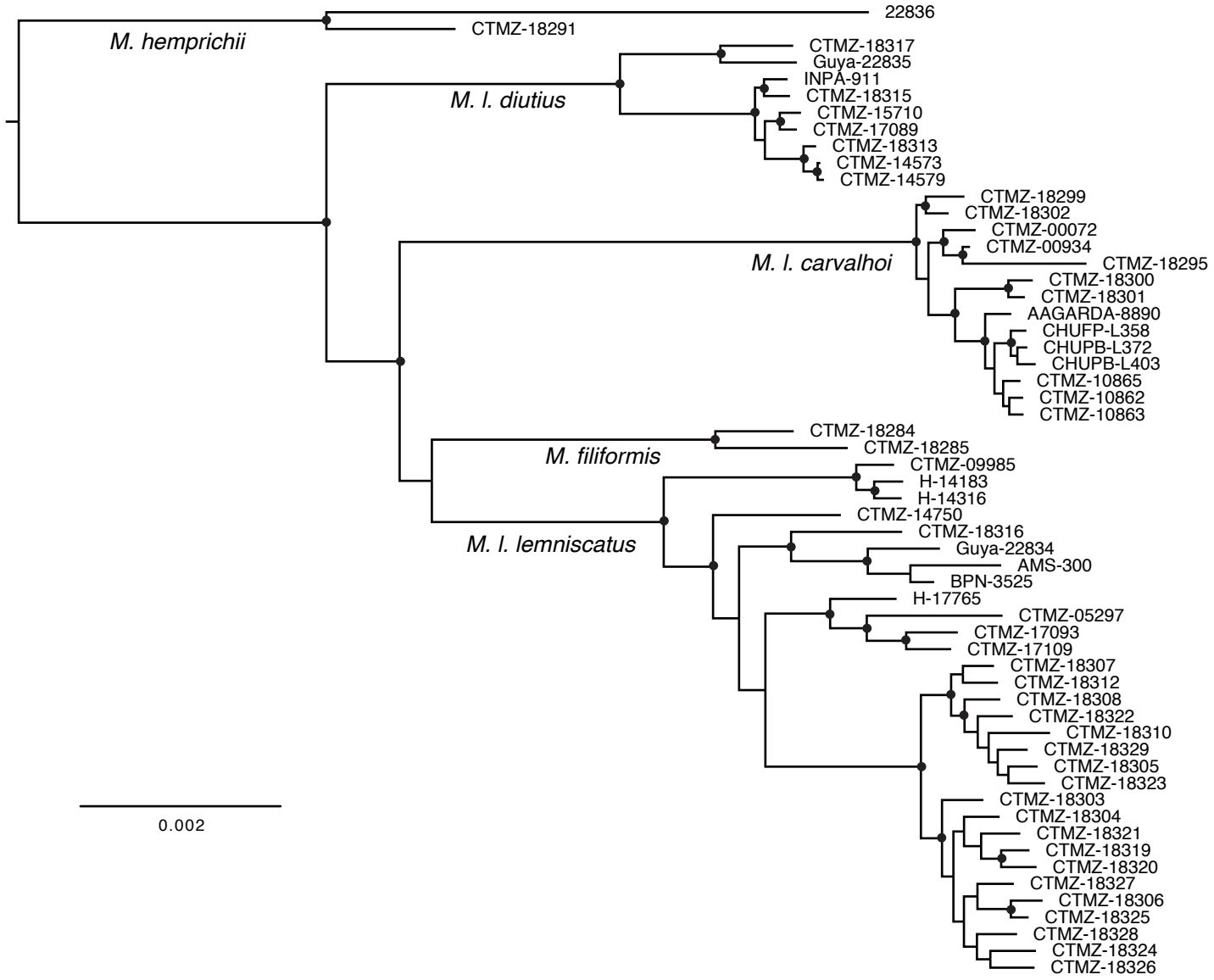

Figure 32. Maximum likelihood tree for the *Micrurus lemniscatus* complex using the software iqtree. Circles represent nodes with ultrafast bootstrap values with support ≥ 95%.

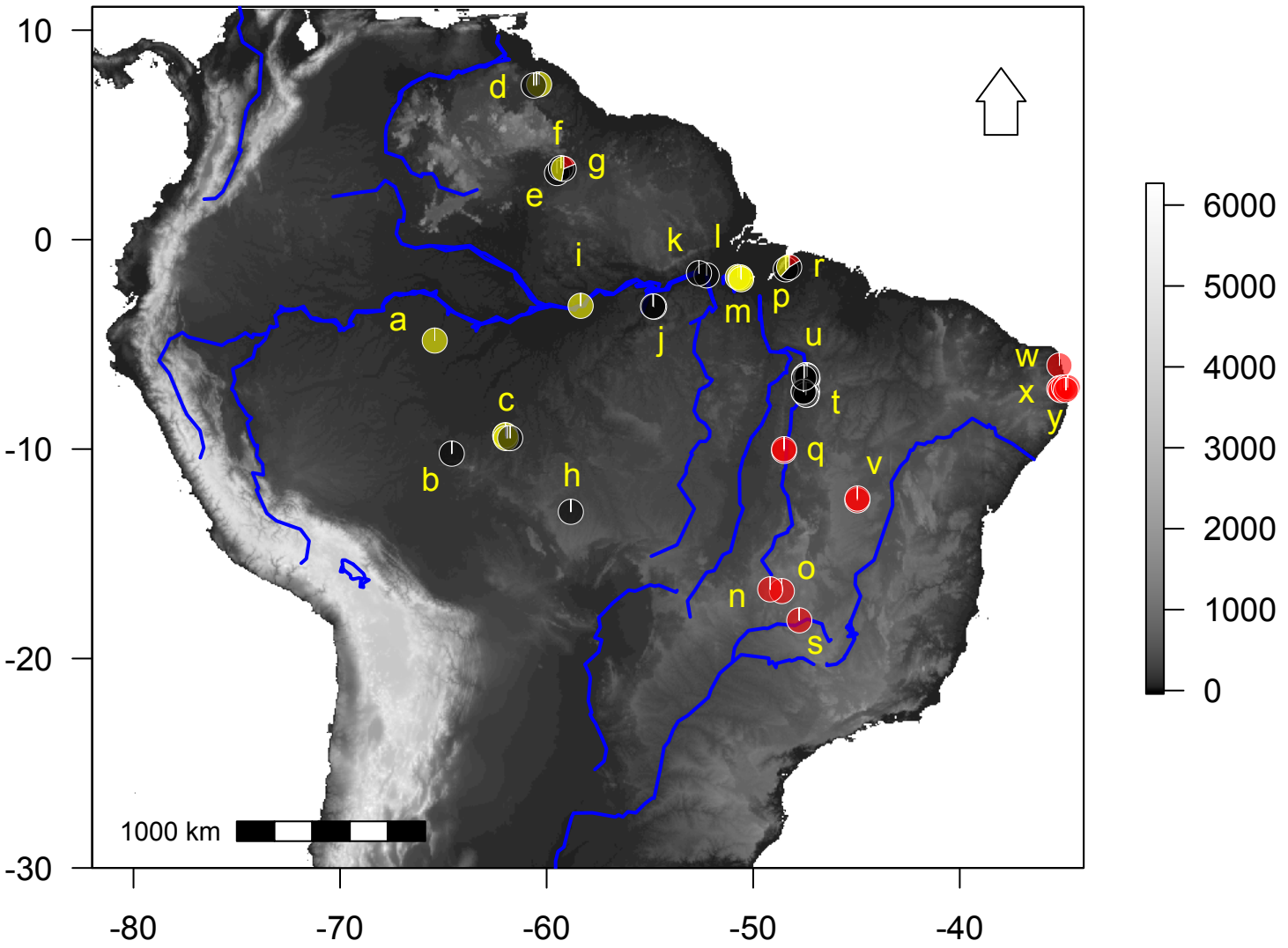

Figure 33. Map showing the samples used to reconstruct the phylogenetic history of the *M. lemniscatus* complex. Pie chart areas represent probability of assignment to each of one species of the M. lemniscatus complex from the fastStructure analysis. Yellow: *M. l. diuiuts*, Black: *M l. lemniscatus*, Red: *M. l. carvalhoi*. Tricolored represents *Micrurus filiformis*. Letters correspond to groups on fastSTRUCUTURE barplot of Fig 34. Gray scale represents altitude in meters.

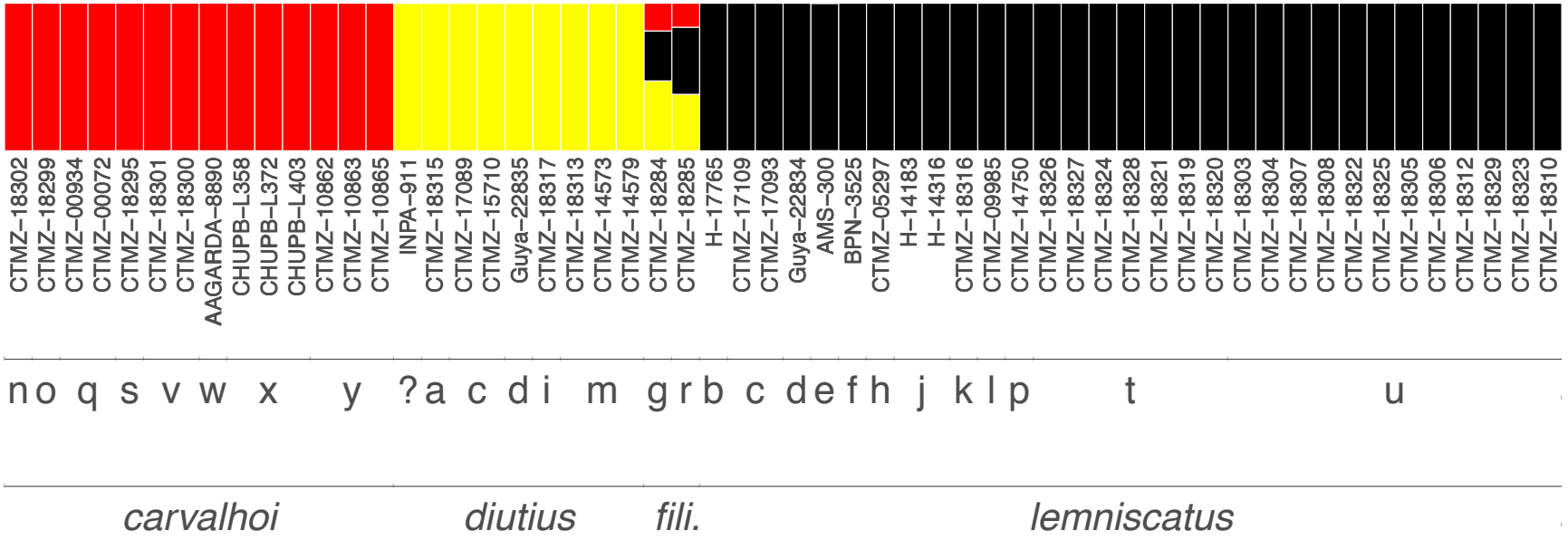

Figure 34. fastStructure analysis Barplot using samples of the *M. lemniscatus* complex. Best k=3. Letters correspond to geographic locations of Fig 33. Each vertical bar represents one sample and each color represents one admixture group.fili = *Micrurus filiformis.*

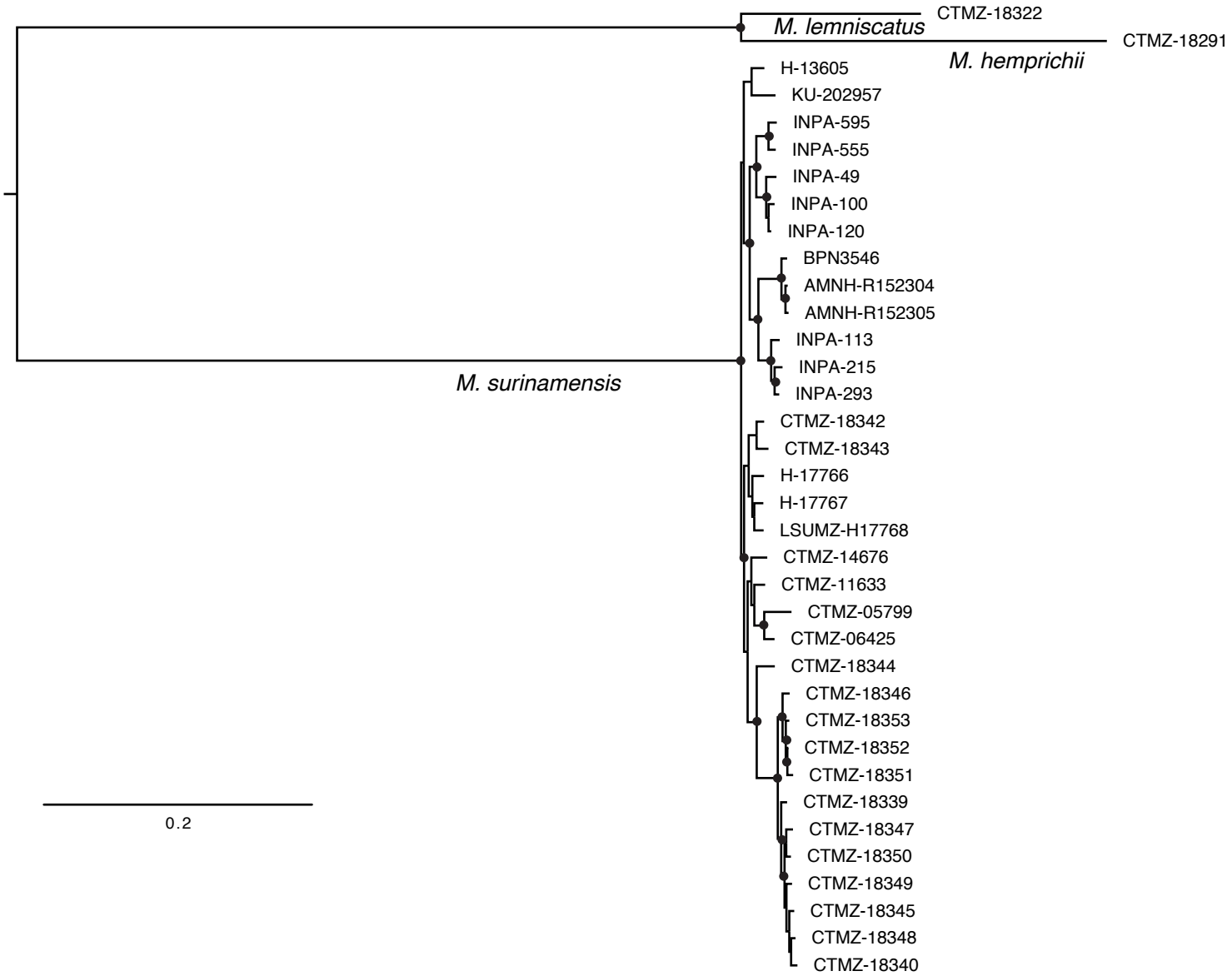

Figure 35. Maximum likelihood tree for *Micrurus surinamensis* using the software RAxML. Circles represent nodes with bootstrap values with support ≥ 75%.

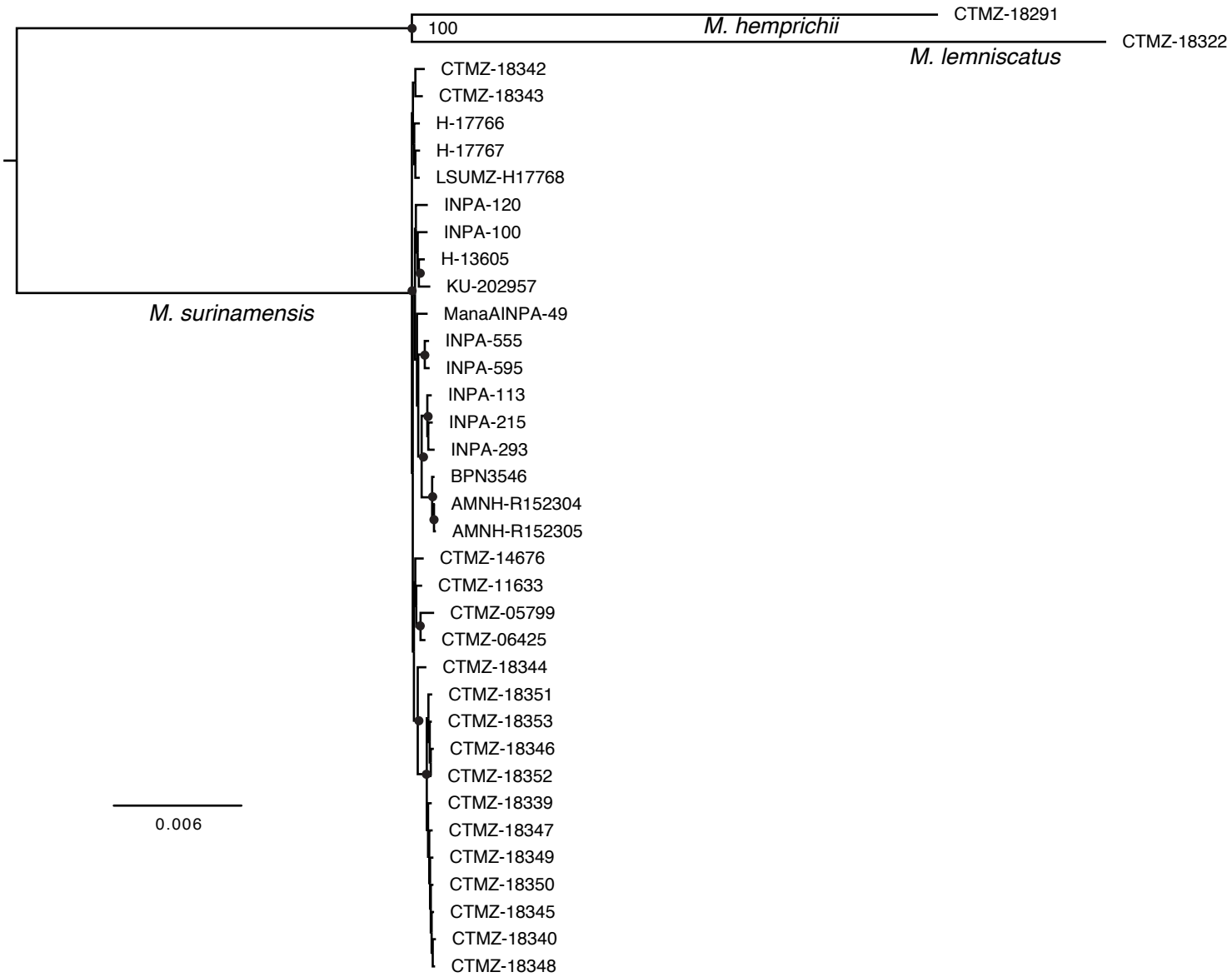

Figure 36. Maximum likelihood tree for the Micrurus surinamensis using the software iqtree. Circles represent nodes with ultrafast bootstrap values with support ≥ 95%.

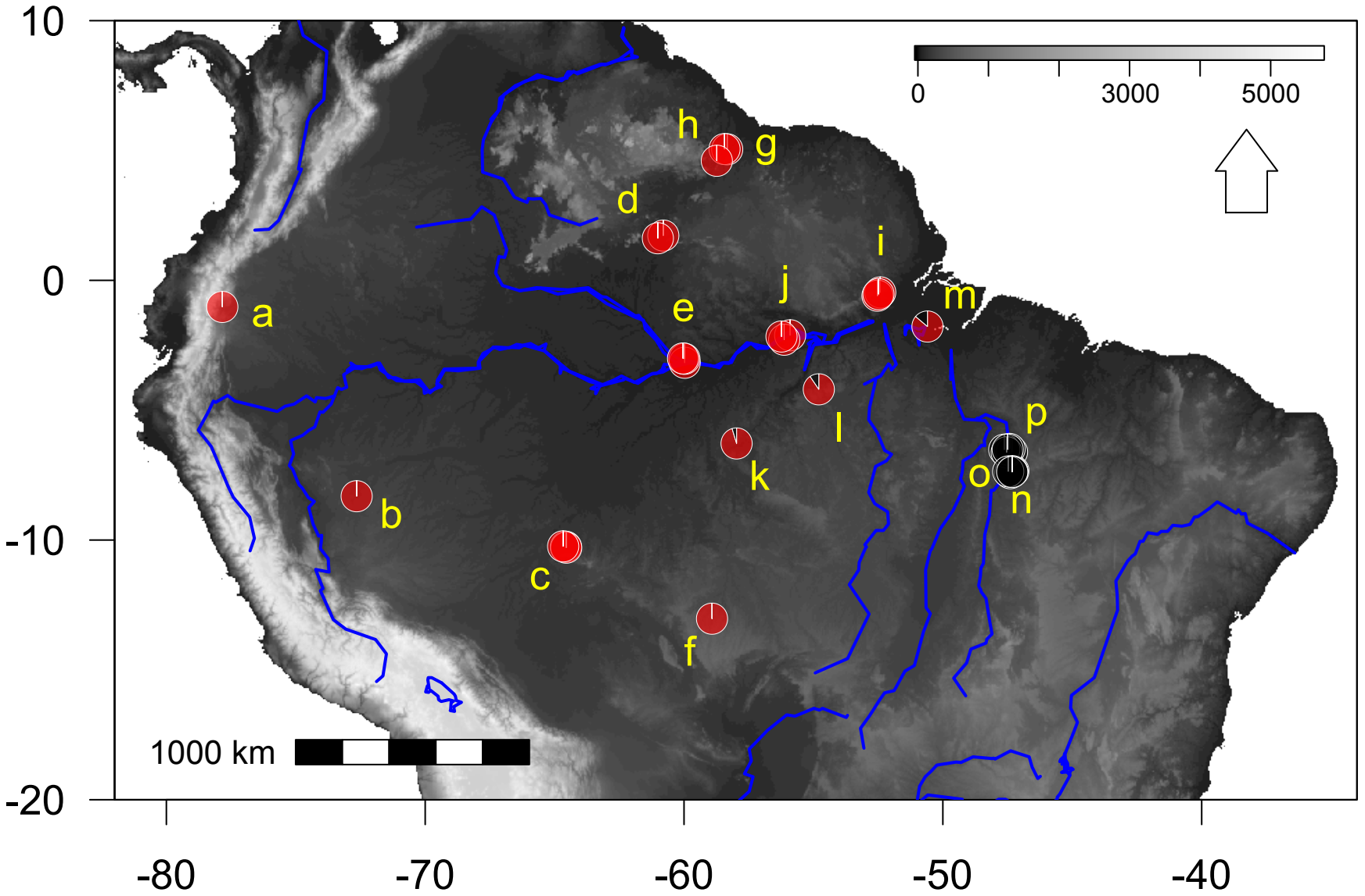

Figure 37. Map showing the samples used to reconstruct the phylogenetic history of the M. surinamensis. Pie chart areas represent probability of assignment to each of one populations of M. surinamensis from the fastStrucuture analysis. Red: Amazon group, Black: Tocantins/Araguaia group. Gray scale represents altitude in meters.

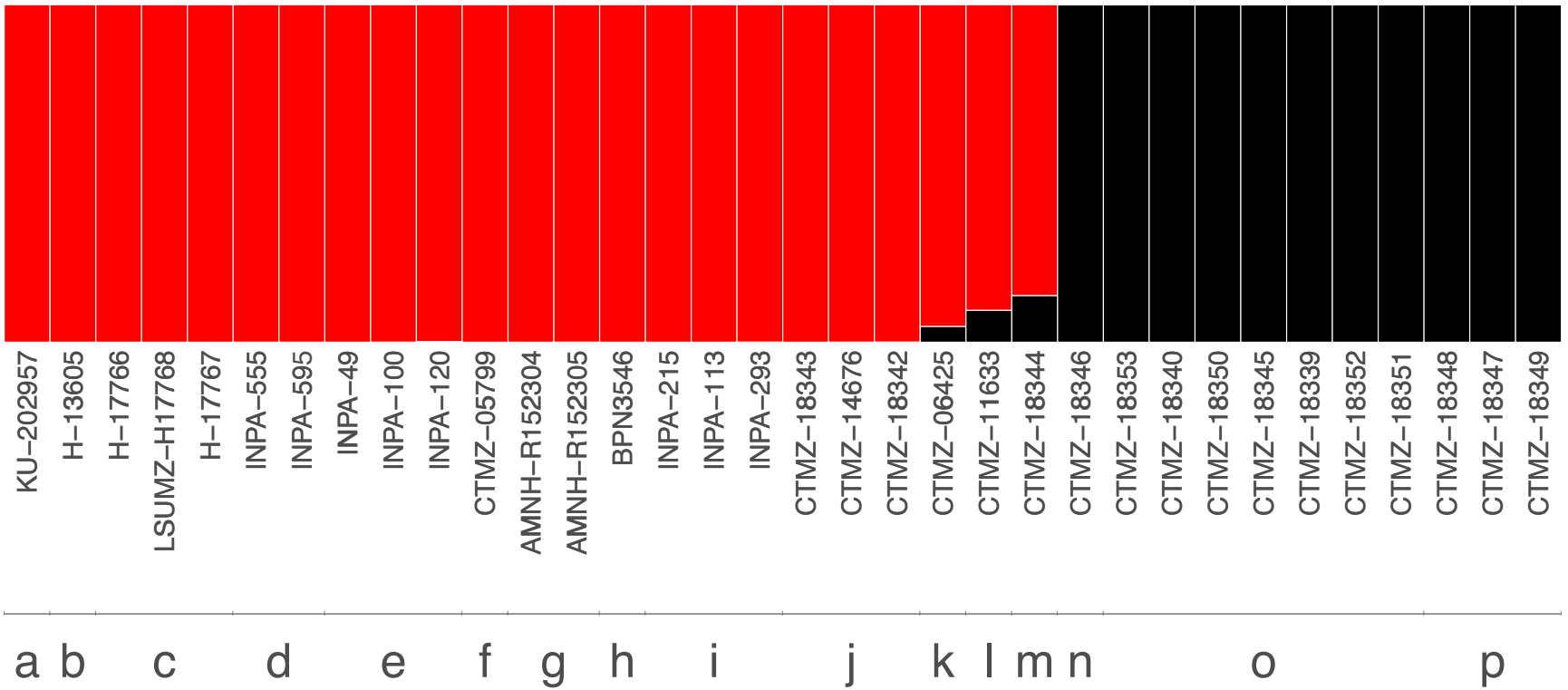

Figure 38. fastStrucuture analysis Barplot using samples of the *M. surinamensis*. Best k=2. Letters correspond to geographic locations of Fig 37. Each vertical bar represents one sample and each color represents one admixture group.

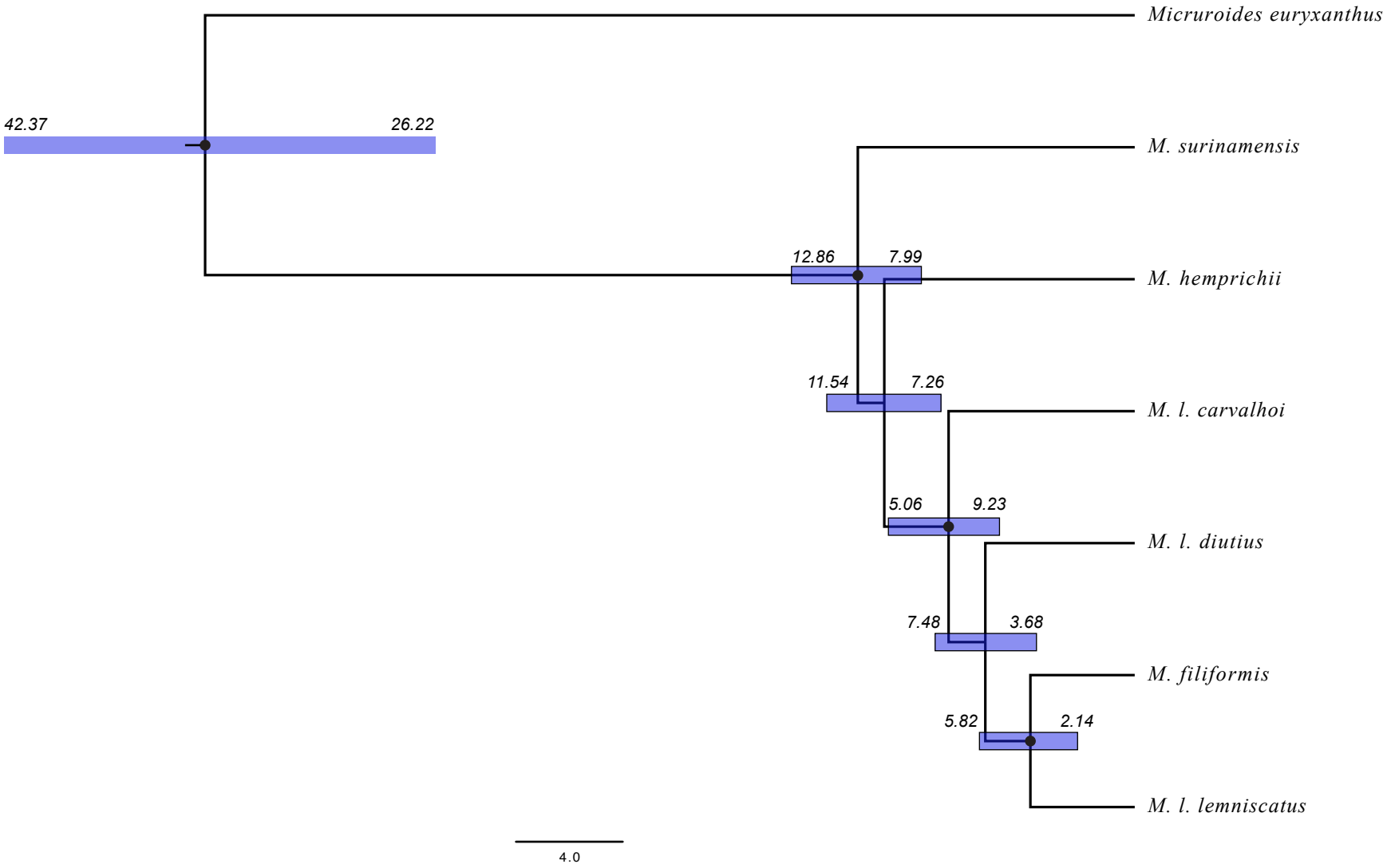

Figure 39. Coalescent tree for *Micruroides, M. hemprichii* and *M. lemniscatus* complex using the software SNAPP blue bars represent the 95% credibility interval of divergence time estimates at each node. Numbers above each blue bar correspond to time before present in million years. Nodes with black circles: posterior probability = 1, nodes without black circles: posterior probability < 0.7.

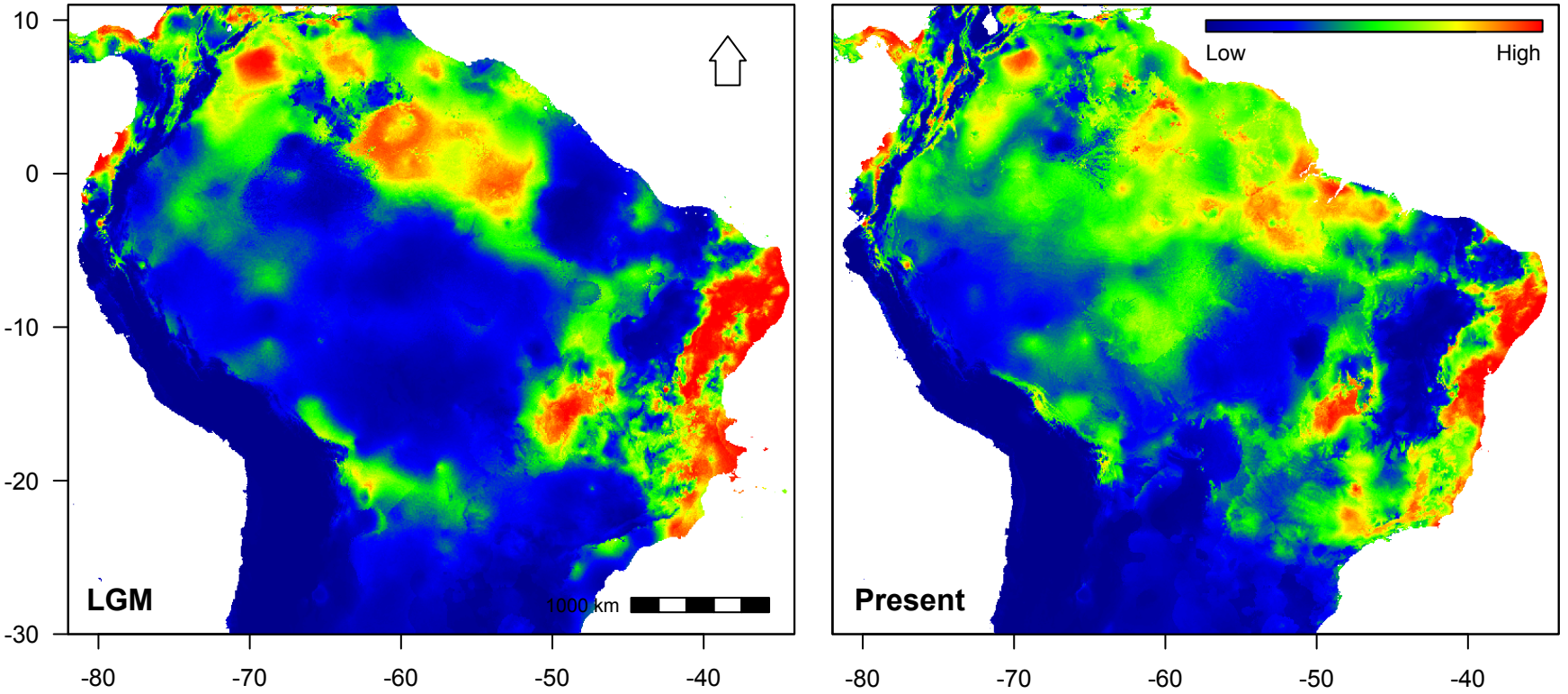

Figure 40. Distribution modeling of the *Micrurus lemniscatus* complex under past climatic conditions (left map, Last Glacial Maximum - 21 thousands years ago) and present climatic conditions (right map) using Maxent. Warmer colors represent areas with higher probability of niche suitability.

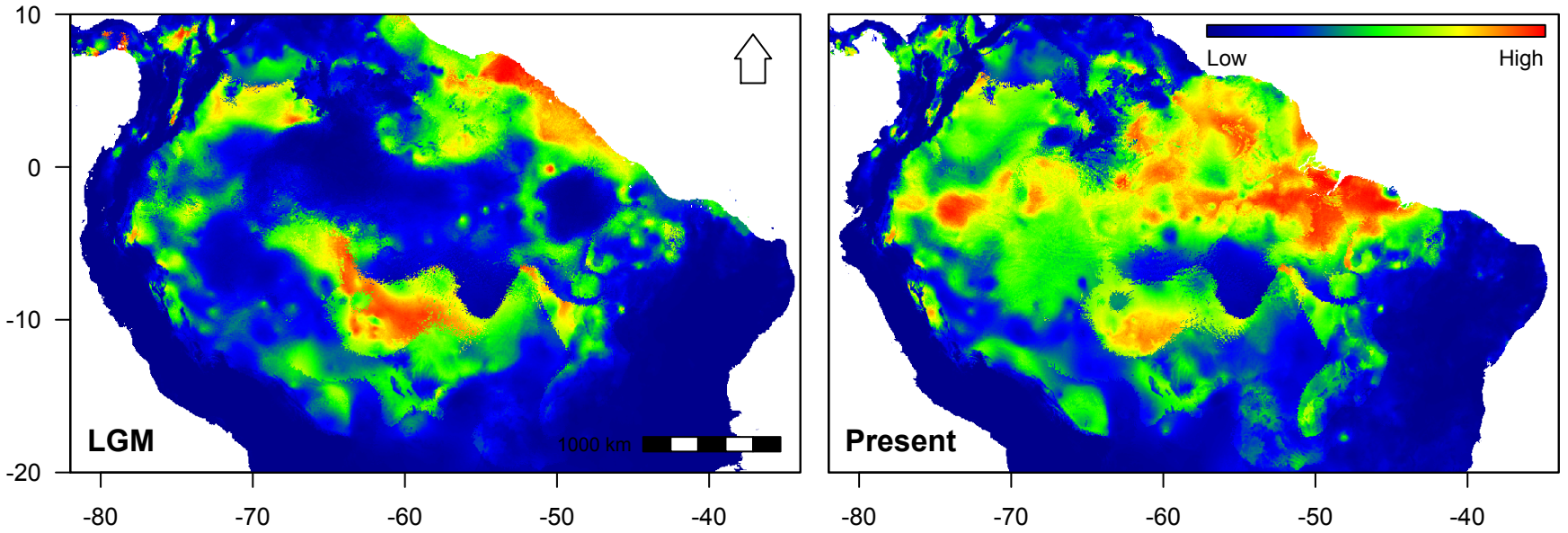

Figure 41. Distribution modeling of the *Micrurus surinamensis* under past climatic conditions (left map, Last Glacial Maximum - 21 thousands years ago) and present climatic conditions (right map) using Maxent. Warmer colors represent areas with higher probability of niche suitability.

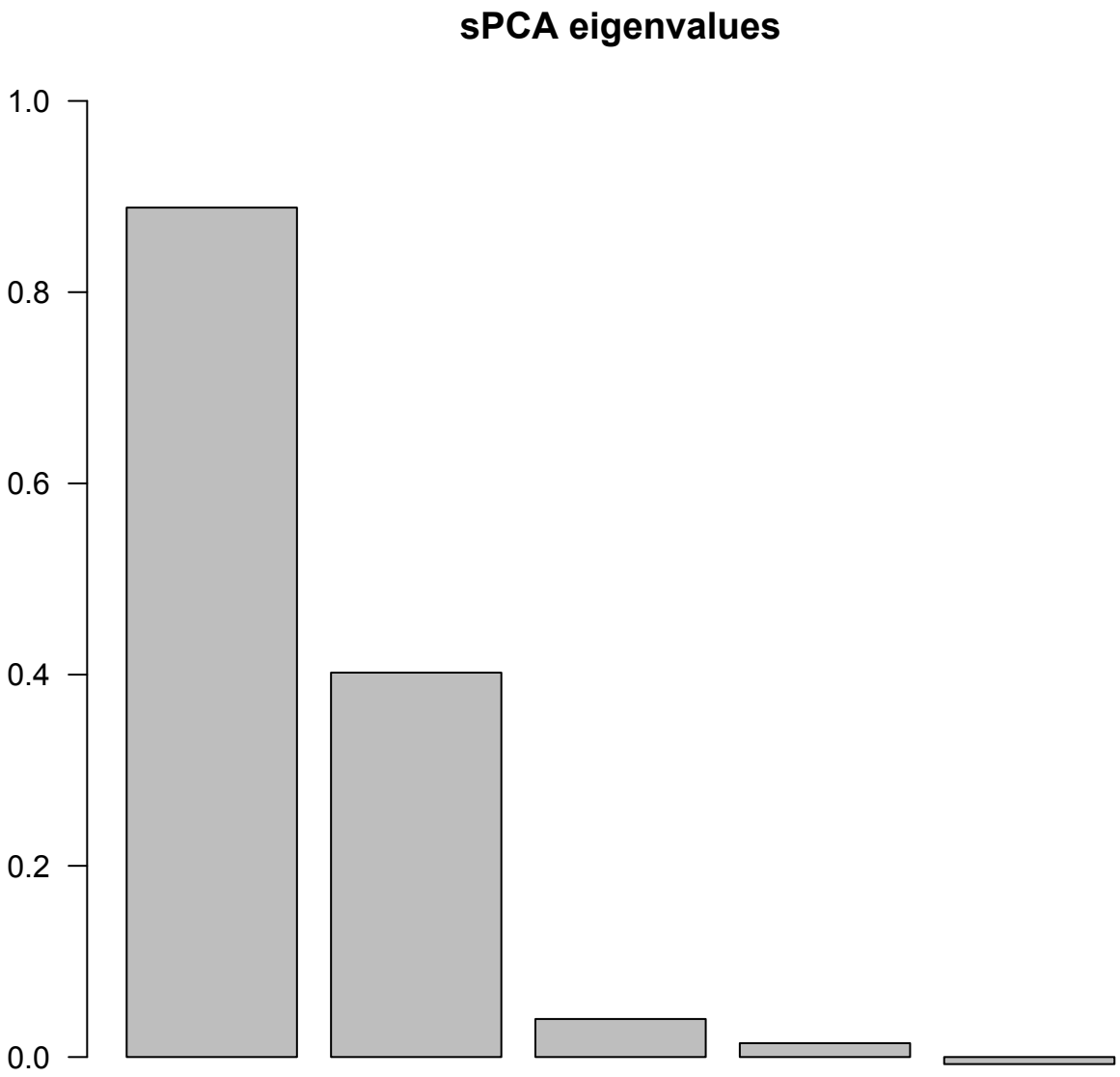

Figure 42. Barplot displaying the importance of each spatial principal component analysis axis for *Micrurus lemniscatus* complex.

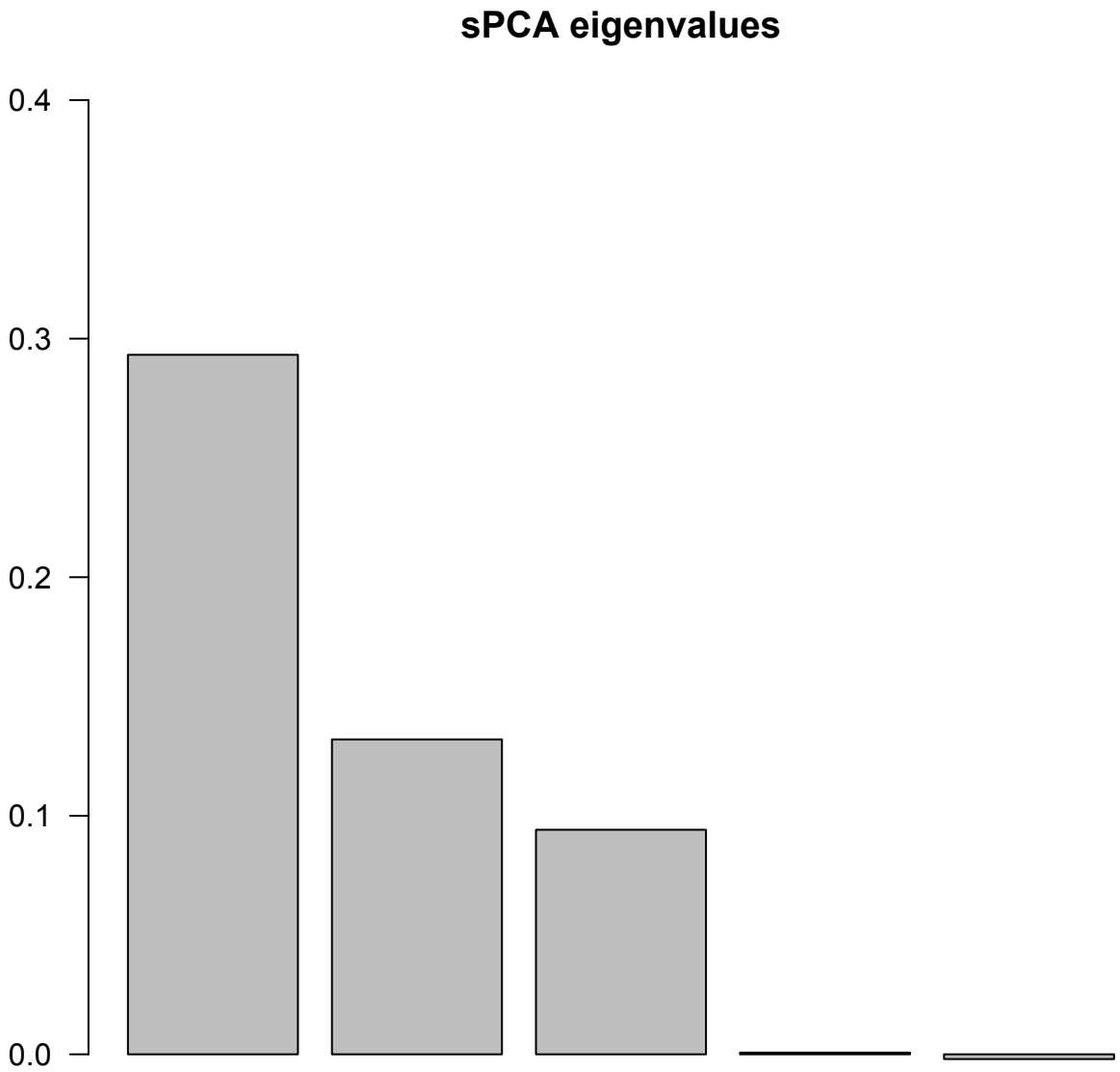

Figure 43. Barplot displaying the importance of each spatial principal component analysis axis for *Micrurus surinamensis.*

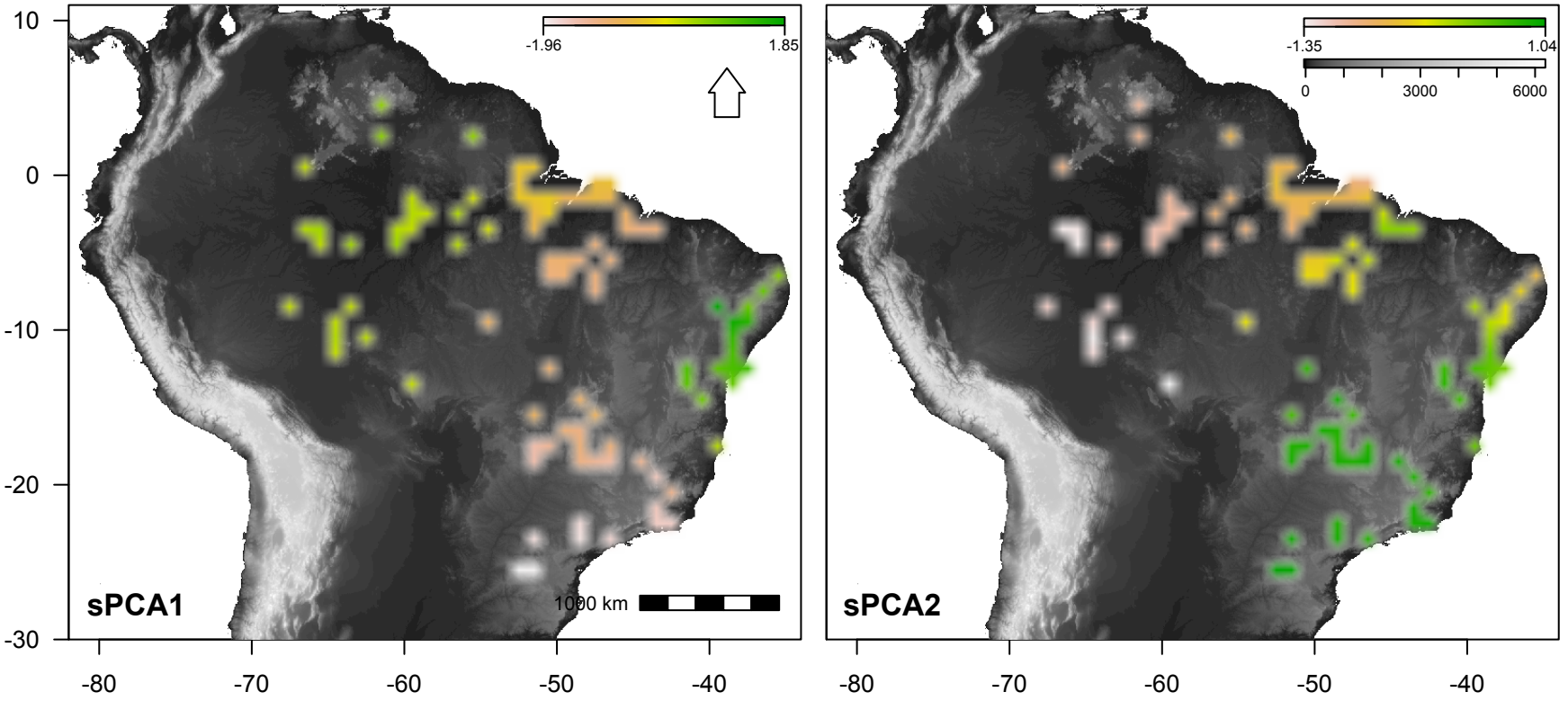

Figure 44. Map displaying the morphological variation of the *Micrurus lemniscatus* complex. Each cells has one degree latitude x longitude (ca. 111 km2). Colors represent the averaged lagged score of each cell. Gray scale represents altitude in meters.

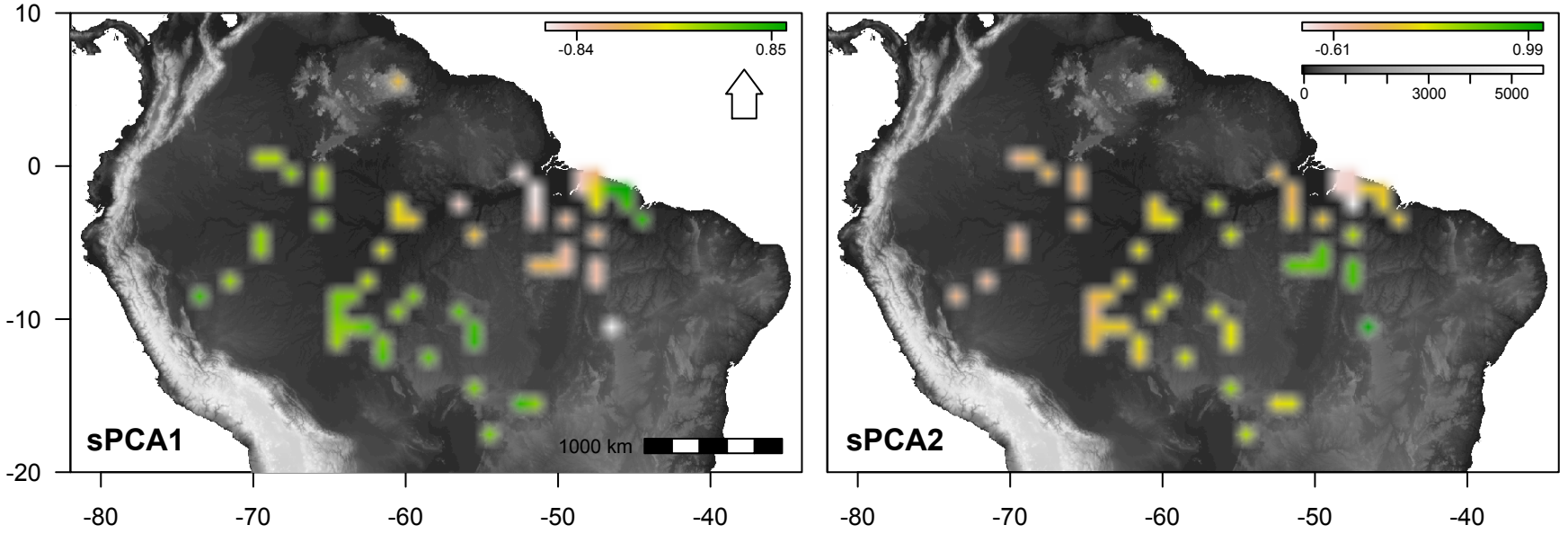

Figure 45. Map displaying the morphological variation of *Micrurus surinamensis*. Each cells has one degree latitude x longitude (ca. 111 km2). Colors represent the averaged lagged score of each cell. Gray scale represents altitude in meters.

Appendix C: List of specimens of the *Micrurus* genus used in chapter 2 and 3 with museums acronyms.

Micrurus brasiliensis: **CEPB:** 4540. **CHUNB:** 14163, 52143, 12012, 44683. **MNRJ:** 19531, 18663, 9089, 18660, 18662, 14977. **MNRJ:** 19531, 18663, 9089, 18660, 18662, 14977. **MPEG:** 24136, 24144, 24143, 24142, 24139, 24146, 24138, 24140, 24147, 24145, 24135, 24141, 24137. **MZUSP:** 20969, 20948, 21054, 20954, 21050, 19370, 21044, 20959, 21029, 21031, 21045, 21056, 20935, 17295, 21021, 20933, 21034, 20960, 21025, 21049, 21046, 20930, 20941, 20924, 21041, 21057, 20961, 21027, 20952, 20923, 21037, 20922, 17215, 20925, 19377, 20931, 21043, 20965, 20926, 19376, 20950, 20936, 20927, 21028, 21033, 21040, 21023, 20962, 20949, 21030, 20938, 19378, 20944, 19371, 20946, 20956, 17212, 21048, 20958, 21035, 19375, 20943, 21042, 20929, 20955, 19372, 19369, 16734, 20942, 21038, 20957, 21055, 21036, 20940, 20951, 21032, 20963, 15119, 21023-2, 20937, 21026, 21053, 21024, 21058, 19381, 20921, 19368, 20953, 20947, 20945, 17296, 20939, 16733, 19367, 20928, 21039, 19374, 19379, 20934, 20932, 21051, 19373, 19364, 21047, 19380. **UFMT:** 8616.
Micrurus frontalis: **CEPB:** 304, 4498, 2475, 345, 1873, 8520, 1659, 8861, 336, 1813, 6812, 3277, 8840, 605, 1659, 1587, 1968, 1658, 2235, 1915, 2363, 6565, 3827, 4320, 614, 3179, 3208, 1770, 770, 1657, 8396, 1762, 1217, 3192, 2688, 2432, 2365, 1874, 2284, 2076, 2433, 3824, 4497, 6811, 2989, 3061, 2817, 2140, 2301, 2686, 2817. **CHUNB:** 35989, 29298, 42648, 67596, 3937, 20315, 3923, 3931, 37442, 3919, 62265, 20314, 3920, 3935, 62388, 3926, 58391, 3921, 37441, 24380, 43654, 3932. **MHNCI:** 9628, 6977, 360, 11524, 426, 4486, 11523, 7357. **MNRJ:** 25144, 8265, 8258, 23021, 8263, 8262, 17304, 1361, 8260, 17303, 8264, 8261, 20683, 8266, 9061, 8259, 1353, 1360, 17227, 1356, 9251, 1359, 17777, 1355, 21107, 1357, 1351, 1350, 15318, 15127, 1349, 9097, 1348, 1352, 1354, 1358, 9080. **MPEG:** 10415. **MZUFBA:** 1832. **MZUSP:** 1772, 616, 15283, 10186, 8640, 131, 17223, 15000, 9945, 81, 7995, 10185, 80, 15286, 17377, 5379, 10187, 5248, 14412, 9605, 11731, 17375, 17370, 17371, 17373, 14549, 14999, 17372, 14926, 12063, 17376, 17374, 17475. **UFMT:** 607, 736, 732, 8502, 254, 669, 733, 734, 735, 11373, 6962, 267, 1674.
Micrurus ibiboboca: **CHUFPB:** 7055, RT1000, 13216, 13223, 13222, 13228, 7059, 12215, 9252, 13227, 10655, 12205, 7049, 13221, 6950, 4712, 13224, 4697, 12207, 12208, 12581, 12217, 12197, 7061, 12191, 7034, 4715, 13636, 7062, 7058, 12189, 12196, 7048, 13635, 11853, RT1101, 12190, 4703, RT991, 6947, 12210, 7051, 13637, 4718, 13211, 7032, 12204, 6952, 6951, 11852, 12200, 12221, 4706, 7041, 12203, 13212, 9472, 8942, 13226, 11851, 4694, 13213, 7056, 4704, 7033, 13229, 13209, 7053, 9214, 7057, 7029, 4689, 7021, RT986, 6948, 4698, 12216, 7025, 4713, 7043, 12220, 7047, 7052, GU05, 12202, 4711, 4696, GU06, 8943, 13959, 13210, 4695, 5509, 12206, 7020, 4707, 11854, 7045, 12199, 12195, 12212, 7038, 13217, 4837, 4687, 11445, 7046, 4716, 12198, 13631, RT327, 4682, 7064, 7065, 13639, 4686, 7022, 7031, 12192, 4702, 12219, 12201, 13634, 9333, 6949, 12218, RT1016, 11751, 13638, 7044, 13632, 8494, 4685, 7066, 4705, 13215, 5506, 4693, 13160, 13219, 13562, 4681, 7060, 7024, 7054, 4710, 13220, 5901, 13161, 9325, 5899, 13633, 7039, 12852, 4690, 4683, 13214, 4714, 4680, 4688, 4709, 14135, 4691, 8657, GU027, 4684, 4700, 4701, 5908, 6777, 9348, 9193, 7063, 7035, 583, 4708, 4717, 4692, 11898, 5872, 7023, 9924. **CHUNB:** 64753, 61174, 64752, 29981, 64751, 29286, 25352, 61175, 3925. **LARUFRN:** 2782, 5060, 5769, 3776, 7263, 7202, 2629, 3258,

9793, 2891, 3150, 3512, 6763, 6832, 9765, 2961, 11311, 6484, 11347. **MHNCI:** 7516, 11346, 13390, 3138, 11470, 13394, 7099, 3137. **MNRJ:** 19013, 18191, 9045, 19014, 19774, 20051, 13116, **MPEG:** 23355, 23350, 23352, 23351, 20531, 22793, 22803, 22772, 23349, 23353, 20804, 19165, 26156, 17211, 22789, 20529, 23354, 20528, **MZUFBA:** 1948, 147, 176, 150, 2111, 146, 165, 1160, 151, 145, 169, 99, 168, 999, 178, 158, 2110, 172, 2106, 173, 162, 160, 166, 170, None_1, 171, 159, 142, 148, 149, 174, 177, 143, 157, 161, 167, 164, 163, 175, **MZUSP:** 20616, 7253, 6905, 7252, 6503, 6907, 6564, 3268, 20287, 7002, 8935, 20431, 9005, 12377, 10963, 7255, 6932, 20403, 6904, 8934, 3546, 9021, 13372, 12376, 8953, 8952, 3547, 20433, 7191, 6934, 8909, 7193, 20429, 6561, 9004, 6903, 6902, 6933, 20289, 20428, 7190, 83, 5853, 20430, 20288, 20434, 6563, 6901, 6562, 13959, 77, 9006, 10463, 18269, 5441, 18277, 76, 10967, 13011, 6502, 12637, 612, 7189, 5175, 18796, 18762, 15582, 12636, 10035, 18270, 20617, 13012, 8099, 6906, 3548, 10962, 7801, 8908, 17728, 17727.
Micrurus lemniscatus: **CEPB:** 7567, 603, 8605, 8561, 1875, 8608, 4475, 8563, 6337, 4474, 8559, 6354, 2068, 8558, 2678, 352, 8606, 8555, 3614, 3837, 178, 275, 8604, 8556, 5274, 3838, 369, 6352, 8562, 1163, 609, 7426, 892, 1542, 223, 4395, 1761, 4856, 1969, 8607, 6353, 5375, 2801, 1768, 8557, 8560, 4449, 4429, 4462, 32, **CHUFPB:** 7028, 12187, 6946, 7030, 7026, 7036, 7042, 12188, 12185, 7037, 13231, 4, 2, 3, 12186. **CHUNB**: 3913, 3911, 72311, 66423, 66426, 72310, 72307, 3910, 72333, 20316, 72315, 72304, 72374, 3930, 32640, 72346, 72334, 72329, 72320, 72331, 66421, 72327, 72347, 72323, 28876, 72317, 72355, 72308, 72359, 72353, 72305, 72336, 72330, 72337, 72349, 72299, 72312, 72332, 72322, 72325, 72354, 72339, 72338, 72343, 72321, 72300, 32309, 72318, 72373, 72319, 72342, 72326, 72335, 72324, 72348, 72316, 72341, 72340, 72345, 72306, 72358, 72352, 72357, 22031, **INPA:** 31577, 28650, 18768, 2220, 15758, 20835, 28595, 32003, 11122, 34261, 32007, 32096, 17641, 32313, 20690, 34140, 31494, 20482, 21174, 25536, 34124, 32251, 12012, 13764, 17275, 34268, 2175, **LARUFRN:** 8890, **MHNCI**: 3105, 12081, 4966, 4463, 4309, 10010, 12762, 4541, 2779, 14105, 12571, 13302, 4932, 15177, 13915, 11177, 14517, 11942, **MNRJ:** 19332, 20517, 957, 19514, 22781, 17308, 19316, 24418, 17840, 4899, 15226, 17492, 16496, 24114, 19761, 8274, 14920, 9252, **MPEG:** 18657, 16198, 10178, 15281, 13001, 10119, 15444, 25032, 5021, 5382, 20127, 1516, 16695, 18879, 5600, 5020, 25969, 19904, 22401, 24098, 8852, 23720, 8466, 13652, 12691, 23147, 23146, 10374, 15552, 16489, 5026, 24151, 3669, 388, 24237, 14513, 16162, 23544, 8887, 23237, 3043, 24446, 20083, 6551, 25445, 20001, 16408, 24385, 8886, 19054, 1371, 25629, 24236, 4146, 8837, 13517, 16488, 18698, 25968, 22052, 17606, 8455, 23387, 3044, 18687, 6833, 8853, 8850, 23386, 8885, 19772, 24152, 24153, 2618, 3906, 20373, 22054, 13905, 266, 26078, 18444, 8877, 24154, 5602, 19814, 12854, 8878, 4319, 12899, 5548, 19150, 22511, 18707, 23097, 25067, 24150, 22184, 8845, 5390, 19303, 17260, 17144, 26075, 5551, 16833, 219, 16791, 8849, 17579, 18963, 8454, 2193, 24063, 6552, 21397, 17513, 5533, 23196, 25066, 13763, 18686, 23195, 20530, 17784, 8851, 22827, 20913, 25625, 26076, 24234, 24238, 8848, 2856, 10118, 8879, 3220, 24536, 8838, 3904, 15280, 20787, 5603, 429, 15026, 25068, 13645, 14186, 13004, 21559, 26077, 23494, 24149, 21167, 19693, 25630, 24148, 5542, 22281, 20458, 22176, 16164, 21168, 24235, 19694, 23769, 21169, 17762, 19692, 25627, **MZUFBA**: 1358, 567, 982, 801, 1318, 1974, 270, 635, 337, 1388, 271, 1441, 436, 470, 409, 1562, 441, 2072, 195, 983, 1637, 1336, 979, 768, 1354, 1002, 2000, 613, 2414, 1460, 2024, 1325, 1872, 1356, 450, 626, 879, 859, 1442, 389, 775, 273, 1375, 1480, 787, 860, 614, 451, 1977, 1161, 1635, 1433, 792, 338, 858, 1439, 471, 5793, 1444, 864, 578, 1462, 612, 1543, 1425, 371, 998, 1355, 758, 1276, 1440, 1972, 1505, 1353, 1871, 980, 861, 445, 1357, 866, 412, 1773, 632, 1906, 757, 1371, 984, 1016, 813, 572, 863, 636, 469, 1645, 1289, 1163, 577, 1279, 815, 1316, 1324, 144, 403, 1956, 1164, 394, 995,

767, 978, 1903, 977, **MZUSP:** 19431, 19417, 19420, 19428, 19419, 19400, 17352, 19390, 19391, 19421, 19429, 19416, 5465, 20036, 19410, 19366, 19383, 19424, 19426, 19407, 19408, 19365, 14518, 19399, 19395, 19404, 19430, 2972, 19427, 19458, 19415, 19382, 19385, 19403, 18758, 19384, 19392, 18622, 4400, 18643, 9306, 19386, 19411, 10812, 19425, 14517, 17355, 19423, 20840, 19406, 19393, 18644, 20034, 3965, 19412, 17351, 19397, 19402, 8357, 4901, 9097, 19409, 19418, 20035, 1224, 13163, 8042, 19422, 19706, 19396, 17327, 4792, 10135, 18930, 6108, 19414, 19398, 10809, 19707, 17354, 19413, 71, 9258, 17326, 9411, 9243, 19394, 72, 20432, 8641, 8896, 17325, 19405, 19708, 15534, 19389, 19401, 17353, 2944, **UFMT:** 11718.

Micrurus surinamensis: **CHUNB:** 33906, 3912, 47131, **INPA:** 12621, 1345, 27642, 28913, 18759, 34219, 21668, 12623, 32054, 1566, 19218, 32802, 9719, 28914, 1567, 32138, 34851, 34221, 16366, 34220, 30285, 12639, 21667, 31482, 12622, 12090, 21699, **MHNCI:** 13635, 14037, 12908, **MNRJ:** 10046, 8229, 10833, 8269, 10957, 10048, 10848, 8270, 10847, **MPEG:** 22060, 24132, 24133, 22056, 5594, 22058, 22055, 23388, 20118, 1863, 23630, 22059, 21741, 2553, 23629, 2651, 8880, 20218, 10150, 12606, 26019, 24134, 3064, 1509, 12759, 20152, 9434, 25016, 15002, 4606, 2713, 1437, 21318, 4113, 8854, 2165, 5601, 16319, 22057, 26084, 17610, 5585, 20741, 859, 18734, 26083, 21747, 2855, 24935, 14768, 25626, 568, 5511, 20217, 16812, 2194, 10151, 23115, 21549, 25013, 20735, 25633, 18501, 20947, 2554, 26088, 17336, 6838, 19384, 18751, 12611, 2421, 10145, 3709, 12980, 18892, 23802, 12890, 24068, 19135, 26022, 26085, 18989, 2484, 10146, 18510, 19112, 919, 25634, 8856, 21116, 21016, 20280, 25635, 4980, 25702, 5584, 8884, 16556, 4786, 5544, 14844, 20499, 2322, 20729, 12811, 20378, 15954, 15337, 4141, 13757, 1510, 13761, 10144, 13653, 2552, 18243, 20374, 20375, 20728, 14767, 14437, 10147, 15001, 14136, 12760, 23992, 10149, 18337, 14137, 8094, 8201, 26087, **MZUSP:** 19337, 19332, 19331, 19336, 19340, 19334, 19335, 19330, 19997, 20838, 19338, 17837, 11453, 18384, 19339, 10703, 17381, 19333, 19067, 19709, 20839, 17472, 11467, 17379, 11468, 17383, 18630, 20837, 19859, 20863, 20679, 17211, 17380, 8716, 15601, 17382, 17308, **UFMT:** 7210, 6942, 10521, 9270, 7798, 7164, 7379, 731, 7170, 7799, 8432, 8668.

Museum acronyms

CEPB: Centro de Estudos e Pesquisas biológicas da PUC Goiás.
CHUFPB: Coleção Herpetológica da Universidade Federal da Paraíba.
CHUNB: Coleção Herpetológica da Universidade de Brasília.
INPA: Instituto Nacional de Pesquisas da Amazônia.
LARUFRN: Laboratório de anfíbios e répteis da Universidade Federal do Rio Grande do Norte.
MHNCI: Museu de História Natural Capão da Imbuia.
MNRJ: Museu Nacional do Rio de Janeiro
MPEG: Museu Paraense Emílio Goeldi
MZUFBA: Museu de Zoologia da Universidade Federal da Bahia
MZUSP: Museu de Zoologia da Universidade de São Paulo
UFMT: Universidade Federal do Mato Grosso.

Appendix D: List of specimens of the *Oxyrhopus* genus used in chapter 3 with museums acronyms.

Oxyrhopus guibei: **CHUFBP:** 04788, 04789, 04790, 04791. **CHUNB:** 03643, 03648, 03650, 03652, 03653, 03657, 03659, 03660, 03661, 03662, 03688, 03792, 06165, 06166, 06167, 13751, 13752, 13753, 13754, 13755, 13756, 13757, 13758, 13760, 17170, 17171, 17172, 17173, 17590, 18324, 18366, 18367, 20282, 20283, 20284, 20285, 20286, 20287, 20288, 20290, 20291, 20292, 20294, 20295, 20296, 20297, 2103, 23731, 23823, 24163, 24382, 24598, 24617, 24749, 24896, 25340, 25341, 25354, 25356, 26486, 26486, 26919, 26922, 27645, 28149, 28891, 28949, 2931, 29621, 30341, 30397, 30412, 32638, 3823, 38477, 38941, 39061, 39062, 39063, 39065, 40286, 40287, 40627, 40673, 40721, 40722, 40733, 40734, 40737, 40741, 40742, 40743, 40795, 40796, 40845, 40895, 40960, 41310, 41721, 42296, 42297, 42298, 42299, 4230, 4232, 4233, 4235, 4237, 42579, 44044, 44045, 44046, 44047, 44048, 44113, 44114, 44115, 4427, 4428, 45390, 45392, 45393, 49447, 49685, 50272, 50426, 52258, 52356, 52357, 52361, 52410, 52762, 53187, 53271, 53312, 55218, 55219, 56358, 56381, 5656, 56859, 56893, 57347, 57348, 57436, 59161, 59164, 59165, 59166, 62417, 65112, 65113, 65257, 67258, 67479, 67482, 67487, 69250, 69256, 6941, 69430, 69447, 73439, 73454. **LARUFRN:** 6791. **MHNCI:** 10167, 10185, 10217, 10361, 10591, 10598, 1065, 10725, 10926, 1126, 11282, 11287, 11289, 1130, 11333, 11349, 11353, 11367, 11370, 11394, 1141, 1151, 1152, 11593, 11595, 11597, 11598, 1163, 1164, 1165, 1166, 1167, 1169, 11610, 11613, 11614, 12128, 12139, 1219, 1268, 12688, 1269, 13597, 1364, 1367, 13611, 13613, 14076, 14081, 1424, 14256, 14329, 14348, 14351, 14367, 14495, 1453, 14572, 14579, 14622, 14756, 14763, 14787, 14883, 14894, 1490, 14931, 1523, 1654, 1655, 1757, 1876, 1877, 1905, 2007, 2020, 2029, 2391, 2409, 2413, 2414, 2432, 2433, 2436, 2441, 2449, 2494, 2495, 2646, 2696, 2726, 2909, 3273, 3280, 3349, 3356, 3376, 3388, 3402, 3413, 3416, 3468, 3551, 3556, 3681, 3682, 3700, 3896, 3897, 3999, 4215, 4246, 4251, 4278, 4383, 4397, 4451, 4472, 4480, 4486, 4487, 4500, 4618, 4762, 4781, 4787, 4812, 4813, 4877, 5832, 5866, 5867, 5916, 5917, 5960, 6170, 6171, 6171, 6259, 6263, 6347, 6348, 6383, 6385, 6431, 6433, 6465, 6472, 653, 6544, 655, 6564, 6628, 6662, 6887, 6981, 7017, 7056, 7284, 7376, 7435, 7452, 749, 7928, 7985, 7994, 8106, 8339, 8472, 8473, 8474, 8475, 8486, 8541, 8850, 8969, 8970, 9104, 9175, 9240, 9301, 9352, 9353, 9354, 953, 963, 9940. **MZUFBA:** 1293, 1376, 1377, 1830, 1919, 1925, 1926, 2311, 790, 791, 892. **MZUSP:** 10137, 10148, 10170, 10172, 10176, 1056, 11096, 1118, 11588, 1161, 11679, 1171, 1173, 11814, 11815, 11824, 12051, 12055, 12060, 12079, 12086, 12099, 12110, 12159, 12160, 1224, 12283, 1238, 12354, 12416, 12426, 12434, 12438, 12454, 12514, 12721, 12727, 12728, 12742, 12745, 12750, 12756, 1283, 12812, 12813, 12814, 12815, 12821, 12837, 12838, 12847, 12849, 12862, 12864, 12897, 1297, 12914, 12915, 12922, 12929, 12932, 12939, 12940, 12952, 12974, 12984, 13019, 13021, 13023, 13060, 13125, 13127, 13190, 1322, 1329, 13211, 13213, 13228, 13243, 14414, 14742, 15152, 15688, 16249, 16255, 16270, 16272, 16274, 16275, 16276, 16277, 16280, 16283, 16284, 16290, 16291, 16312, 16313, 16317, 16318, 16319, 16573, 16845, 16861, 16862, 16863, 16864, 16864, 16865, 16866, 17193, 17482, 17624,

17772, 17772, 17799, 17818, 17841, 17849, 17868, 17924, 18141, 18638, 18781, 18826, 18843, 19594, 1995, 20442, 20858, 20911, 21436, 21443, 21444, 2353, 2610, 2648, 2800, 2869, 311, 315, 319, 322, 328, 330, 333, 3406, 3409, 3692, 3966, 4030, 4032, 4037, 4361, 4365, 542, 5588, 5860, 7578, 8284, 9531, 9904, 9917, 9939. **UFMT:** 00224, 00275, 00287, 00823, 01695, 01711, 02192, 02194, 02205, 02231, 02232, 02233, 03980, 04299, 04319, 04343, 05189, 05813, 06263, 06264, 06265, 06592, 07657, 10650, 11856.

Museum, acronyms
CHUFPB: Coleção Herpetológica da Universidade Federal da Paraíba.
CHUNB: Coleção Herpetológica da Universidade de Brasília.
LARUFRN: Laboratório de anfíbios e répteis da Universidade Federal do Rio Grande do Norte.
MHNCI: Museu de História Natural Capão da Imbuia.
MZUFBA: Museu de Zoologia da Universidade Federal da Bahia.
MZUSP: Museu de Zoologia da Universidade de São Paulo.
UFMT: Universidade Federal do Mato, Grosso.

VITTA

Renan Janke Bosque
Department of Biology
University of Mississippi

Education

Universidade de Brasília	Brasília, Brazil**,**	Biology	Bachelor of Science	**2009**
Universidade de Brasília	Brasília, Brazil	Biology	Fully licensed teacher	**2008**
Universidade de Brasília	Brasília, Brazil	Ecology	Master of Science	**2012**
University of Mississippi	Oxford, MS, USA	Biology	Ph.D.	**2019**

Peer-Reviewed publications

Lawrence, J. P; Rojas, B.; Fouquet, A.; Mappes; J.; Blanchette, A.; Saporito, R. A.; **Bosque R. J.**, Courtois, E. A.; Noonan, B. **2019:** Weak warning signals can persist in the absence of gene flow. *PNAS* 116, 19037-19045.

Rodrigues, P. J. O.; de Oliveira, N.; **Bosque, R. J.** Ferreira, M. F. N.; da Silva, V. M. A.; Magalhães A. C. M.; de Santana, C. J. C.; de Souza, M. C.; **2018:** Histopathological evaluation of the exposure by cyanobacteria cultive containing [d-Leu^1] Microcystin-LR on *Lithobates catesbeianus* tadpoles. *Toxins* 10(8), 318.

Bosque, R. J.; Lawrence, J. P.; Buchholz, R.; Colli, G. R.; Heppard, J.; B. P. Noonan. **2018:** Diversity of warning signal and social interaction influences the evolution of imperfect mimicry. *Ecology and Evolution* 8(15), 7490-7499.

Domingos, F. M. C. B.; Arantes Í. C.; **Bosque R. J.**; Santos M. G. **2017:** Nesting in the lizard *Phyllopezus pollicaris* (Squamata: Phyllodactylidae) and a phylogenetic perspective on communal nesting in the family. *Phyllomedusa* 16(2), 255-267.

Bosque R. J.; B. P. Noonan.; Colli G. R. **2016:** Geographical coincidence and mimicry between harmless snakes (Colubridae: *Oxyrhopus*) and harmful models (Elapidae: *Micrurus*). *Global Ecology and Biogeography*, 25(2), 218-226.

Domingos, F. M. C. B.; **Bosque, R. J.**; Cassimiro, J.; Colli, G. R.; Rodrigues, M. T.; Santos, M. G.; Beheregaray, L. B. **2014:** Out of the deep: Cryptic speciation in a Neotropical gecko (Squamata, Phyllodactylidae) revealed by species delimitation methods. *Molecular*

Phylogenetics and Evolution. 80, 113-124.

Bosque, R. J.; Marcela, M. S. O. C.; Ferreira, M. F. N. **2011:** A Eduação Ambiental na construção do Núcleo de Extensão da Universidade de Brasília em Santa Maria - Distrito Federal. *Revista Participação. Universidade de Brasília*, 15(1), 93-102.

Publications in preparation

de Almeida, P. C. R.; **Bosque, R. J.**; Banci, K. R. da S.; Curcio, F. F.; Rodrigues, M. T.; Prudente, A. L. da C. **2019:** Coral snake mimicry: concepts, evidences and criticisms. Book chapter –International symposium on coral snakes.

Bosque R. J., Hyseni C., Santos, M. L. G. S.; Rangel, E., Dias, C. J. da S., Hearin J., Domingos, F. M. C. B, Colli, G. R., Noonan, B. **2019:** Coral snake Müllerian mimicry. To be submitted to *Evolution*

Posters and Talks

Bosque, R. J.; Lawrence, J. P.; Buchholz, R.; Colli, G.R.; Heppard, J.; Noonan, B. P. **2018:** Diversity of warning signal and social interaction influences the evolution of imperfect mimicry. Joint Meeting of Ichthyologists and Herpetologists.

Anderson, R.; Chamberlain, N.; McPheron, M.; Grays, L.; Landsittel, J.; Rangel, E.; Hearing, J.; Santos, M. L. G.; Dias, C.; Hendricks, M.; Domingos, F. M. C. B.; Colli, G. R.; Noonan, B.; **Bosque, R. J. 2018:** Understanding Coral Snake Mimicry with the Use of Plasticine Replicas. The University of Mississippi School of Pharmacy Poster Session.

Hendricks, M.; Anderson, R.; Chamberlain, N.; McPheron, M.; Grays, L.; Landsittel, J.; Rangel, E.; Hearing, J.; Santos, M. L. G.; Dias, C.; Domingos, F. M. C. B.; Colli, G. R.; Noonan, B.; **Bosque, R. J. 2018:** The Effects of Coral Snake Mimicry on Predator-Prey Interactions. The University of Mississippi School of Pharmacy Poster Session.

Bosque, R. J.; Zaher, H.; Colli; G. R.; Carvajal, O. T.; Rodrigues, M. T.; Junior, N. J. da S.; Prudente, A. L. da C.; Grazziotin, F.; Vitt, L. J.; Noonan, B. **2017:** Phylogegraphy of *Micrurus surinamensis* and *Micrurus lemniscatus*. Evolution. Society for the Study of Evolution.

Bosque, R. J.; Zaher, H.; Colli; G. R.; Carvajal, O. T.; Rodrigues, M. T.; Junior, N. J. da S.; Prudente, A. L. da C.; Grazziotin, F.; Vitt, L. J.; Noonan, B. **2016:** Comparative phylogeography *Oxyrhopus guibei* and *O. trigeminus* and the morphological responses to *Micrurus* presence. Graduate student council symposium

Bosque, R. J.; Zaher, H.; Colli; G. R.; Carvajal, O. T.; Rodrigues, M. T.; Junior, N. J. da S.; Prudente, A. L. da C.; Grazziotin, F.; Vitt, L. J.; Noonan, B. **2016:** Comparative phylogeography *Oxyrhopus guibei* and *O. trigeminus* and the morphological responses to *Micrurus* presence.

Research Showcase Neuroscience Minor - Department of Biology.

Bosque, R. J.; Zaher, H.; Colli; G. R.; Carvajal, O. T.; Rodrigues, M. T.; Junior, N. J. da S.; Prudente, A. L. da C.; Grazziotin, F.; Vitt, L. J.; Noonan, B. **2016:** Phylogegraphy of *Micrurus surinamensis* and *Micrurus lemniscatus*. International Symposium on Coral Snakes.

Bosque, R. J.; Colli, G. R. **2014:** Geographical coincidence and mimicry between harmless snakes (Colubridae: *Oxyrhopus*) and harmful models (Elapidae: *Micrurus*). Evolution. Society for the Study of Evolution.

Bosque, R. J.; Colli, G. R. **2012:** Distribution and color patterns of mimic coral snakes *Oxyrhopus* (Serpentes, Colubridae) and the implications to mimicry. 7th World Congress of Herpetology.

Bosque, R. J.; Domingos, F. M. C. B.; Machado, L. F.; Colli, G. R. **2011:** Cerrado ou Amazônia? Composição da Assembléia de Lagartos numa Área de Transição em Nova Xavantina, MT. IX Congresso Latinoamericano de Herpetologia e V Congresso Brasileiro de Herpetologia.

Bosque, R. J.; Nogueira, C.; Valdujo, P. H.; Recoder, R.; Colli, G. R. **2011:** Répteis Squamata do Parque Nacional Chapada das Mesas, porção norte do Cerrado. IX Congresso Latinoamericano de Herpetologia e V Congresso Brasileiro de Herpetologia.

Bosque, R. J.; Domingos, F. M. C. B.; Machado, L. F., Colli, G. R. **2010:** Cerrado ou Amazônia? Composição da assembléia de lagartos numa área de transição em Nova Xavantina, MT. II Simpósio de Biologia Animal – UnB.

Bosque R. J.; Ledo, M. R. D.; Brasil, M. A.; Colli, G. R. **2009:** Demography of *Mabuya frenata* and *M. nigropunctata* in gallery forests of Central Brazil. IV Congresso Brasileiro de Herpetologia.

Bosque, R. J.; Arantes, I. da Costa: **2009:** Desvendando o segredo das cobras. IV Congresso Brasileiro de Herpetologia.

M. R. D.; Colli, G. R.**; Bosque R. J.;** Silva, M. S. A. **2009:** Estrutura e dinâmica de comunidades de lagartos em matas-de-galeria do Brasil Central. Ledo, IV Congresso Brasileiro de Herpetologia.

Oliveira, H. F. M.; Lobo, Y. P. P.; **Bosque, R. J.**; Coelho, L. A.; Oliveira, C. C. S.; Souza, A. C. O.; Castro, J. P. G. **2008:** Morcegos em caverna de altitude na Mata Atlântica, Bahia. IV Congresso Brasileiro de Mastozoologia.

Grants and fellowships $156,500

2018: University of Mississippi Summer Research Assistantship **$3,000**
2013-2017: Ciências sem Fronteiras fellowship ~**$144,000**

2016: University of Mississippi Graduate Student Council grant **$1,000**
2010-2012: Universidade de Brasília Master of Science assistantship **~$8,500**

Teaching experience

University of Mississippi
2018 – 2018: Teaching assistant - Ecology
2017 – 2017: Teaching assistant - Genetics
2016 – 2016: Teaching assistant - Biological Sciences I
2015 – 2016: Teaching assistant - Inquiry into Life Laboratory
2014 – 2014: Teaching assistant - Inquiry into Life Laboratory

Universidade de Brasília
2011: Teaching assistant - Biology of Reptiles
2011: Teaching assistant - Ecological Statistics
2007: Teaching assistant **-** Vertebrate Biology
2007 – 2007: Biology Instructor, Universidade de Brasília, Brazil – Extension program
2006 – 2006: Environmental Education Instructor, Universidade de Brasília, Brazil - Extension program
2005: Teaching assistant - Histology

Guest lecture

2019: Species interactions –Ecology (BISC 322) University of Mississippi
2018: Species interactions –Ecology (BISC 322) University of Mississippi

Professional experience

2005 – 2012: Assistant Herpetological Collections Manager, CHUNB, Universidade de Brasília, Brazil
2009 – 2010: Scientific Project Manager**,** Universidade de Brasília, Brazil

Special training

2015: Bodega Applied Phylogenetics Workshop. University of California, Davis.
2014: Next-generation sequencing for phylogenetics and phylogeography. National Evolutionary Synthesis Center, Durham NC.
2008: Experimental design. Universidade do Porto, Portugal.
2008: Molecular analysis of biological diversity. Universidade do Porto, Portugal.

Synergistic Activities

Involving undergraduate students in research:

- Mentor of undergraduate students in research projects.
- High School Science Fair judge.